UNIVERSIDAD DE GRANADA

TRABAJO FIN DE MÁSTER

MÁSTER EN MATEMÁTICAS

The Wheeler-DeWitt (WDW) equation and the WKB method

La ecuación de Wheeler-DeWitt (WDW) y el método WKB

Autor
Alejandro José Florido Tomé

Tutor: Elena Blanca Medina Reus
Matemáticas (Universidad de Cádiz)

Rafael de la Rosa Silva
Matemáticas (Universidad de Cádiz)

Julio 2025

MÁSTER EN MATEMÁTICAS

Presentación del Trabajo Fin de Máster

(UNA VEZ CUMPLIMENTADO, DEBERÁ PRESENTARSE JUNTO CON LA MEMORIA)

Máster en: Matemáticas

Curso académico: 24/25.

DATOS DEL ALUMNO

Apellidos: Florido Tomé	**Nombre:** Alejandro José
D.N.I.: 79163457X	**Tlf.:** +34 689776647
Correo electrónico: f92fltoa@correo.ugr.es	

DATOS DEL TRABAJO

TÍTULO:

The Wheeler-DeWitt (WDW) equation and the WKB method

La ecuación de Wheeler-DeWitt (WDW) y el método WKB

NOMBRE DEL TUTOR/CO-TUTOR:

Elena Blanca Medina Reus
Rafael de la Rosa Silva

Declaro explícitamente que el trabajo presentado es original, entendido en el sentido de que no he utilizado fuentes sin citarlas debidamente.

En Granada, a 2 **de** julio **de 20** 25.

Firmado por FLORIDO TOME ALEJANDRO JOSE - ***6345** el día 02/07/2025 con un certificado emitido por AC FNMT Usuarios

.

Firmado: Alejandro José Florido Tomé

Contents

Agradecimientos **1**

Resumen **3**

Abstract **7**

1 Introduction **9**

2 ADM Equations **15**
2.1 Principles of General Relativity 15
2.2 3+1 Formalism 16
2.2.1 The 3+1 Decomposition of Spacetime 16
2.2.2 Extrinsic Curvature 19
2.2.3 Energy-Momentum Tensor Decomposition 20
2.3 ADM Equations Summary 21
2.4 Wheeler-DeWitt Equation 22
2.4.1 Lagrangian Density and Hamiltonian 22
2.4.2 Lagrange Multipliers 23
2.4.3 Quantizing General Relativity 24

3 Classical Inflation **27**
3.1 General Friedmann Equations 27
3.2 Closed Friedmann Universe 30
3.2.1 Redundancy in Friedmann's Equations 31
3.2.2 The Universe as a Perfect Fluid 32
3.2.3 Classical regime 32
3.3 Inflationary regime 33
3.4 Kinetic dominance 33
3.4.1 Expanding universe 34
3.4.2 Contracting universe 36
3.4.3 Discussion of the Kinetic dominance 37
3.5 Constant potential 38
3.5.1 $q = 0$ 39
3.5.2 $q \in (0, 4p^4/27)$ 39
3.5.3 $q = 4p^4/27$ 42
3.5.4 $q > 4p^4/27$ 43
3.6 Slow-Roll Approximation and end of inflation 45

4 Quantum Inflation **47**
4.1 Relationship Between the Wheeler-DeWitt Equation and the Friedmann Equations . . . 47
4.2 WDW Equation for a Closed Universe . . . 48
4.2.1 Quantisation rules . . . 49
4.2.2 WDW equation and WKB solutions . . . 51
4.2.3 Semiclassical Analysis: Consistency with Classical Mechanics 52

5 Case of Study: Constant Potential **55**
5.1 Asymptotic behaviour of the wave functions as $a \to +\infty$ . . . 57
5.2 Asymptotic behaviour of the wave functions as $a \to 0^+$ . . . 58
5.3 Connection between quantum and classical solutions . . . 61
5.4 General wave function of the Universe for different $k-$values . . . 65
5.4.1 $k = 0$ . . . 66
5.4.2 $|k| = 1$ . . . 68
5.4.3 $|k| = \sqrt{8\pi^2 p^2/(27\lambda)}$ . . . 70
5.4.4 $|k| = 2$ . . . 72
5.5 Connection with the asymptotic behaviours . . . 74

6 Conclusion **77**

A Mathematical Foundations **79**
A.1 Manifolds and Differentiable Structures . . . 79
A.2 Tangent Spaces and Vector Fields . . . 80
A.3 Riemannian and Lorentzian Geometry . . . 80
A.4 Vector Bundles and Tensors . . . 82
A.5 Lie Derivatives . . . 83
A.6 Connections and Curvature . . . 84
A.7 Levi-Civita Connection . . . 85
A.8 Foliation of Spacetime . . . 86

B Derivation of the ADM equations **89**
B.1 First Equation: Time Evolution of the Spatial Metric . . . 89
B.2 Gauss-Codazzi and Codazzi-Mainardi Equations . . . 91
B.2.1 Spatial Covariant Derivative and Extrinsic Curvature . . . 91
B.2.2 Gauss-Codazzi Equation . . . 92
B.2.3 Codazzi-Mainardi Equation . . . 93
B.3 Second Equation: Hamiltonian Constraint . . . 93
B.4 Third Equation: Momentum Constraints . . . 94
B.5 Fourth Equation: Extrinsic Curvature Evolution . . . 95

C Lagrangian and Hamiltonian Formalisms **97**
C.1 The Lagrangian Formalism 97
C.2 The Hamiltonian Formalism 98

D Brief review of quantum mechanics **101**

E Numerical implementations **103**
E.1 Derivation of the Friedmann equations 103
E.1.1 Einstein Equations 103
E.1.2 Lagrangian Formalism - Equations of motion 106
E.2 Derivation of the equations of the Kinetic Dominance 108
E.3 Derivation of the 3-D Ricci Scalar for a Closed Universe 109

F Wave function for $\overline{p} = 1$ **113**

Bibliography **119**

Agradecimientos

Agradezco a la Universidad de Granada, al IMAG y a Luis Merino por permitirme realizar este máster, el cual me ha permitido complementar mi formación académica. Ha sido increíble profundizar en temas tan avanzados de matemáticas durante este año, culminando en las páginas que siguen, fruto de muchas horas de dedicación, estudio y tutorías con Rafa y Elena, sin quienes nada de esto habría sido posible. Gracias por vuestro apoyo constante, revisiones y comentarios; os estoy enormemente agradecido.

Aunque la mayor parte del máster fue online, tuve la suerte de conectar con compañeros como Javi, Gerardo, Carlos y Carmen, entre otros, con quienes compartí ordenadores, aulas, risas y horas reflexionando sobre temas complejos.

Y cómo no, mi más sincero agradecimiento a mi familia, especialmente a mi padre por su apoyo incondicional; a mis amigos Blanca, Ali, Jorge, Nanuk, Willy, Eva, Ricardo, Alba, Gea, Simona, entre muchos otros; a mis padres adoptivos Conchi y Jose; y por supuesto, a Mari Tere, mi pareja y compañera de piso, que ha sabido cuidarme en todo momento y ha estado ahí cuando más la he necesitado. Os quiero.

Con todo ello, espero que disfrutes este trabajo y que te aporte algo valioso: desde los conceptos básicos de geometría diferencial presente en los apéndices, hasta la cuantización de la Relatividad General para explorar los primeros instantes del Universo mediante una función de onda.

Resumen

El comienzo del Universo y del tiempo mismo ha sido una incógnita para el ser humano, que desde tiempos inmemoriales ha intentado buscar una solución acorde con su percepción del mundo. No fue hasta los años 20 del siglo pasado cuando Hubble demostró experimentalmente que el Universo se encuentra en expansión, observando que cuanto más lejana era una galaxia, mayor era su velocidad de alejamiento respecto a nosotros, véase la Fig. 1. Si el Universo se expande, en tiempos anteriores debió tener un menor tamaño. De hecho, en los años 60 se obtuvo la primera imagen de nuestro cosmos, asociada al momento en que la luz pudo viajar libremente (Fig. 3), descrita con un comportamiento dual onda-partícula como se muestra en la Fig. 4. Además de presentar un tamaño aparentemente menor, contiene una gran cantidad de inhomogeneidades que con el tiempo darían lugar a las presentes galaxias y estructuras cosmológicas que se conocen.

Para estudiar la expansión del espacio-tiempo, se descompusieron las ecuaciones de la relatividad general de Einstein en sus componentes espacial y temporal mediante la descomposición 3+1, Fig. 5, obteniendo un nuevo sistema de ecuaciones dependientes de: la métrica inducida sobre las hipersuperficies espaciales; y de la curvatura extrínsica asociada con la variación de un vector normal al ser transportado paralelamente, como se muestra en la Fig. 6.

Esta descomposición produce dos ecuaciones de ligadura (igualadas a cero) que pueden incluirse en el Hamiltoniano del sistema (análogo a la energía total), el cual resulta exactamente nulo. Estas ligaduras pueden cuantizarse directamente, definiendo así una función de onda cosmológica que, si 1) carece de singularidades, 2) es no negativa y 3) es de cuadrado integrable, será normalizable. La primera ligadura, llamada ligadura Hamiltoniana, corresponde a la ecuación de Wheeler-DeWitt que estudiamos en este trabajo.

El marco más sencillo para estudiar la expansión es el desarrollado por Friedmann-Lemaître-Robertson-Walker, con ecuaciones homogéneas e isótropas (Fig. 7). Estas ecuaciones permiten describir la expansión para diferentes curvaturas intrínsecas de las hipersuperficies espaciales (Fig. 2), aunque nos centraremos en el caso de curvatura cerrada (esférica).

Se acabarán obteniendo ciertas condiciones que nos limitarán el estudio al caso puramente clásico (es decir, descrito por la relatividad general sin cuantizar, sin la introducción de la mecánica cuántica), y se introducirá un campo inflatón

que describirá la deseada expansión del universo. Este campo presentará dos comportamientos posibles durante la fase de dominancia cinética (cuando la energía cinética asociada a dicho campo domina sobre la energía potencial): un carácter expansivo o contractivo como se representa en las Fig. 8 y 9, respectivamente. Si además se toma un potencial constante, aparece un comportamiento no trivial que restringe las soluciones clásicas a unas regiones representadas en verde en las Figs. 10, 11, 12 y 13, para distintas condiciones impuestas sobre los valores iniciales del factor de escala (parámetro que describe la expansión del espacio en sí) y de la inflación.

La fase de expansión descrita por la dominancia cinética podría estar seguida de una fase de deslizamiento lento, donde el inflatón varía gradualmente hasta alcanzar su valor mínimo como en la Fig. 14.

Con todo esto, se relaciona la ligadura Hamiltoniana con una de las ecuaciones del Universo clásico, y se cuantizará directamente usando como variables independientes el factor de escala y el inflatón, entrando en la descripción del régimen cuántico. Se utilizará la aproximación Wentzel-Kramers-Brillouin, un método semiclásico que proporcionará soluciones analíticas de la ecuación Wheeler-DeWitt. Este estudio se particularizará para un factor de escala que toma tanto valores muy elevados como muy pequeños (el segundo escenario se muestra en la Fig. 15), en lo que llamaremos como comportamientos asintóticos de la función de onda.

A continuación, se conectarán las soluciones clásicas con las cuánticas, mediante analogías entre variables entre ambos regímenes, y condiciones que se deben satisfacer para recuperar las soluciones clásicas. Representamos este análisis para una función más general que la clásica en las Fig. 16, 17, 18 y 19, mostrando regiones clásicamente permitidas (verde) y prohibidas (rojo). La novedad es que cuánticamente podemos representar la solución en las regiones prohibidas clásicamente mediante la función de onda, que será una función compleja. Se representarán sus partes reales e imaginarias, así como su módulo cuadrado (asociado a la densidad de probabilidad de encontrar el universo para cada valor del factor de escala), véasen las Fig. 20, 21, 22 y 23. Por último, se valorará si los comportamientos asintóticos se ajustan correctamente a las funciones de ondas recién mostradas en la Fig. 24.

Nuestro estudio muestra que la singularidad inicial (asociada a un factor de escala nulo) no aparece como tal, sino como un instante donde el cosmos tiene una probabilidad finita de comenzar. Esto garantiza que las funciones de onda estudiadas son normalizables y tienen sentido físico, al menos en el límite semiclásico. Además, se presenta un efecto de túnel cuántico en ciertas condiciones, correspondientes a regiones clásicamente prohibidas rodeadas de regiones permitidas.

Como continuación natural de este trabajo, podríamos estudiar las inho-

mogeneidades del universo temprano observadas en el fondo cósmico de microondas, Fig. 3, perturbando tanto el campo inflatón como la métrica misma, poniendo así a prueba el comienzo del tiempo y nuestros modelos teóricos.

Palabras clave: expansión del espacio-tiempo, descomposición 3+1, singularidades, ecuación de Wheeler-DeWitt, Friedmann-Lemaître-Robertson-Walker, inflatón, potencial constante, aproximación Wentzel-Kramers-Brillouin, factor de escala, función de onda, regiones clásicamente prohibidas, límite semiclásico, efecto de túnel cuántico.

Abstract

The early stages of the Universe are nowadays among the most fascinating mysteries in modern astrophysics, quantum cosmology, and theoretical physics. Although its fundamental nature and initial conditions are still unknown, several models have been proposed. In this work, we quantize Einstein's equations of general relativity to explain the first moments of the Universe, when it was sufficiently small to be described as a wave-particle in the so-called "microcosmos".

Our approach combines quantum cosmology techniques with semiclassical approximations to connect quantum gravity and classical cosmology. Our basic formalism for this quantum picture is the Wheeler-DeWitt equation.

Using the Wentzel–Kramers–Brillouin approximation, we obtain and analyze the wave function's behavior in different scenarios, comparing these semiclassical solutions with their classical counterparts. This treatment naturally avoids the initial singularity (the Big Bang), which represents a breakdown point for classical theories, instead of describing the beginning of time as an instant where the Universe emerges with a specific probability distribution.

Notably, our results display how quantum effects can cross the initial singularity while maintaining classical cosmological solutions for appropriate limits. Our examination of probability density determines preferred quantum states of the primordial Universe, and a non-null probability in the forbidden regions, enabling the quantum tunneling effect.

Throughout this study, both expanding and contracting universe solutions naturally emerge, providing a complete picture of the possible quantum cosmological scenarios. The model successfully reproduces key features of the kinetic dominance phase while maintaining consistency with standard inflationary cosmology in later stages.

Keywords: quantum cosmology, Wheeler-DeWitt equation, WKB approximation, wave function, quantum effects, kinetic dominance, inflationary cosmology.

1 Introduction

The beginning of the Universe is one of the biggest mysteries in modern physics, connecting cosmology, astrophysics, theoretical physics, and quantum field theory. But what do we know about it, and how is it related to the Wheeler-DeWitt equation that gives this dissertation its title?

From ancient times, the human race has been searching for an explanation of how the Universe began and how it works. Until 1610, when Galileo discovered moons orbiting Jupiter, Earth was believed to be the center of the Universe, with all stars, planets, and even the Sun following circular orbits around it. This discovery shifted the paradigm to heliocentrism, where the Sun became the new center, and only moons orbited planets, defended theoretically by Copernicus (1543) a century before this discovery (without much popular support). This idea didn't last long, as the entire Universe was later thought to be contained within the Milky Way -this white band visible in our night sky-, our galaxy.

In the 1920s, Edwin Hubble established and demonstrated experimentally two concepts that revolutionized our understanding of the Universe:

- Galaxies exist beyond the Milky Way (1925, Hubble's Cepheid variable observations, [1]), dramatically expanding the known size of the Universe.

- The Universe's expansion (1929, Hubble-Lemaître law) by measuring how fast distant galaxies recede from us, following a linear relationship with distance, see Fig. 1 [2, 3, 4]. The slope of this relationship, called the Hubble constant, quantifies the expansion rate [5, 6, 7].

  This idea was supported theoretically by a previous work of Georges Lemaître in 1927 [8], being the law presented by Hubble known as the Hubble-Lemaître law.

Today, we observe the expansion of spacetime itself through the Hubble constant [3], which provides direct evidence for cosmic expansion. Once this expansion was confirmed, physicists realized the Universe must have been smaller in the past. But how much smaller? Did it have a beginning?

To address this, the Friedmann-Lemaître-Robertson-Walker (FLRW) model (between 1920 and 1930) emerged as the simplest solution to Einstein's equations of General Relativity (1915), the theory describing spacetime curvature caused by mass-energy [9, 10, 11].

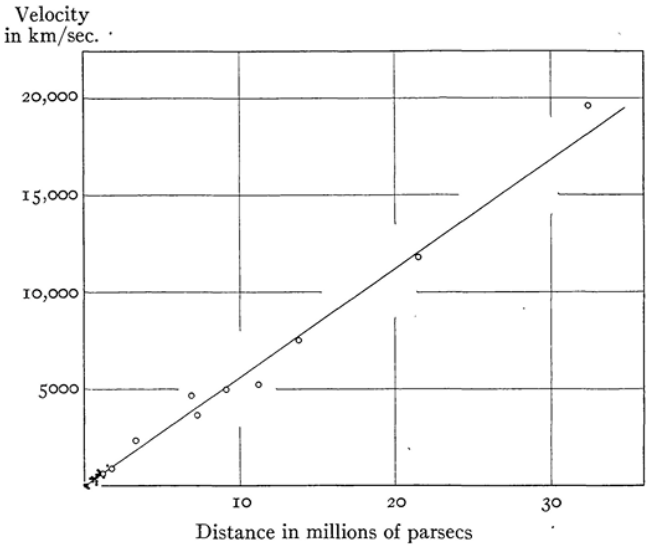

Figure 1: Recession velocities and distances of different nebulae, showing a linear correlation: the farther away a nebula is, the faster it moves away from us due to the Universe's expansion. Image extracted from [3].

The FLRW model describes three possible Universe geometries: open, closed, and flat, depending on the sign of the curvature of spatial hypersurfaces, see Fig. 2 [12, 13]. These equations link cosmic expansion to the Hubble parameter $H(t)$, analogous to the Hubble constant but time-dependent, with the scale factor $a(t)$ as the key parameter.

This model effectively describes the Universe's early stages, including inflation, a brief period of expansion where the Universe grew from subatomic to macroscopic scales at all points of spacetime (idea developed between 1981 and 1982 by Alan Guth and Andrei Linde, respectively, [14, 15]). Inflation requires coupling a scalar field to Einstein's equations, modifying the FLRW framework,

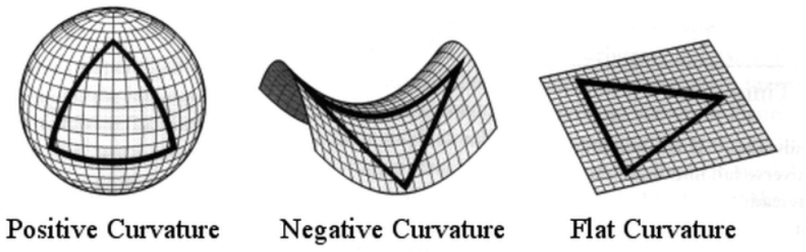

Figure 2: Possible Universe geometries based on spatial curvature. Image extracted from [13].

and which is described by a potential term. The field's potential is not unique, and various forms have been proposed.

Despite its success, how can today's Universe exhibit inhomogeneities - with vast cosmic voids and galaxy-filled filaments - while the FLRW model assumes perfect isotropy and homogeneity on large scales [16]? The resolution lies in scale. The cosmic microwave background (CMB), discovered by Penzias and Wilson (1965), reveals remarkable isotropy (no matter in which direction of the sky we observe, the CMB will always be detected) and homogeneity, with temperature fluctuations of just 10^{-6} K around 2.73 K (2018) [17, 18]). But these tiny primordial temperature variations (related with density fluctuations), see Fig. 3 [19], gave rise to all later structure formation. Through gravitational instability over billions of years, overdense regions collapsed into the galaxy clusters and filaments we observe - all while maintaining the large-scale homogeneity assumed by FLRW cosmology.

To explain these inhomogeneities produced before the CMB era, when the Universe was sufficiently small, quantum physics becomes essential. But what is quantum physics?

This field emerged from the debate between supporters of wave and corpuscular theories of light: the first argued that light behaves as waves, with Huygens being the pioneer in 1678 [20]; while the second maintained that light behaves as particles following classical trajectories, with Newton as the principal advocate in 1704 [21], see Fig. 4. However, it was not until the last century that the dual particle-wave nature of light (and all known particles) was mathematically

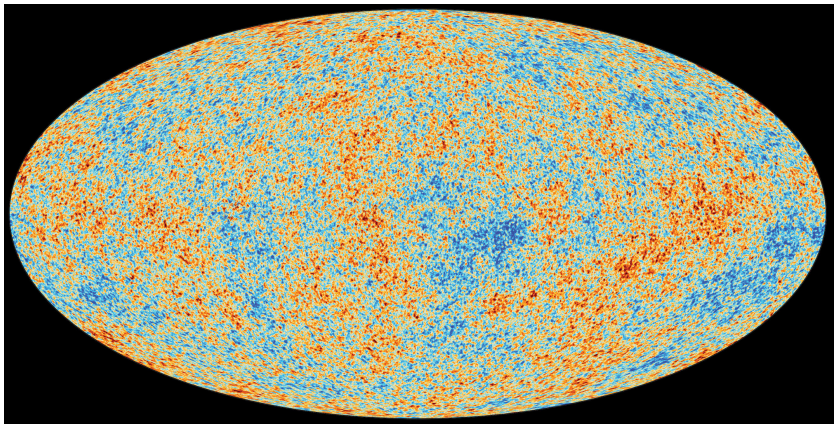

Figure 3: The CMB, the so-called oldest light in our cosmos, imprinted on the sky when the Universe was 380.000 years old, reveals temperature fluctuations that are associated to regions of slightly different densities, representing the stars and galaxies of today. Image extracted from [19].

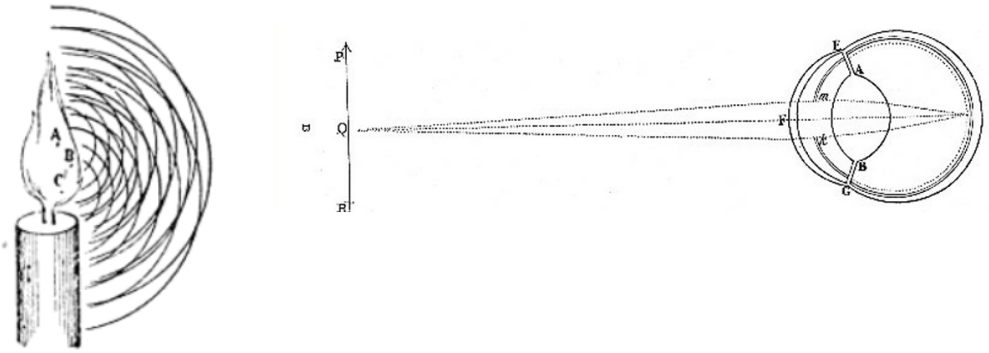

Figure 4: On the left panel, we observe a candlelight illustration with three point sources emitting light in spherical wavefronts, representing Huygens' wave theory of light [20]. The right panel shows the rectilinear light propagation from an object to the eye, exemplifying Newton's corpuscular theory [21].

established. This wave-particle duality, described by a complex wave function whose squared magnitude gives the probability of finding a particle at a specific point in spacetime, fundamentally altered our understanding of reality. Rather than being localized at a single point, particles exist across space, with their positions probability as the unique information we can extract in a flat spacetime framework (without gravity).

Once the beginning of the Universe and the foundations of quantum physics became somewhat understood, efforts began to combine the theory describing our Universe at large scales (governed by Einstein's field equations) with the theory describing the micro-universe (particles and scales far beyond our everyday experience). In 1967, DeWitt [22], starting from the 3+1 formalism of general relativity (which allows spacetime to be described as spatial hypersurfaces at each time), discovered that the total energy within a volume, excluding surface terms, was null. He recognized that the independent variable is the induced spatial metric on the hypersurface, which in the FLRW formalism corresponds to the scale factor we previously discussed in relation to the Hubble parameter. This pioneering work established the field of **quantum cosmology**, which has become essential for understanding the origin of time.

With the scale factor as an independent variable, we can obtain the Wheeler-DeWitt (WDW) equation, expressed in terms of this factor and its associated conjugate momentum, effectively achieving first quantization of the system.

This represents the simplest approach to quantizing general relativity, yielding a null quantized energy.

To account for the Universe's expansion in its earliest moments, Hartle and Hawking in 1983 [23] coupled the inflaton field to the WDW equation. This allowed the authors to describe the early stages of the Universe and its dynamical behavior, which could evolve into our current Universe with a certain probability. Thus, the state of the Universe can be described by its wave function. Naturally, the WDW equation is extremely challenging to solve. The simplest approach involves expanding the wave function as a series of progressively smaller contributions using the WKB approximation. This enables us to derive analytical expressions that provide at least an intuitive understanding of the Universe's beginning.

This wave function does not vanish at $a = 0$, implying a finite probability of the Universe appearing from nothing. Moreover, cosmological wave functions in minisuperspace models exhibit "tunneling", predicting initial states that lead to inflation [24]. Although the Universe begins nonsingularly, it will develop future singularities (black holes, big crunch). Space and time originate from the Big Bang - the state with scale factor $a = 0$ marking the Universe's beginning - making it meaningless to inquire about a "previous moment" since time itself started then [25].

The key advantage of this approximation lies in its semiclassical nature, enabling direct comparison with classical studies [26].

Thus, the objectives of our work are to:

- Decompose spacetime as a Cauchy initial value problem with a well-defined time direction, enabling us to move from one spatial hypersurfaces to the following.
- Rewrite the Einstein field equations into two equations of motion and two constraints.
- Use the scalar constraint from this reformulation to quantize general relativity and derive the general WDW equation.
- Particularize this study to classical inflation in a closed Universe (see Fig. 2) described by the FLRW equations, which naturally explains both contraction and expansion of spacetime.
- Explain inflation at the beginning of time, where the behavior is particularly complex, employing simplifications that lead to the kinetic dominance phase.

- Apply all this framework to a constant potential to identify classically allowed and forbidden regions - where only the first allows universe formation in the classical approximation.
- Quantize the FLRW equations using the scale factor and inflaton field as independent system variables.
- Implement the WKB approximation to obtain the Universe's wave function for the constant-potential case, characterizing both classically allowed and forbidden regions while recovering classical solutions in this same limit.

This work is organised as follows: In Section 2, we theoretically introduce the decomposition of spacetime into spatial hypersurfaces labeled by time, deriving a new set of equations equivalent to the Einstein field equations, and obtaining the most general form of the WDW equation. In Section 3, we derive the Friedmann equations from the FLRW model to describe a closed universe, where we obtain and discuss both inflation and kinetic dominance phases. In Section 4, we quantize the Friedmann equations and apply the WKB approximation to derive the general expression for the early-Universe wave function. In Section 5, we particularize this study to a constant potential case, demonstrating how classical universe solutions emerge from the quantum description. Finally, for readers with advanced mathematical background, we recommend first reviewing Appendix A.

2 ADM Equations

2.1 Principles of General Relativity

General relativity describes the gravitational force and its relationship with spacetime curvature. The theory is based on three fundamental principles [27, 28, 29]:

- Spacetime can be described as a curved, four-dimensional pseudo-Riemannian manifold:

  Definition 2.1 *A **Lorentzian metric** on a $(d+1)$-dimensional manifold has signature $(1,d)$ on each tangent space T_pM, with one negative and d positive eigenvalues. They are also known as **pseudo-Riemannian metrics**, where the negative eigenvalue is associated with the time coordinate. A **Lorentzian or pseudo-Riemannian manifold** is a differentiable manifold with such a metric.*

  For more details, see Appendix A and Definition A.10.

- At every point in spacetime, we can construct a locally inertial frame where the nongravitational laws of physics are indistinguishable from those of special relativity (laws of physics are identical in all systems moving at constant velocity relative to each other).

- The density and flux of nongravitational energy and momentum curve spacetime according to Einstein's field equations.

The equations that governs how spacetime curves and describes its energy-momentum content, relating both, is famously known as Einstein's field equations for gravity, expressed as [30]:

$$G_{\mu\nu} = R_{\mu\nu} - \frac{1}{2}g_{\mu\nu}R + \Lambda g_{\mu\nu} = \frac{8\pi G}{c^4}T_{\mu\nu}, \tag{2.1}$$

where $R_{\mu\nu}$ is the Ricci tensor, R the Ricci scalar, Λ the cosmological constant, G the gravitational constant, c the speed of light, $T_{\mu\nu}$ the stress-energy tensor, and $G_{\mu\nu}$ the Einstein Tensor.

These equations form the basis of general relativity, illustrating the relationship between the geometry of spacetime (encoded in $G_{\mu\nu}$) and the distribution of matter and energy within it (encoded in $T_{\mu\nu}$). They show how the stress-energy tensor generates curvature in its neighborhood, governs the propagation of spacetime ripples (gravitational waves), and determines the external spacetime of static sources, among other phenomena.

The stress-energy tensor encodes complete information about the energy density, momentum density, and stress as measured by all possible observers at a given event.

From this point onward, we will adopt the geometrized unit system, where we set $G = c = 1$. We will only explicitly mention these constants when necessary.

2.2 3+1 Formalism

Equations (2.1) are presented in a manifestly covariant form, treating space and time as equal entities. However, this approach can pose challenges when we try to understand the evolution of the universe from the Big Bang to the present day.

Several mathematical approaches have been developed to decompose Einstein's equations for the purpose of establishing well-posed initial data and subsequently evolving the gravitational field [31, 32, 33, 34]. Among these, the *3+1 formalism* has emerged as particularly powerful, providing a rigorous framework that separates the four-dimensional spacetime into a foliation of three-dimensional spatial hypersurfaces parametrized by a time coordinate.

Our spacetime will describe a topologically manifold $M = \Sigma_t \times \mathscr{R}$, where Σ_t is a three-dimensional spacelike hypersurface, and $\mathscr{R}$ is related with the cosmic time.

In Appendix A, we present the mathematical framework necessary for a comprehensive understanding of the theoretical basis of our work. This framework serves as a foundation for the concepts discussed in the main text, ensuring that readers have the requisite knowledge to fully engage with our findings and analyses.

2.2.1 The 3+1 Decomposition of Spacetime

The 3+1 formalism offers a rigorous reformulation of Einstein's equations as a Cauchy initial value problem. This means that, given appropriate initial conditions on a spacelike hypersurface and suitable boundary conditions, the fundamental equations uniquely determine the future (or past) state of the system. What distinguishes this formalism is its ability to clearly distinguish between spatial and temporal components, enabling the analysis of the temporal

evolution of physical systems within the framework of general relativity. This approach is particularly valuable for studying dynamic processes, such as the evolution of the universe or the behavior of compact objects like black holes and neutron stars, and serves as the foundation for modern numerical relativity [35, 36, 37, 38, 39].

Consider a spacetime $(M, g_{\mu\nu})$ with Lorentzian metric $g_{\mu\nu}$, with M a manifold of class C^∞. We restrict our attention to globally hyperbolic spacetimes that possess Cauchy surfaces - a necessary condition for well-posed evolution (see Definition A.27 for more details).

Using the following theorem:

Theorem 2.1 *Let (M, g_{ab}) be a globally hyperbolic spacetime that is stably causal. Then, a global time function f can be chosen such that each surface of constant f is a Cauchy surface. Consequently, M can be foliated by Cauchy surfaces, and the spacetime topology becomes $\Sigma \times \mathbb{R}$, where Σ denotes any Cauchy surface.*

(see Theorem A.6 for more details), we can foliate $(M, g_{\mu\nu})$ by Cauchy surfaces Σ_t (three-dimensional C^∞ spatial manifolds) parameterized by a global time function t. Let n^a be the unit normal vector field to the hypersurfaces Σ_t. The spacetime metric $g_{\mu\nu}$ induces a spatial metric $\gamma_{\mu\nu}$ on each Σ_t:

$$\gamma_{\mu\nu} = g_{\mu\nu} + n_\mu n_\nu, \tag{2.2}$$

such that the spatial metric acts as a projection operator onto the hypersurfaces. $\gamma_{\alpha\beta}$ is a defined positive symmetric metric, and because all of its eigenvalues are positive, on the spatial hypersurfaces this metric will be a Riemannian one (see Definition A.8).

Let's consider a vector field t^μ on M satisfying $t^\mu \nabla_\mu t = 1$, representing the flow of time. This can be decomposed into normal and tangential components relative to Σ_t, via the definitions of the **lapse function** α and the **shift vector** β^i:

$$\alpha = -t^\mu n_\mu = (n^\mu \nabla_\mu t)^{-1} = (-\nabla t \cdot \nabla t)^{-1/2}, \tag{2.3}$$

$$\beta_\mu = \gamma_{\mu\nu} t^\nu. \tag{2.4}$$

That is, we can combine n^μ (normal component) and $\beta^\mu = g^{\mu\nu}\beta_\nu$ (tangential component) to obtain an expression of the time vector:

$$t^\mu \equiv \alpha n^\mu + \beta^\mu. \tag{2.5}$$

From (2.3), α measures the magnitude of the gradient of the time coordinate function. The unit normal vector can alternatively be expressed as $n^\mu = -\alpha \nabla^\mu t$, with the negative sign ensuring that it is future-directed.

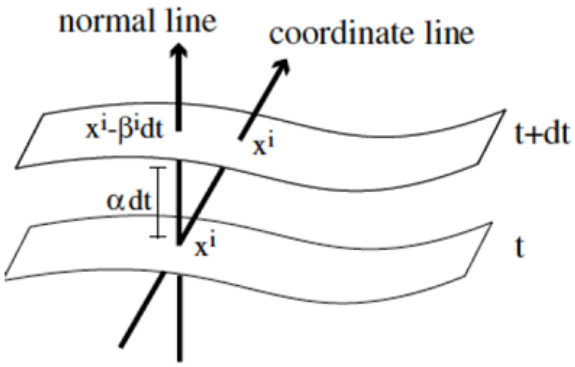

Figure 5: Adjacent spatial hypersurfaces illustrating the geometric interpretation of the lapse function α and shift vector β^i. Image extracted from [37].

The shift vector can also be defined through three scalar functions β^i such that the change in spatial coordinates when moving from one hypersurface to the next along the normal direction satisfies:

$$x^i_{t+dt} = x^i_t - \beta^i dt. \tag{2.6}$$

These scalars form a 4-vector with adapted components $\beta^\mu = (0, \beta^i)$, which is orthogonal to n^μ, $n^\mu \beta_\mu = 0$.

Examining a specific foliation with adjacent hypersurfaces Σ_t and Σ_{t+dt}, see Fig. 5, the intervening spacetime geometry is completely determined by:

1. The 3-metric γ_{ij} $(i, j = 1,2,3)$ which measures proper distances within the hypersurface:
$$dl^2 = \gamma_{ij} dx^i dx^j. \tag{2.7}$$

2. The proper time lapse $d\tau$ between hypersurfaces for observers moving normal to them (Eulerian observers):
$$d\tau^2 = \alpha^2(t, x^i) dt^2. \tag{2.8}$$
Here α, the lapse function, encodes the relationship between coordinate time and proper time.

3. And the shift vector β^i, that is also seen as the relative velocity between Eulerian observers and lines of constant spatial coordinates via (2.6).

The foliation and coordinate propagation between hypersurfaces are highly non-unique. Consequently, the lapse function α and shift vector β^i represent

gauge freedom in the theory, encoding our choice of coordinate system and time slicing.

In terms of $\{\alpha, \beta^i, \gamma_{ij}\}$, the spacetime metric takes the Arnowitt-Deser-Misner (ADM) form [40]:

$$ds^2 = g_{\mu\nu}dx^\mu dx^\nu = (-\alpha^2 + \beta_i\beta^i)dt^2 + 2\beta_i dt dx^i + \gamma_{ij}dx^i dx^j, \tag{2.9}$$

which represents the complete 3+1 metric decomposition. From this point forward, we will utilize the Greek alphabet to denote four-dimensional objects, while the standard alphabet will be reserved for three-dimensional ones.

Explicitly in matrix form:

$$g_{\mu\nu} = \begin{pmatrix} -\alpha^2 + \beta_k\beta^k & \beta_i \\ \beta_j & \gamma_{ij} \end{pmatrix}, \tag{2.10}$$

$$g^{\mu\nu} = \begin{pmatrix} -1/\alpha^2 & \beta^i/\alpha^2 \\ \beta^j/\alpha^2 & \gamma^{ij} - \beta^i\beta^j/\alpha^2 \end{pmatrix}. \tag{2.11}$$

The 4D volume element in this decomposition becomes:

$$\sqrt{-g} = \alpha\sqrt{\gamma}, \tag{2.12}$$

where g and γ denote the determinants of $g_{\mu\nu}$ and γ_{ij} respectively.

The unit normal vector n^μ to the spatial hypersurfaces has components:

$$n^\mu = (1/\alpha, -\beta^i/\alpha), \quad n_\mu = (-\alpha, 0). \tag{2.13}$$

This vector field represents the 4-velocity of Eulerian observers and satisfies:

$$n^\mu n_\mu = -1. \tag{2.14}$$

Consequently, the worldlines of Eulerian observers are orthogonal to Σ_t, meaning that Σ_t locally comprises events that are simultaneous from their perspective under Einstein's simultaneity convention.

2.2.2 Extrinsic Curvature

In the context of foliated spacetime, we must carefully distinguish between two fundamental geometric quantities: intrinsic curvature, which characterizes the geometry of the hypersurfaces themselves, and extrinsic curvature, which encodes how these hypersurfaces are embedded within the four-dimensional spacetime manifold.

The intrinsic curvature is fully described by the 3D Riemann tensor constructed from the spatial metric γ_{ij}, capturing the hypersurface's internal

geometric properties. In contrast, the extrinsic curvature tensor $K_{\alpha\beta}$ quantifies how the normal vector $\vec{n}$ varies under parallel transport along the hypersurface, thereby measuring how the hypersurface is curved within the spacetime that encompasses it, see Fig. 6.

To rigorously define the extrinsic curvature, we first introduce the spatial projection operator:

$$P^{\alpha}{}_{\beta} \equiv \delta^{\alpha}{}_{\beta} + n^{\alpha} n_{\beta}, \tag{2.15}$$

which is mathematically equivalent to the induced spatial metric ($P_{\alpha\beta} = \gamma_{\alpha\beta}$). The extrinsic curvature tensor is then given by:

$$K_{\mu\nu} \equiv -P^{\alpha}{}_{\mu} \nabla_{\alpha} n_{\nu} = -(\nabla_{\mu} n_{\nu} + n_{\mu} n^{\alpha} \nabla_{\alpha} n_{\nu}). \tag{2.16}$$

The purely spatial nature of $K_{\mu\nu}$ becomes evident through the orthogonality condition:

$$n^{\mu} K_{\mu\nu} = -(n^{\mu} \nabla_{\mu} n_{\nu} + n^{\mu} n_{\mu} n^{\alpha} \nabla_{\alpha} n_{\nu}) = -(n^{\mu} \nabla_{\mu} n_{\nu} + (-1) n^{\alpha} \nabla_{\alpha} n_{\nu}) = 0, \tag{2.17}$$

where we have employed Einstein summation and the normalization condition $n^{\mu} n_{\mu} = -1$. This implies that in adapted coordinates, the components $K^{00} = K^{0i} = 0$ vanish identically (though K_{00} and K_{0i} may be non-zero in general). Therefore, we typically focus only on the spatial components K_{ij}.

An important symmetry property of the extrinsic curvature is:

$$K_{\mu\nu} = K_{\nu\mu}, \tag{2.18}$$

demonstrating its tensor nature. Remarkably, $K_{\mu\nu}$ can alternatively be expressed as the Lie derivative of the spatial metric along the normal direction:

$$K_{\mu\nu} = -\frac{1}{2} \mathcal{L}_{\vec{n}} \gamma_{\mu\nu}. \tag{2.19}$$

This has been demonstrated in Appendix B.1, proving that the extrinsic curvature encodes the variation of the unit normal vector across the spatial hypersurfaces.

2.2.3 Energy-Momentum Tensor Decomposition

The decomposition of the energy-momentum tensor follows an analogous pattern to our geometric spacetime decomposition. We express $T_{\alpha\beta}$ in terms of quantities defined on the spatial hypersurfaces:

$$T_{\alpha\beta} = \rho n_{\alpha} n_{\beta} + j_{\alpha} n_{\beta} + j_{\beta} n_{\alpha} + S_{\alpha\beta} \tag{2.20}$$

where the components are defined as:

$$\rho \equiv n^{\alpha} n^{\beta} T_{\alpha\beta}, \tag{2.21}$$

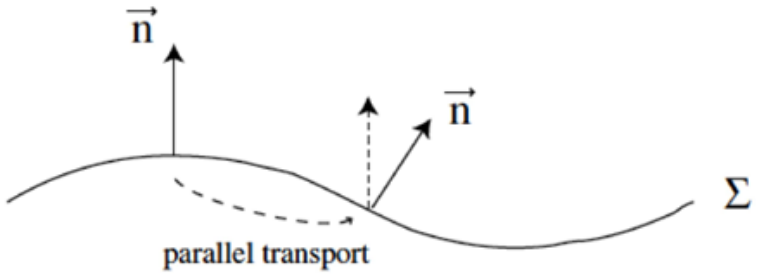

Figure 6: Visualization of the geometric interpretation of the extrinsic curvature tensor, showing how it measures the variation of the normal vector under parallel transport. Image extracted from [37].

$$j_\alpha \equiv -n^\beta \gamma^\mu{}_\alpha T_{\beta\mu}, \tag{2.22}$$

$$S_{\alpha\beta} = \gamma^\mu{}_\alpha \gamma^\nu{}_\beta T_{\mu\nu}. \tag{2.23}$$

Here, ρ represents the energy density as measured by Eulerian observers, j_α is the momentum density, and $S_{\alpha\beta}$ is the spatial stress tensor. This decomposition completes our mathematical framework for reformulating Einstein's equations as a Cauchy problem, which we will show comprises four key equations: two evolution equations and two constraint equations.

2.3 ADM Equations Summary

Following all the calculus done in Appendix B, we derive the following four equations that constitute the complete ADM system [35, 37, 41, 42, 40, 43], fully equivalent to Einstein's equations but within the 3+1 formalism:

$$\partial_t \gamma_{ij} = -2\alpha K_{ij} + D_i\beta_j + D_j\beta_i, \tag{2.24}$$

$$\begin{aligned}\partial_t K_{ij} = {} & \beta^k \partial_k K_{ij} + K_{ki}\partial_j\beta^k + K_{kj}\partial_i\beta^k - D_i D_j \alpha \\ & + \alpha\left[R_{ij} + KK_{ij} - 2K_{ik}K_j{}^k\right] + 4\pi\alpha[\gamma_{ij}(S-\rho) - 2S_{ij}],\end{aligned} \tag{2.25}$$

$$H^0 = R + K^2 - K_{ij}K^{ij} - 16\pi\rho - 2\Lambda = 0, \tag{2.26}$$

$$H^i = D_j(K^{ij} - \gamma^{ij}K) - 8\pi j^i = 0. \tag{2.27}$$

The first equation, (2.24), provides the time evolution of the spatial metric. The second equation, (2.25), describes the time evolution of the extrinsic curvature. The third equation, (2.26), represents a constraint that must be

satisfied at all times, governing energy conservation within our spacetime foliation; for this reason, we refer to it as H^0, or the Hamiltonian constraint. Lastly, the fourth equation, (2.27), consists of three constraint equations that regulate momentum conservation in our foliation, ensuring the consistency of our physical model, refered as H^i, or the momentum constraint.

The constraints possess two notable properties: they are time-independent and gauge-invariant, encoding fundamental relationships between hypersurface geometries. The Hamiltonian and momentum constraints represent four of Einstein's ten equations, leaving six for gravitational evolution.

These 6+6+1+3 equations constitute the ADM formulation. In numerical implementations, typically only the evolution equations are solved directly, with the constraints serving as accuracy checks. While the constraints remain satisfied analytically, discrete numerical implementations inevitably accumulate constraint-violating errors.

The gauge quantities α (lapse) and β^i (shift) lack evolution equations—they embody coordinate freedom and must be specified independently through gauge conditions, as we said before.

2.4 Wheeler-DeWitt Equation

2.4.1 Lagrangian Density and Hamiltonian

Once we have derived the equations that describe our spacetime as a Cauchy problem, we will translate it into the Lagrangian and Hamiltonian formalism to explore whether we can uncover any relationships. Our goal is to ultimately obtain the expression for the total energy of the system.

As is done in classical mechanics, the Hamiltonian density $\mathscr{H}$ arises from the Legendre transform of the Lagrangian density $\mathscr{L}$, with Π as the dual variables [44]:

$$\mathscr{H} := \sum_q \Pi \dot{q} - \mathscr{L}. \tag{2.28}$$

This means that we need the Lagrangian formulation of the system in order to derive its Hamiltonian formulation.

In physics, it is common to describe systems using the action S, which is formally defined from a Lagrangian $L = L(q^a(t), \dot{q}^a(t), t)$. The Lagrangian is a function that depends on the generalized coordinates $q^a(t)$, their temporal derivatives $dq^a(t)/dt := \dot{q}^a(t)$ and time t, such that: $S = \int_M L\sqrt{-g}\, d^4x$ [45]. In our case, the Einstein-Hilbert action is the one that describes our physical problem [46] (we could use it to derive equation (2.1) in the absence of energy-

matter, $T_{\mu\nu} = 0$, using the principle of least action, $\delta S = 0$):

$$S_{EH} = \frac{1}{16\pi}\int_M \left({}^{(4)}R - 2\Lambda\right)\sqrt{-g}\; d^4x = \int_M \mathscr{L}\; d^4x, \tag{2.29}$$

where M represents the spacetime manifold and $\mathscr{L} = L\sqrt{-g}$ the Lagrangian density. We can derive a more useful expression of the Lagrangian density (volume term), see Appendix C for details of the derivation, given by:

$$\mathscr{L}_0 = \frac{1}{16\pi}\left[\alpha\sqrt{\gamma}\,(R - 2\Lambda) + \frac{\alpha}{\sqrt{\gamma}}\left(\Pi^{ij}\Pi_{ij} - \frac{1}{2}\Pi^2\right)\right], \tag{2.30}$$

where Π^{ij} is the canonical momenta density associated to the variable γ_{ij},

$$\Pi^{ij} = \frac{\partial\mathscr{L}_0}{\partial\dot{\gamma}_{ij}} = \frac{\sqrt{\gamma}}{16\pi}\left(\gamma^{ij}K - K^{ij}\right). \tag{2.31}$$

The Hamiltonian (volume term) of the system, using (2.28),is:

$$H_\Sigma = \frac{1}{16\pi}\int_{\Sigma_t}\left[-2(D_i\Pi^{ij})\beta_j - \alpha\sqrt{\gamma}\,(R - 2\Lambda) + \frac{\alpha}{\sqrt{\gamma}}\left(\Pi_{ij}\Pi^{ij} - \frac{\Pi^2}{2}\right)\right]\mathrm{d}^3x. \tag{2.32}$$

Here, D_α projects all indices of the 4D derivative ∇_α onto Σ_t such that $D_i\Pi^{ij} = \gamma^k{}_i\gamma^i{}_m\gamma^j{}_n\nabla_k\Pi^{mn}$. This Hamiltonian is the total energy of the system (except for the boundary terms which may include non-trivial contributions, but their study its out of the scope of this thesis), which can be rewritten in terms of the ADM equations.

2.4.2 Lagrange Multipliers

Once we have the Hamiltonian (2.32), let us finally rewrite it in terms of the constrains (2.26) and (2.27).

The Hamiltonian constraint (2.26) can be rewritten in the absence of sources, using (C.11) and (C.14), as:

$$\overline{H}^0 = \sqrt{\gamma}H^0 = -\sqrt{\gamma}(R - 2\Lambda) + \frac{1}{\sqrt{\gamma}}\left(\Pi_{ij}\Pi^{ij} - \frac{\Pi^2}{2}\right) = 0. \tag{2.33}$$

Analogously, using (C.10), (2.27) is given by:

$$\overline{H}^i = H^i/\sqrt{\gamma} = -2D_j\Pi^{ij} = 0. \tag{2.34}$$

Thus the Hamiltonian (2.32) vanishes identically:

$$H_\Sigma = \int_{\Sigma_t}\{\alpha\overline{H}^o + \beta_i\overline{H}^i\}\,d^3x = \int_{\Sigma_t}\beta_\mu\overline{H}^\mu d^3x = 0, \tag{2.35}$$

with $\beta_0 = \alpha$, $\overline{H}^0 = \sqrt{\gamma}H^0$ and $\overline{H}^i = H^i/\sqrt{\gamma}$. That is, written in this way, its clear that α and β_i are Lagrange multipliers of the problem, and indeed do not describe any physical variable [47]. The constraints (2.26) and (2.27) are essential to describe our system with null energy (except for the boundary terms).

This constrained structure leads naturally to quantum gravity via (2.26). Let us see how.

2.4.3 Quantizing General Relativity

Knowing that our canonical variables are γ_{ij} and Π^{ij}, we can promote them to the quantum domain. This quantisation can be done when its being described as a microsystem. In our case, with our equations we are trying to describe the whole universe, so its associated microuniverse will be when the universe was little enough to describe it as it. This condition is given at the first instances of the universe, just after the Big Bang (physical singularity at the beggining of the universe) where the Universe expanded in a huge way in a fraction of a second [48].

First, we need the Poisson brackets derived from Hamiltonian mechanics [49]. For our canonical variables of our system, γ_{ij} and Π^{ij}, it can be defined two differentiable functions in the phase space ($\Gamma = \{(\gamma_{ij}, \Pi^{ij}) / \gamma_{ij}\}$ is positive defined, soft and symmetric, and Π^{ij} is symmetric and of kind (2,0) over our hypersurface), f and g such that:

$$\{f, g\} := \frac{\delta f}{\delta \gamma_{ij}} \frac{\delta g}{\delta \Pi^{ij}} - \frac{\delta f}{\delta \Pi^{ij}} \frac{\delta g}{\delta \gamma_{ij}}. \tag{2.36}$$

This definition of the Poisson bracket satisfy, for three functions f, g and h of our phase space, the Leibniz's rule,

$$\{fg, h\} = f\{g, h\} + \{f, h\}g, \tag{2.37}$$

and the Jacobi identity,

$$\{f, \{g, h\}\} + \{g, \{h, f\}\} + \{h, \{f, g\}\} = 0. \tag{2.38}$$

Then, we can calculate the different Poisson brackets among the canonical variables of the system, knowing that γ_{ij} and Π^{ij} are independent variables between them:

$$\{\gamma_{ij}, \gamma_{kl}\} = 0, \tag{2.39}$$

$$\{\Pi^{ij}, \Pi^{kl}\} = 0, \tag{2.40}$$

$$\{\gamma_{ij}, \Pi^{kl}\} = \frac{\delta \gamma_{ij}}{\delta \gamma_{pn}} \frac{\delta \Pi^{kl}}{\delta \Pi^{pn}} - 0 = \delta_i{}^p \delta_j{}^n \delta_p{}^k \delta_n{}^l = \delta_i{}^k \delta_j{}^l. \tag{2.41}$$

And the quantisation of this Hamiltonian system is straight forward mathematical by promoting the canonical variables into their corresponding quantum operator, $\hat{\gamma}_{ij}$ and $\hat{\Pi}^{ij}$, satisfying now the following conmutation relation:

$$[\hat{\gamma}_{mj}, \hat{\Pi}^{kl}] = i\hbar\delta_m{}^k\delta_j{}^l, \tag{2.42}$$

in total analogy to what we have explained in the Appendix D, where $\hbar$ is the reduced Planck constant that typically appears in quantum contexts. Introducing a wave functional $\Psi[\gamma_{ij}]$ defined on the space of field configurations γ_{ij} [50], the operators act over it as:

$$\hat{\gamma}_{ij}\Psi[\gamma_{ij}] = \gamma_{ij}\Psi[\gamma_{ij}], \tag{2.43}$$

$$\hat{\Pi}^{kl}\Psi[\gamma_{mj}] = -i\hbar\frac{\delta}{\delta_{kl}}\Psi[\gamma_{mj}]. \tag{2.44}$$

At the quantum level, constraint equations (2.26) and (2.27) becomes in the momentum representation $\hat{\Pi}^{kl}$ in:

$$\hat{H}^0\Psi[\gamma_{kl}] = \left[-\sqrt{\gamma}\,(R-2\Lambda) - \frac{\hbar^2}{\sqrt{\gamma}}\left(\frac{1}{2}\gamma_{ab}\gamma_{cd} - \gamma_{ac}\gamma_{bd}\right)\frac{\delta}{\delta\gamma_{ab}}\frac{\delta}{\delta\gamma_{cd}}\right]\Psi[\gamma_{kl}] = 0, \tag{2.45}$$

$$\hat{H}^m\Psi[\gamma_{kl}] = 2i\hbar D_j\frac{\delta}{\delta_{mj}}\Psi[\gamma_{kl}] = 0. \tag{2.46}$$

This two equations are known as the Wheeler-DeWitt equations, such that (2.45) will be the Wheeler-DeWitt equation that will be studied in this work in depth, and (2.46) is called the quantum diffeomorphism equation. The physical states $\Psi[\gamma_{kl}]$ are solutions to the Wheeler-DeWitt equation (2.45) and span a Hilbert space $\mathscr{H}_S$ [51]. The inner product in this space, analogous to the Schrödinger inner product, is given by [50, 22]:

$$\langle\Psi_1|\Psi_2\rangle = \int_{\mathrm{Riem}(\Sigma)}\Psi_1^*[\gamma_{ij}]\Psi_2[\gamma_{ij}]\mathscr{D}\gamma_{ij}, \tag{2.47}$$

where $\mathrm{Riem}(\Sigma_t)$ denotes the space of all Riemannian metrics γ_{ij} defined on the spatial hypersurface Σ_t. This inner-product can be defined in several ways, depending on the theory used such as loop quantum gravity, quantum field theory, string theory... (see [52, 53, 54] for more details).

The Hilbert space associated is $\mathscr{H}_S := L^2(\mathrm{Riem}(\Sigma), \mathbb{C})$, and the normalization condition is:

$$\int_{\mathrm{Riem}(\Sigma)}|\Psi[\gamma_{ij}]|^2\mathscr{D}\gamma_{ij} = 1. \tag{2.48}$$

The Wheeler-DeWitt equation has a strong interest because its one of the paths to quantum gravity: one theory which is able to merge general relativity

and quantum field theory. However, this approach faces several problems: why only appears the three-metric, and where is the time coordinate? Is it quantum gravity timeless? How can we describe correctly this quantum universe? [55].

Equation (2.45) may seem timeless at first sight, with an absence of a traditional time variable as it may appear in the Schrodinger equation, $\hat{H}\Psi[\gamma_{kl}] = i\hbar\partial_t\Psi[\gamma_{kl}]$. But the time evolution is encoded in the changes of the wave function $\Psi[\gamma_{kl}]$, which depends on configuration space variables, and describing then a dynamical evolution [56, 57].

As we will see in the following sections, this equations may be adequate for calculating and studying the wave function of the quantum universe in the semiclassical regime, where the Wentzel-Kramers-Brillouin (WKB) approach will take a crucial part.

3 Classical Inflation

3.1 General Friedmann Equations

It is usual to study cosmology with the Friedmann-Lemaitre-Robertson-Walker (FLRW) line element, which fits with the cosmological principle. This one states that there is no priviliged position in the Universe, and it is spatially homogeneus and isotropic [58]. More precisely (see [59, 60] for further details):

- The manifold is spatially homogeneous if for any time t and for any pair of points (P,Q) of the hypersurfaces Σ_t, there exists an isometry of M taking P into Q. See the left image of Fig. 7.
- And it is spatially isotropic if at any point P and for any pairs of unit spatial tangent vectors $e_1^\mu, e_2^\mu \in T_pM$ (T_pM is the tangent space to M at $p \in M$, i.e., is the space of equivalence classes of curves through p, for more details see Definition A.7), there exists an isometry that leaves P and the tangent vector at that point, $u^\mu \in T_pM$, fixed and that rotates the vectors e_1^μ into e_2^μ. See the right picture of Fig. 7.

This means physically that we observe approximately the same density in any

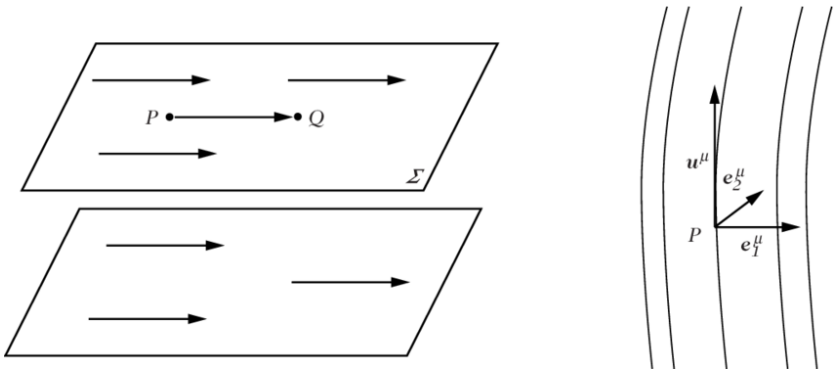

Figure 7: Visualization of (left): for an homogeneous space, how a manifold can be foliated by a family of Σ_t in which there is an isometry that takes the point P into Q; and (right): for an isotropic space, there is an isometry that rotates any unit spatial tangent vector e_1^μ to any other e_2^μ, while the tangent vector u^μ remains invariant. Image extracted from [59].

direction we observe the Universe, and this statement holds true for any point in spacetime. The best way to incorporate this into the metric or line element is by imposing spherical symmetry (i.e., that all geodesics lie along the axis of rotation, ensuring that their points remain invariant under a rotation of the coordinate system) [29].

In (t, r, θ, φ) coordinates, the FLRW line element is given by [61]:

$$\begin{aligned} ds^2 &= -\alpha(t)^2 dt^2 + a^2(t)\left(\frac{dr^2}{1-Qr^2} + r^2(d\theta^2 + \sin^2\theta^2\, d\varphi^2)\right) \\ &= -\alpha(t)^2 dt^2 + a^2(t)\overline{g}_{ij} dx^i dx^j. \end{aligned} \tag{3.1}$$

In equation (3.1) we have the scale factor, $a(t)$; the spatial curvature of the three-space, Q, normalized to $Q = +1$ (closed Friedmann model), $Q = -1$ (open Friedmann model), and $Q = 0$ (Einstein de-Sitter static model); $\overline{g}_{ij}$ is the metric of the spatial slices of constant curvature (in total analogy with the spatial metric γ_{ij}).

In this line element is encoded via $a(t)$ the Hubble parameter that describes how the universe expand, such that $a \to 0$ describes a microuniverse and $a \to \infty$ an infinite one. Thus, $a(t)$ provides a measure of the universe's relative size.

At cosmological level, there are several questions that arise naturally when we look into the sky [42]:

1. Why the universe is almost flat? (It is thought that it has a curvature $Q \approx 0$).

2. How is possible that the cosmic microwave background is so homogeneus? That is, the first 'picture' of the universe we have it is so homogeneus and isotropic. And also nowadays the density is very homogeneous and isotropic (for that reason we imposed spherical symmetry in equation (3.1)).

3. Why are we made of particles and not antiparticles?

Two of these problems can be handled in such an elegant way by introducing a spatially homogeneous scalar field that here will be called *inflaton*, $\phi(t) : M \to \mathbb{R}$, that is a soft function. Now, our manifold M is the spacetime described by the FLRW metric.

To solve the first two problems exposed, it would be needed (one of the solutions among others) that our scale factor a would behave exponentially $a(t) \sim e^{t/R_0}$, with $R_0 = \sqrt{3/(8\pi G\Lambda)}$, for a fraction of a second, just after 10^{-35} seconds following the Big Bang [62], until 10^{-32} seconds. Then, during this process called *inflation*, every part of the universe would inflate from microscopic ($\ell_{\text{Pl}} \sim 10^{-35}$ m) to Hubble scale ($H^{-1} \approx 10^{26}$ m actually). With

this expansion, the universe would be really flat and it would explain why it is homogeneus and isotropic: before inflation, the whole universe was causally-connected (inside the light cones, see Fig. 26), but after it, some regions of it would be no longer connected (spacelike vectors, see Definition A.10).

The third problem is beyond the scope of this thesis, but there are several works that test it, see for example [63, 64].

Then, let us consider the Einstein-Hilbert action minimally coupled to a scalar field described by a potential $V(\phi)$ [36]:

$$S = \int_M \sqrt{-g}\left(\frac{R-2\Lambda}{16\pi} - \frac{1}{2}g^{\mu\nu}\partial_\mu\phi\partial_\nu\phi - V(\phi)\right)d^4x = \int_M \mathscr{L}(\phi,\dot{\phi},a,\dot{a},\alpha,\dot{\alpha},t)d^4x. \tag{3.2}$$

With this two expressions, (3.1) and (3.2), we can obtain and describe all the dynamics of the universe. For that, we will calculate the Einstein equations, and the equations of motions.

Thanks to the metric in the (t,r,θ,φ) coordinates:

$$g_{\mu\nu} = \begin{pmatrix} -\alpha(t)^2 & 0 & 0 & 0 \\ 0 & a^2(t)\frac{1}{1-Qr^2} & 0 & 0 \\ 0 & 0 & a^2(t)r^2 & 0 \\ 0 & 0 & 0 & a^2(t)r^2\sin^2\theta^2 \end{pmatrix}, \tag{3.3}$$

and to the Levi-Civita connection ($\Gamma^\mu{}_{\nu\alpha} = \Gamma^\mu{}_{\alpha\nu}$ and $\nabla_\alpha g_{\mu\nu} = 0$, see Theorem A.3), we have the neccesary to calculate the curvature part of the Einstein field equations (2.1), i.e., $G_{\mu\nu} = R_{\mu\nu} - \frac{1}{2}g_{\mu\nu} + \Lambda g_{\mu\nu}$.

On the other hand, considering our action minimally coupled to the scalar field that we called inflaton, the energy-momentum tensor is given by:

$$T_{\mu\nu} = \partial_\mu\phi\partial_\nu\phi - g_{\mu\nu}\left(\frac{1}{2}g^{\rho\sigma}\partial_\rho\phi\partial_\sigma\phi + V(\phi)\right). \tag{3.4}$$

Now, we have all the ingredients to calculate the different components of the Einstein equations. We performed these calculations in Python (as they involve extensive computations just to derive two equations). The code can be found in Appendix E.1.1. For simplicity, $db(t)/dt = \dot{b}(t)$, notation that will be used from now on only for time derivatives.

Only two independent components emerged: $G_{00} - 8\pi T_{00} = 0$, given by:

$$\boxed{\left(\frac{\dot{a}}{a}\right)^2 = \frac{8\pi}{3}\left(V\big(\phi(t)\big)\cdot\alpha^2(t) + \frac{1}{2}\dot{\phi}^2\right) + \frac{\Lambda}{3}\alpha^2 - \frac{Q}{a^2}\alpha^2}, \tag{3.5}$$

and $G_{ii} - 8\pi T_{ii} = 0$, for example $i = 1$,

$$\boxed{\alpha\left(\frac{\ddot{a}}{a} + \frac{1}{2}\left(\frac{\dot{a}}{a}\right)^2\right) = \dot{\alpha}\frac{\dot{a}}{a} - 4\pi\left(\frac{1}{2}\dot{\phi}^2 - V(\phi(t))\right)\alpha - \frac{Q}{2a^2}\alpha^3 + \frac{\Lambda}{2}\alpha^3}. \tag{3.6}$$

Additionally, we can derive one more equation from the Lagrangian associated with the action (3.2), using the equation of motion for the scalar field, the inflaton (this expression may be derived from the least minimum action principle, $\delta S = 0$, see for example [42]):

$$\frac{d}{dt}\left(\frac{\partial \mathscr{L}}{\partial \dot{\phi}}\right) - \frac{\partial \mathscr{L}}{\partial \phi} = 0. \tag{3.7}$$

In Appendix E.1.2, we provide another Python implementation to calculate the previous equation, yielding:

$$\boxed{\ddot{\phi} + 3\dot{\phi}\frac{\dot{a}}{a} + \alpha^2 \frac{dV(\phi(t))}{d\phi} - \dot{\phi}\frac{\dot{\alpha}}{\alpha} = 0}. \tag{3.8}$$

Thus, equations (3.5), (3.6), and (3.8) are fully analogous to the Einstein field equations and the equations of motion derived from the action, but expressed in terms of a (the scale factor), α (the lapse function), and ϕ (the inflaton scalar field). The first two equations are the well-known Friedmann equations [65, 66], generalized for the case where $\alpha(t) \neq 1$ and $\Lambda \neq 0$.

At this stage, it is common to define the Hubble parameter $H = \dot{a}/a$, whose expression is given by equation (3.5). This parameter describes the expansion rate of the Universe.

In the following sections, we will consider simplified versions of these equations admitting analytical solutions. The WKB approximation arises naturally in this context because the early universe represents a semiclassical regime where quantum gravitational effects are small but non-negligible, making WKB suitable for studying the transition from quantum to classical behavior [23, 67].

3.2 Closed Friedmann Universe

As we said before, $Q = 1$ it is associated to a closed universe, that will be the case taken from now on. For simplicity, $\alpha = 1$ and $\Lambda = 0$, such that this two things will make our equations easier to solve.

Up to this point, it is quite normal in all papers to take $\alpha = 1$ and $\beta^i = 0$, but this is a natural choice. As we said before, they are Lagrange multipliers and they do not enconde any physical information. Therefore, we can take them as constant to remain with the physical-meaningful quantities.

In this case, our manifold $M = \Sigma_t \times \mathbb{R}$, will be such that the hypersurfaces Σ_t are 3-spheres $\mathbb{S}^3$.

Now, our Friedmann equations and equation of motion will just be:

$$H^2 = \left(\frac{\dot{a}}{a}\right)^2 = \frac{8\pi}{3}\left(V + \frac{1}{2}\dot{\phi}^2\right) - \frac{1}{a^2}, \tag{3.9}$$

$$\frac{\ddot{a}}{a}+\frac{1}{2}\left(\frac{\dot{a}}{a}\right)^2=-4\pi\left(\frac{1}{2}\dot{\phi}^2-V\right)-\frac{1}{2a^2}, \tag{3.10}$$

$$\ddot{\phi}+3\dot{\phi}\frac{\dot{a}}{a}+\frac{dV}{d\phi}=\ddot{\phi}+3\dot{\phi}H+\frac{dV}{d\phi}=0. \tag{3.11}$$

These well-known equations were obtained after doing a lot of simplifications. They are normally called as the Friedmann equation (3.9), the acceleration equation (3.10) and the evolution equation (3.11).

3.2.1 Redundancy in Friedmann's Equations

At this stage, it is noteworthy that one of the three previous equations, Eq. (3.10), is actually a consequence of the other two. To demonstrate this, we first compute $\dot{H}$:

$$\dot{H}=\frac{d}{dt}\left(\frac{\dot{a}}{a}\right)=\frac{\ddot{a}}{a}-\frac{\dot{a}^2}{a^2}=\frac{\ddot{a}}{a}-H^2. \tag{3.12}$$

The first term on the right-hand side corresponds to the first term appearing in Eq. (3.10). By adding its second term, $\dot{a}^2/(2a^2)$, we obtain:

$$\frac{\ddot{a}}{a}+\frac{1}{2}\left(\frac{\dot{a}}{a}\right)^2=\dot{H}+\frac{3}{2}H^2. \tag{3.13}$$

The quantity H^2 is known from equation (3.9), while $\dot{H}$ can be determined by differentiating equation (3.9) with respect to time:

$$2H\dot{H}=\frac{8\pi}{3}\left(V'(\phi)\dot{\phi}+\ddot{\phi}\dot{\phi}\right)+2\frac{\dot{a}}{a^3}. \tag{3.14}$$

Substituting $\ddot{\phi}$ from Eq. (3.11) and assuming $H\neq 0$, we find:

$$\dot{H}=-4\pi\dot{\phi}^2+\frac{1}{a^2}. \tag{3.15}$$

We now have all the necessary components to substitute into Eq. (3.13):

$$\begin{aligned}\frac{\ddot{a}}{a}+\frac{1}{2}\left(\frac{\dot{a}}{a}\right)^2&=-4\pi\dot{\phi}^2+\frac{1}{a^2}+\frac{3}{2}\left(\frac{8\pi}{3}\left(V+\frac{1}{2}\dot{\phi}^2\right)-\frac{1}{a^2}\right)\\&=-4\pi\left(\frac{1}{2}\dot{\phi}^2-V\right)-\frac{1}{2a^2}.\end{aligned} \tag{3.16}$$

This calculation demonstrates that only two of the Friedmann system equations are independent, namely equations (3.9) and (3.11). Remarkably, these same two equations will re-emerge when we quantize the system and subsequently recover the classical limit through the WKB approximation.

3.2.2 The Universe as a Perfect Fluid

Returning to the cosmological description of our universe, we will model it as a perfect fluid based on Weyl's postulate, which states that at cosmological scales, galaxies and clusters move with velocities small compared to the overall cosmic expansion, implying no significant viscosity or heat conduction, and no intersection between them [68]. In other words, the trajectories of galaxies trace out a smooth, non-crossing flow of geodesics in spacetime, all receding from a common past.

Thus, the components of the energy-momentum tensor (3.4) are given by:

$$T_{00} = \dot{\phi}^2 - \frac{1}{2}\dot{\phi}^2 + V(\phi) = \frac{1}{2}\dot{\phi}^2 + V(\phi) = \rho, \tag{3.17}$$

$$T_{ii} = 0 - g_{ii}\left(-\frac{1}{2}\dot{\phi}^2 + V(\phi)\right) = g_{ii}\left(\frac{1}{2}\dot{\phi}^2 - V(\phi)\right) = g_{ii}P, \tag{3.18}$$

where $\rho = V(\phi) + \dot{\phi}^2/2$ and $P = -V(\phi) + \dot{\phi}^2/2$ are the total density and pressure of the Universe, respectively, being both the sources of the cosmological gravitational field [69].

3.2.3 Classical regime

To prevent the generation of quantum-induced inhomogeneities, the system must remain in the classical regime, which imposes the constraint $\rho < M_{\text{pl}}^4$, where $M_{\text{pl}} = (8\pi G)^{-1/2} = (8\pi)^{-1/2}$ in our units is the mass Planck. This limit arises because if the density were of this order, microscopic black holes would form, disrupting the smooth spacetime structure and leading to a manifold riddled with singularities, and a chaotic inflation would take place [48, 70].

This constraint impose a classical minimal value for $a(t)$. To derive it, we substitute the density expression (3.17) into the closed-universe Friedmann equation (3.9), obtaining:

$$\rho = 3M_{\text{pl}}^2\left(H^2 + \frac{1}{a^2}\right). \tag{3.19}$$

Since $H^2 > 0$ by construction (as $a(t)$ is a real function), the following inequality must hold:

$$\frac{1}{a^2} \leq \frac{1}{3M_{\text{pl}}^2}\rho < \frac{M_{\text{pl}}^2}{3}, \tag{3.20}$$

where in the last inequality we have used the condition $\rho < M_{\text{pl}}^4$. This implies that the scale factor must satisfy:

$$a > \frac{\sqrt{3}}{M_{\text{pl}}}. \tag{3.21}$$

This condition establishes a lower bound on $a(t)$, preventing the initial singularity at $a = a_0$ associated to $t = t_0 = 0$ (the Big Bang), and ensuring that the scale factor remains larger than the Planck length—the regime where quantum perturbations become significant.

3.3 Inflationary regime

Focusing now on that hypothetical inflationary regime in which the accelerated expansion of the Universe takes place, it is clear that the term $\ddot{a}/a$ of the acceleration equation (3.10) must be positive. If we introduce (3.9) into (3.10), we obtain:

$$\frac{\ddot{a}}{a} = \frac{\dot{\phi}^2}{2}\left(-4\pi - \frac{4\pi}{3}\right) + V(\phi)\left(4\pi - \frac{4\pi}{3}\right) = -\frac{1}{3M_{\text{pl}}^2}\left(\dot{\phi}^2 - V(\phi)\right) > 0, \tag{3.22}$$

and therefore the inequality $V(\phi) > \dot{\phi}^2$ holds, which can be combined with (3.17), i.e., $\dot{\phi}^2 = 2\rho - 2V(\phi)$, and with the density expression we derived at (3.19), such that $\rho < 3V/2$. Therefore:

$$a > \sqrt{\frac{3M_{\text{pl}}^2}{3V/2 - 3M_{\text{pl}}^2 H^2}} > \sqrt{\frac{2}{V(\phi)}} M_{\text{pl}}. \tag{3.23}$$

Having again a minimum value of $a(t)$, that now it is dependent on $V(\phi)$, such that lower is his value, greater will be the scale factor, having associated a greater expansion of the Universe during the inflation epoch.

3.4 Kinetic dominance

There are some models that say that the first step was dominated by the kinetic energy of the inflaton field, $\dot{\phi}^2 \gg V(\phi)$, to be later followed by a slow-roll regime in which the inflation happened, $V(\phi) \gg \dot{\phi}^2$ [71].

For that, we will impose that we are evaluating the equations in a time t in which the expansion made $Q/a^2 \ll 4\pi\dot{\phi}^2/3$ (it will be justified in Section 3.4.3). That is, the evolution equation (3.11) will reduce to

$$\ddot{\phi} \sim -3H\dot{\phi} = -3\frac{\dot{a}}{a}\dot{\phi}, \tag{3.24}$$

and (3.9) to:

$$H^2 \sim \frac{1}{6M_{\text{pl}}^2}\dot{\phi}^2 \quad \text{and its square root is} \quad H = \frac{\dot{a}}{a} \sim \pm\frac{|\dot{\phi}|}{\sqrt{6}M_{\text{pl}}}. \tag{3.25}$$

We can introduce this last expression in (3.24) to obtain two decoupled equations:

$$\ddot{\phi} \sim \mp\sqrt{\frac{3}{2}}\frac{|\dot{\phi}|}{M_{\rm pl}}\dot{\phi}. \tag{3.26}$$

From here, we can differentiate between two cases because of the $\pm$ sign, that are going to be the asympotic solutions of (3.11) and (3.9) when $a \to 0^+$.

3.4.1 Expanding universe

In this case, the plus sign have been taken in equation (3.25), such that the equations to be solved are:

$$\frac{\dot{a}}{a} \sim \frac{|\dot{\phi}|}{\sqrt{6}M_{\rm pl}}, \quad \ddot{\phi} \sim -\sqrt{\frac{3}{2}}\frac{|\dot{\phi}|}{M_{\rm pl}}\dot{\phi}. \tag{3.27}$$

See that $\dot{\phi}$ can be positive or negative, but $\dot{a}$ will not change its sign, and for that reason it will be associated with an expansion in which $\dot{a} > 0$.

The solutions to both equations can be obtained using Wolfram Mathematica, as done in Appendix E.2. For the case when the derivative is positive, $\dot{\phi} > 0$, we obtain for ϕ:

$$\phi_+(t) \sim c_2 + \sqrt{\frac{2}{3}}M_{\rm pl}\log\left(\sqrt{6}t - 2M_{\rm pl}c_1\right). \tag{3.28}$$

This solution can be further simplified by introducing $\phi_0 = c_2 + \sqrt{2/3}\,M_{\rm pl}\log(\sqrt{6})$ and $t_0 = 2M_{\rm pl}\,c_1/\sqrt{6}$, where t_0 represents an initial time that for an expanding universe will coincide with the beginning of time. Thus,

$$\phi_+(t) \sim \phi_0 + \sqrt{\frac{2}{3}}M_{\rm pl}\log(t - t_0). \tag{3.29}$$

Clearly, the form of $\phi(t)$ with negative derivative will be analogous but with a minus sign before the square root:

$$\phi_-(t) \sim \phi_0 - \sqrt{\frac{2}{3}}M_{\rm pl}\log(t - t_0). \tag{3.30}$$

Since the sign of the derivative is irrelevant when calculating the scale factor via (3.25), we can also solve for it (see Appendix E.2), obtaining:

$$a(t) \sim a_0(t - t_0)^{1/3}. \tag{3.31}$$

Fig. 8 shows how $a(t)$ increases with time, clearly indicating the universe is in an expansive phase with $\dot{a} > 0$. This behavior occurs for both ϕ_+ and ϕ_-,

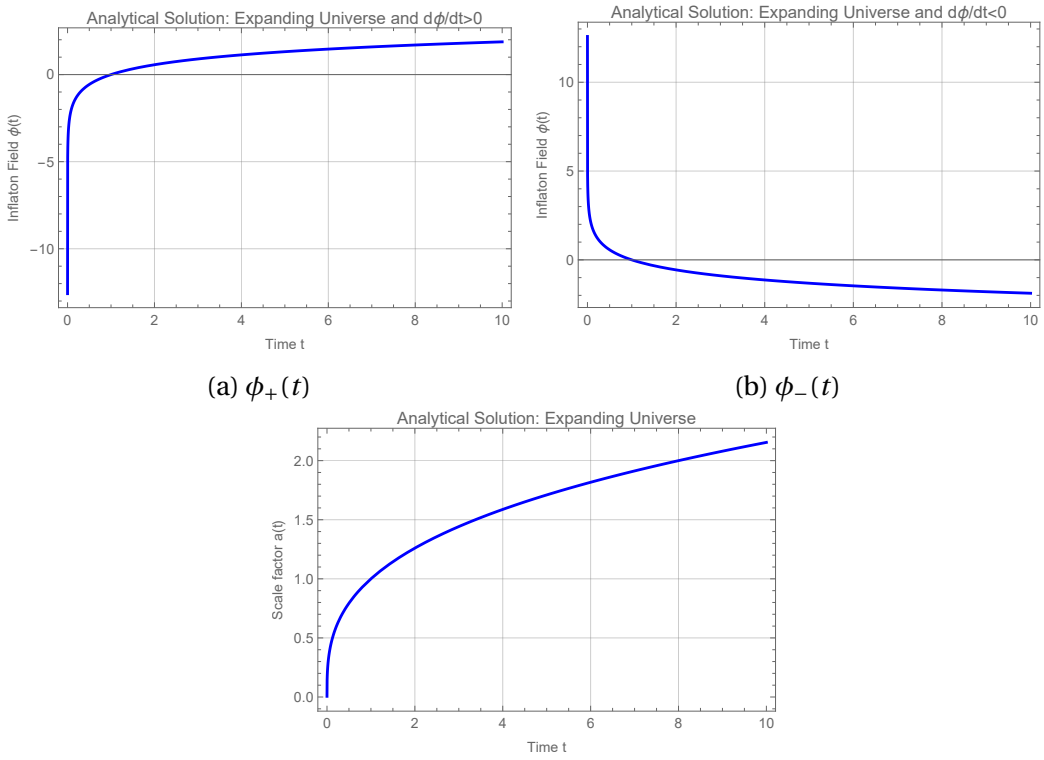

(a) $\phi_+(t)$ (b) $\phi_-(t)$

(c) $a(t)$

Figure 8: For the expanding universe in kinetic dominance, we have plotted as functions of time: (8a) ϕ_+ from (3.29), (8b) ϕ_- from (3.30), and (8c) a from (3.31), for parameter values $M_{\text{pl}} = 1$, $\phi_0 = 0$, $t_0 = 0$ and $t_{\text{max}} = 10$.

though both fields exhibit strong variation near $t = t_0$, where they approach the limits $\phi_+|_{t\to t_0^+} = -\infty$ and $\phi_-|_{t\to t_0^+} = +\infty$.

It can be shown that the condition $\dot{\phi}^2 \gg V(\phi)$ is entirely generic for any form of the potential, and that, in fact, a model described by any potential in (3.9) and (3.11) coincides with this expanding universe with $a(t) \sim a_0(t - t_0)^{1/3}$ as $a \to 0$. Therefore, kinetic dominance represents a robust model that could satisfactorily explain the beginning of the universe, where the kinetic energy density of the inflaton dominated [26, 71].

Initially, $\dot{\phi}$ has a high value around $t \to t_0$, but it becomes significantly smaller as ϕ undergoes drastic changes near $a \to 0$ and then evolves more smoothly as $a \gg 1$. Eventually, a point is reached where $\dot{\phi}^2 \approx V(\phi)$, meaning they are of the same order of magnitude. At this stage, a process known as fast-roll inflation begins in which the inflaton field evolves rapidly, but not yet under the slow-roll conditions. This phase transitions into the slow-roll inflation, characterized by

the condition $V(\phi) \gg \dot{\phi}^2$. During slow-roll inflation, the universe undergoes a sustained period of exponential expansion, driven by the potential energy of the inflaton field. This phase eventually leads to oscillations around a minimum of the potential, marking the end of inflation.

3.4.2 Contracting universe

On the other hand, the minus sign have been taken in equation (3.25),

$$\frac{\dot{a}}{a} \sim -\frac{|\dot{\phi}|}{\sqrt{6}M_{\rm pl}}, \quad \ddot{\phi} \sim \sqrt{\frac{3}{2}}\frac{|\dot{\phi}|}{M_{\rm pl}}\dot{\phi}. \tag{3.32}$$

It is evident that our solutions will now be analogous to those obtained in the previous sections. The primary distinction is that, due to the condition $\dot{a} < 0$, the universe will be contracting until it reaches a final point at $t = t_0$, where the universe concludes. In this context, we have $t_0 \geq t$ in general. Therefore, our solutions can be expressed as follows:

$$\phi_{\pm}(t) \sim \phi_0 \mp \sqrt{\frac{2}{3}} M_{\rm pl} \log(t_0 - t), \tag{3.33}$$

$$a(t) \sim a_0 (t_0 - t)^{1/3}. \tag{3.34}$$

Again, ϕ_+ is associated with $\dot{\phi} > 0$, and ϕ_- with $\dot{\phi} < 0$.

By observing Fig. 9, we find a singularity at $t = t_0$ that we call Big Crunch [72]. However, this time coincides with the end of the universe, where the values of the inflaton diverge again, leading to the formation of a singularity. This is possible thanks to the fact that we are dealing with a closed universe. We will not go deeply into this point, as it is not the focus of our discussion.

An interesting point to mention here is that the commutation relations we derived in (2.42) can be modified, as it were done in [73]. This modification leads to a relation analogous to the Heisenberg uncertainty principle x (space) or p (momentum), $\triangle x \triangle p \geq \hbar/2$ [74], where $\triangle$ indicates an unvertainty in the variable. Specifically, the modified relation is given by:

$$\triangle a \triangle p_a = 1 - 2\alpha\langle p_a\rangle + 4\alpha^2\langle p_a^2\rangle, \tag{3.35}$$

where p_a is the momentum operator associated with a, $\langle p_a\rangle$ its expected value, and α a parameter.

This implies that there exists a minimum length for the universe, meaning it cannot shrink to zero. As a result, both the Big Bang and Big Crunch singularities are avoided.

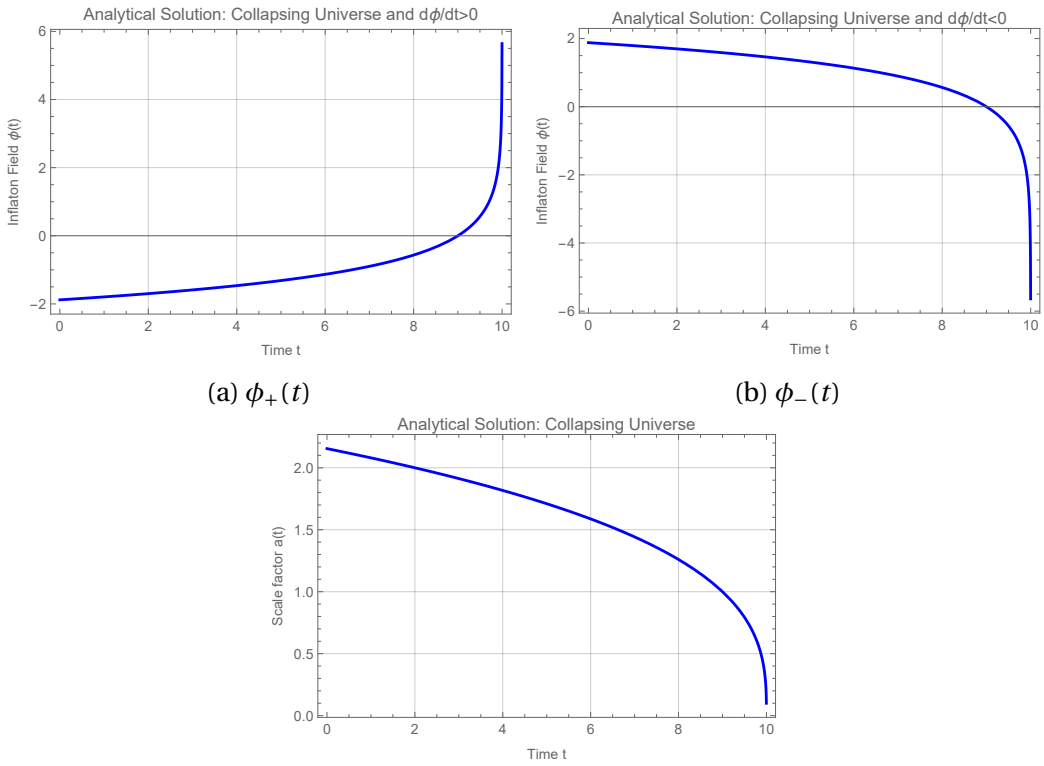

(a) $\phi_+(t)$ (b) $\phi_-(t)$

(c) $a(t)$

Figure 9: For the contracting universe in kinetic dominance, we have plotted as functions of time: (9a) ϕ_+ from (3.33), (9b) ϕ_- from (3.33), and (9c) a from (3.34), for parameter values $M_{\text{pl}} = 1$, $\phi_0 = 0$, $t_{\text{max}} = t_0 = 10$, and $a_0 = 1$.

In other words, our universe could begin, expand until reaching a maximum point, and then start contracting until it reaches a minimum non-zero value of a, only to begin again all this process. However, the null energy condition would need to be violated, and there is no evidence of this happening. Thus, the concept of a bouncing universe is considered highly improbable [75]. It is worth mentioning that this idea has been contemplated by humanity for centuries, from Ragnarok in Norse mythology to the eternal return defended by Nietzsche [76].

3.4.3 Discussion of the Kinetic dominance

To conclude, we are now in a position to support the initial assumption that $\dot{\phi} \gg 1/a^2$. To justify this, we will explain it for the case of an expanding universe, noting that the argument is analogous for a contracting one.

From equations (3.29) and (3.30), we find that $\dot{\phi}^2 \propto 1/(t-t_0)^2$, while from

equation (3.31), $1/a^2 \propto 1/(t-t_0)^{2/3}$. Thus, as $t \to t_0^+$, it follows that $\dot{\phi}^2 \gg 1/a^2$, which justifies that the approximation taken in the kinetic dominance regime, in equations (3.24) and (3.25), is valid as long as we are considering a stage very close to the beginning of the universe.

That is, for an expanding universe, these solutions will correspond to the asymptotic behaviours of the classical ones associated with $t \to t_0^+$ [77], provided that the condition (3.21), $a > \sqrt{3}/M_{\rm pl}$, is satisfied. In this regime, we will relate quantum and classical solutions.

3.5 Constant potential

Let us consider a constant potential, $V(\phi) \approx V(\phi_0) = V_0 \in \mathbb{R}^+$, which is of interest because, in some inflationary models, inflation occurs when the potential varies slowly around its minimum value. Thus, the evolution equation (3.11) becomes:

$$\frac{\ddot{\phi}}{\dot{\phi}} + 3\frac{\dot{a}}{a} = 0, \tag{3.36}$$

if $\dot{\phi} \neq 0$ and $a \neq 0$, so we can integrate equation (3.36):

$$\int_{t_0}^{t} \frac{\ddot{\phi}}{\dot{\phi}} dt = -3\int_{t_0}^{t} \frac{\dot{a}}{a} dt = \log\left(\frac{\dot{\phi}(t)}{\dot{\phi}(t_0)}\right) = -\log\left(\frac{a(t)}{a(t_0)}\right)^3 = \log\left(\frac{a(t_0)}{a(t)}\right)^3,$$

$$a^3\dot{\phi} = a^3(t_0)\dot{\phi}(t_0). \tag{3.37}$$

This new relationship obtained is quite interesting because it connects the values of the scale factor and the inflaton field with themselves, evaluated at an arbitrary time $t_0 > 0$.

We can also evaluate the Friedmann equation (3.9) for this case:

$$\dot{a}^2 = \left(\frac{da}{dt}\right)^2 = \frac{1}{3M_{\rm pl}^2}\left(\frac{1}{2}\dot{\phi}^2 + V_0\right)a^2 - 1 = \frac{a^6(t_0)\dot{\phi}(t_0)^2}{6M_{pl^2}}\frac{1}{a^4} + \frac{V_0}{3M_{\rm pl}^2}a^2 - 1 = \frac{a^2}{p^2} + \frac{q}{a^4} - 1. \tag{3.38}$$

Two constants have been defined to simplify the last equation: $p = M_{\rm pl}\sqrt{3/V_0}$ and $q = \dot{\phi}(t_0)^2 a(t_0)^6/6M_{\rm pl}^2$. The equation (3.38) is an ordinary differential equation that can be solved by separating the variables a and t:

$$t - t_0 = \pm\int_{a(t_0)}^{a(t)} \frac{da}{\frac{1}{a^2 p}\sqrt{a^6 - p^2a^4 + p^2q}} = \pm\int_{a(t_0)}^{a(t)} \frac{da}{\sqrt{f(a)}}. \tag{3.39}$$

Defining $f(a) = (a^6 - p^2a^4 + p^2q)/(a^4p^2)$ and $P(A) = P(a^2) = A^3 - p^2A^2 + p^2q$, we will find ourselves in different situations depending on the value of q.

It is evident that both $f(a)$ and $P(A)$ must be positive to solve equations (3.38) and (3.39). The minimum value of $P(A)$ occurs when

$$P'(A_{\min}) = 0 = 3A_{\min}^2 - 2p^2 A_{\min} \Rightarrow A_{\min} = \frac{2p^2}{3}, \quad \text{assuming } A_{\min} \neq 0. \tag{3.40}$$

This critical point leads to a minimum value of $P(A_{\min}) = p^2(q - 4p^4/27)$. This result allows us to distinguish among different cases depending on the value of q, as this minimum can be negative, zero, or positive.

3.5.1 $q = 0$

In this first scenario where $P(A_{\min}) < 0$, there exists a range of values for which we cannot solve equations (3.38) and (3.39). That is, $P(A) = A^3 - p^2A^2$ is null when $A = 0$ and $A = p^2$ (its positive solutions), and inside this range its the negative minimum at $A_{min} = 2p^2/3$. From the first equation, we observe that $\dot{a}^2 \geq 0$ only when $a^2 \geq p^2$. This behavior is illustrated in Fig. 10.

The upper panel displays $P(A)$, clearly showing positivity when $A > p^2$. The lower panel presents the phase space diagram ($\dot{a}$, a), featuring two distinct curves for $a \geq p$:

- A contracting universe (lower blue curve with $\dot{a} < 0$) that reaches a minimum size $a_{\min} = p$.
- An expanding universe (upper red curve with $\dot{a} > 0$) that emerges from this minimum size.

Both trajectories describe classical inflation without kinetic dominance, suggesting a cosmological scenario where our universe shrank to a minimum size (analogous to a Big Crunch but avoiding the $a = 0$ singularity), and another that is in an expansion phase, both asymptotically approaching $a = p$ as the minimum universe size at $t \to +\infty$ and $t \to -\infty$, respectively.

3.5.2 $q \in (0, 4p^4/27)$

In this second scenario with $P(A_{\min}) < 0$, we again encounter negative values of the potential function. While the cubic polynomial $P(A) = A^3 - p^2A^2 + p^2q$ appears simple, its analytical solution is non-trivial, although it is straightforward to visualize it numerically as shown in Fig. 11.

The potential exhibits two distinct regimes: $P(A) > 0$ for $A < p_1$ (below the first root) and for $A > p_2$ (above the second root); and $P(A) < 0$ in the intermediate region between roots p_1 and p_2.

This behavior gives rise to two distinct cosmological solutions, as seen in the lower panel of Fig. 11:

1. For $A \leq p_1$ where $P(A) > 0$, we obtain:
   - An expanding universe (left red curve) emerging from the initial singularity ($a = 0$) and reaching a maximum size of a_1 (kinetic dominance).
   - A subsequent contracting phase (left blue curve) collapsing back to $a = 0$.
2. For $A \geq p_2$, we recover behavior similar to the case $q = 0$ but with

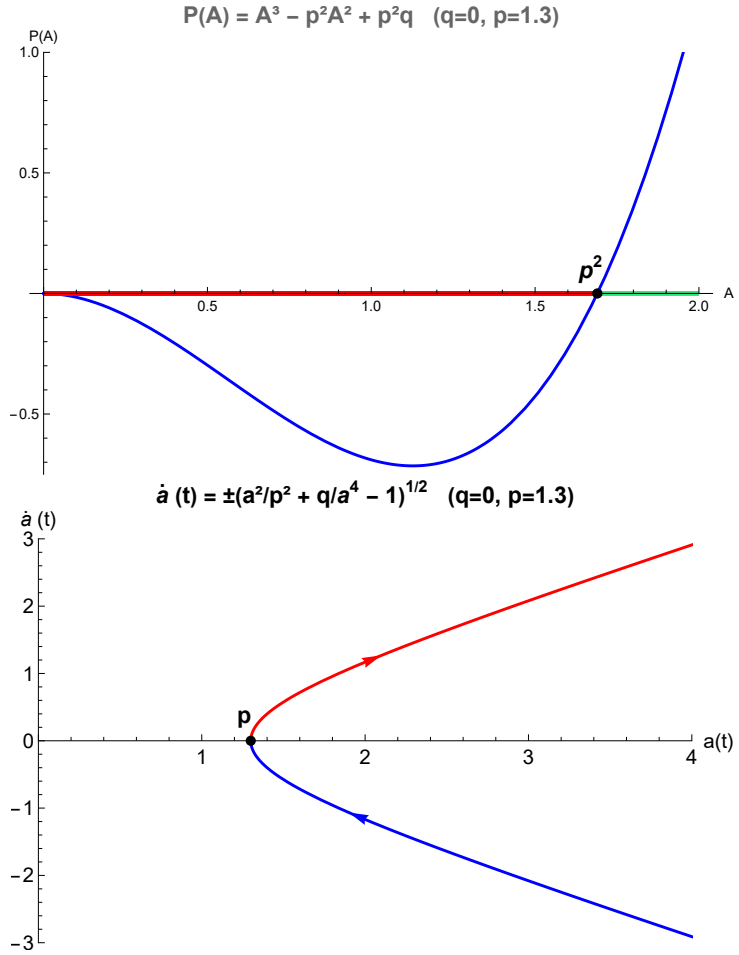

Figure 10: For the specific case where $q = 0$ and $p = 1.3$: (Top) The function $P(A)$ versus A, with red indicating $P(A) < 0$ and green showing $P(A) > 0$; (Bottom) The phase space diagram $(\dot{a}, a)$ representing a contracting universe for $\dot{a} < 0$ and an expanding one for $\dot{a} > 0$, both asymptotically approaching p as the minimum universe size.

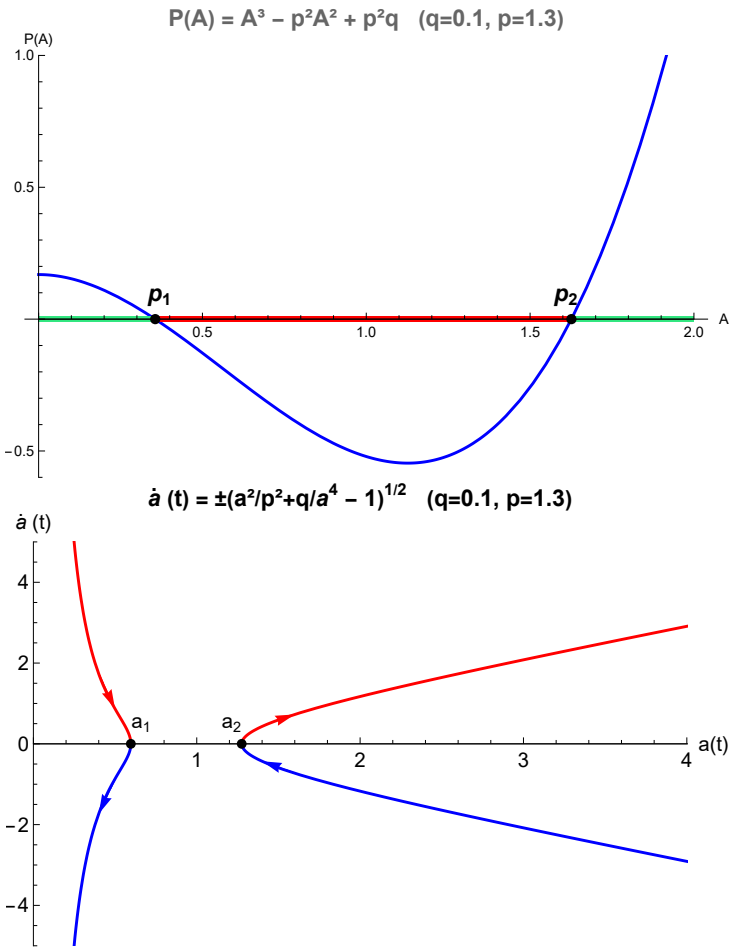

Figure 11: For the parameter values $q = 0.1$ and $p = 1.3$: (Top) The potential function $P(A)$ shows regions where $P(A) < 0$ (red) and $P(A) > 0$ (green); (Bottom) Phase space diagram $(\dot{a}, a)$ illustrating two distinct regimes: 1) For $a \geq a_2$, a contracting universe ($\dot{a} < 0$, blue curve) and an expanding universe ($\dot{a} > 0$, red curve), acting a_2 as their minimum size and as a turning point (i.e., the Universe went from contraction to its minimum size to expansion); and 2) For $a \leq a_1$, a contracting universe that diverges at $a = 0$, and an expanding universe emerging from the initial singularity at $a = 0$, acting a_1 as the maximum size and as an another turning point (i.e., the Universe went from expansion to its maximum size to contraction).

minimum size a_2 (inflation).

This scenario naturally incorporates kinetic dominance near the singularity while maintaining the bounce behavior at finite scale factor $a = a_1$. The solution space now includes both singularity-approaching and singularity-avoiding

trajectories, providing a more complete picture of possible cosmological dynamics in this model.

3.5.3 $q = 4p^4/27$

This represents the critical case where $P(A_{\min}) = 0$. The special point $p_0 = 2p^2/3 = A_{\min}$ corresponds to $a_0 = \sqrt{p_0}$ where $\dot{a} = 0$, and it separates the four

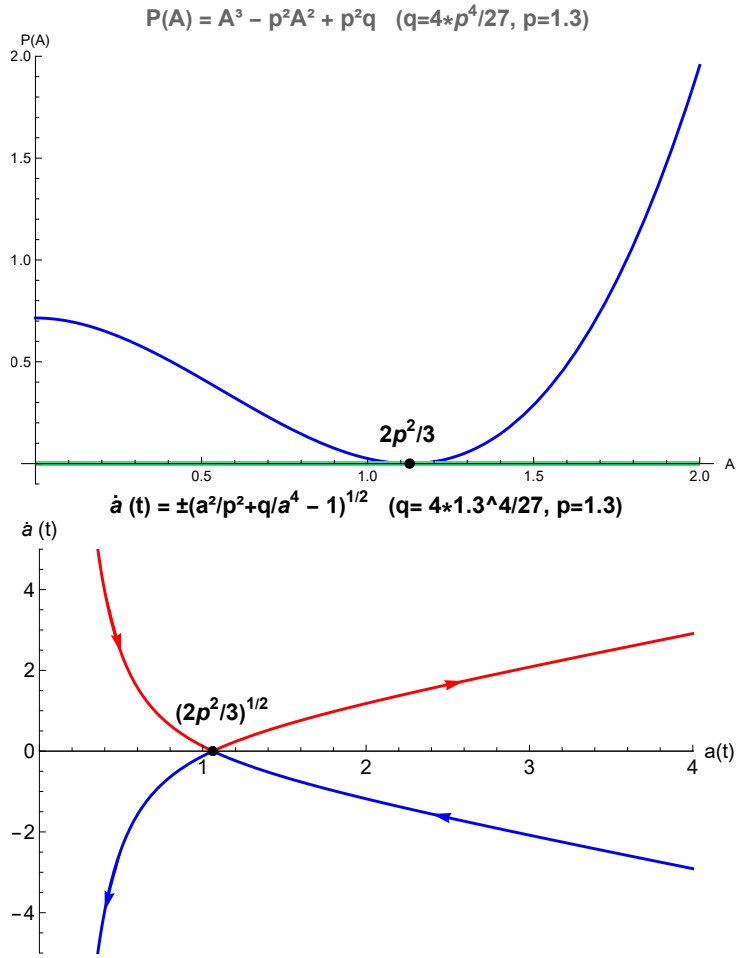

Figure 12: For the parameter values $q = 4 \cdot 1.3^4/27$ and $p = 1.3$: (Top) Potential function $P(A)$ shows exclusively positive values ($P(A) > 0$, green region); (Bottom) Phase space diagram ($\dot{a}$, a) displaying: 1) For $a \geq \sqrt{2p^2/3} = a_0$ - both contracting ($\dot{a} < 0$, blue curve) and expanding ($\dot{a} > 0$, red curve) solutions asymptotically approaching a_0 as the minimum size, and 2) For $a \leq a_0$ - an expanding universe originating from the initial singularity at $a = 0$ that reaches a maximum size at a_0 before recollapsing.

different solutions. As shown in Fig. 12, this scenario exhibits several important features:

- The solution space now contains a unique zero-crossing point at a_0.
- The four different cosmological solutions merge into two classes, each encompassing both expansion and contraction behaviours:
  - Two left solutions (from $a = 0$ to a_0) with identical maximum size a_0.
  - Two right solutions (from a_0 to ∞) sharing the same minimum size a_0.
- New dynamical behaviors emerge at the left part (the solutions to the right of $(2p^2/3)^{1/2}$ are analogous to those obtained for $q = 0$):
  - Expanding solutions ($\dot{a} > 0$) that decelerate to $\dot{a} = 0$ at a_0.
  - Contracting solutions ($\dot{a} < 0$) that accelerate toward the singularity.

This critical case provides a smooth transition between the previously discussed scenarios, with the special point a_0 serving as both the maximum size for singularity-originating solutions and the minimum size for bounce solutions. The phase space structure reveals how the different cosmological behaviors connect at this critical parameter value.

3.5.4 $q > 4p^4/27$

In this final scenario where $P(A_{\min}) > 0$, all values of $A = a^2$ are allowed, but unlike previous cases, there exists no extremal size for the universe (neither minimum nor maximum), as shown in Fig. 13. The model presents two fundamental cosmological behaviors:

- **Expanding solution** ($\dot{a} > 0$):
  - Originates near the singularity with high expansion rates in a kinetic dominance phase.
  - Decelerates to a minimum expansion rate $\dot{a}_{\min} > 0$.
  - Continues expanding indefinitely (inflation).
- **Contracting solution** ($\dot{a} < 0$):
  - Begins with gradual contraction from $\dot{a} < 0$ to $\dot{a}_{\max} < 0$.
  - Decelerates toward the singularity in a kinetic dominance phase.

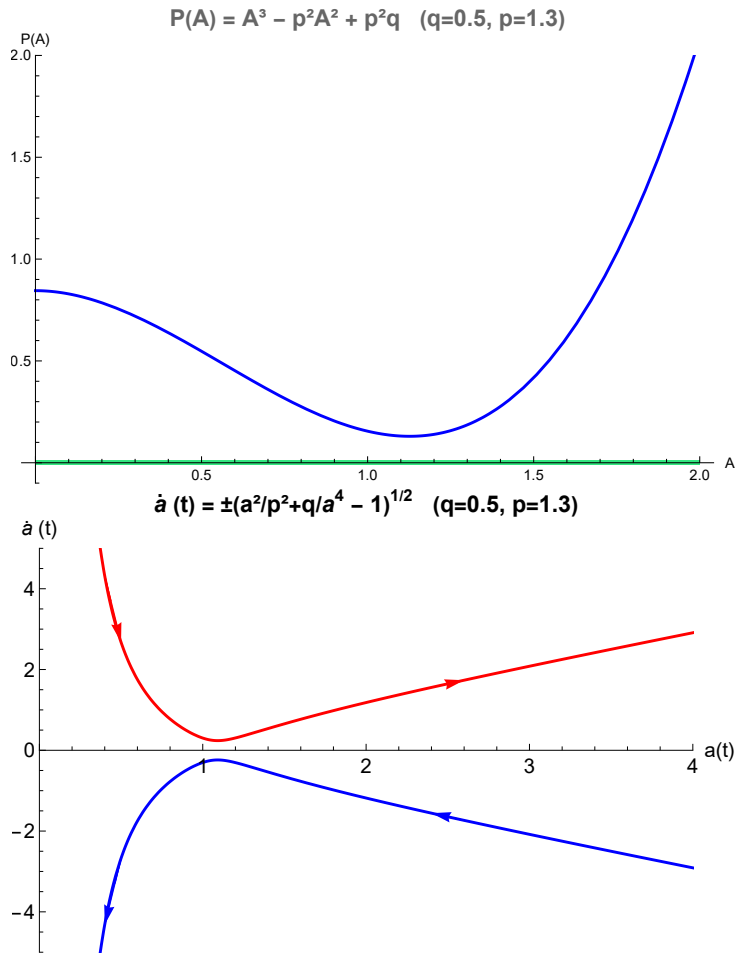

Figure 13: For parameters $q = 0.5$ and $p = 1.3$: (Top) Potential function $P(A)$ showing exclusively positive values ($P(A) > 0$, green region); (Bottom) Phase space diagram ($\dot{a}$, a) illustrating two distinct cosmological scenarios: (1) An expanding universe (red curve) originating from the initial singularity ($\dot{a} > 0$), and (2) A contracting universe (blue curve) collapsing toward $a = 0$ ($\dot{a} < 0$).

  - Ends in a Big Crunch.

The expanding solution of this model aligns remarkably well with modern cosmological observations, featuring:

- An initial kinetic dominance regime with rapid expansion.
- Subsequent transition to classical inflation.
- Final phase of increasing expansion where $\dot{a}/a \sim$constant (consistent with Hubble-Lemaître's law).

This scenario successfully describes our current understanding of cosmic evolution: an initial kinetic dominance phase burst followed by the observed gradual expansion of the universe, a classical inflation. The model naturally incorporates both the early universe dynamics and the current accelerated expansion without introducing artificial cutoffs or boundaries.

3.6 Slow-Roll Approximation and end of inflation

If we look at equation (3.11), it is analogous to the equation of motion given by Newton second law, $\ddot{a} = -V'$, but with an extra term that it has been called as friction term, $3H\dot{\phi}$ [78].

Then, if the potential $V(\phi)$ dominates after the kinetic dominance phase, via (3.9), will lead to a large H, and therefore to a great friction in (3.11), being the scalar field forced to move slowly [79]. Because of the rapid growth of the scale of the universe and the slow motion of ϕ, this stage is characterized by $\dot{\phi}^2 \ll V(\phi)$, i.e. $\ddot{\phi} \ll dV(\phi)/d\phi$, and $H^2 \gg 1/a^2$. Then, in the slow-roll aproximation, equations (3.9) and (3.11) are reduced to:

$$3H\dot{\phi} \sim -\frac{dV(\phi)}{d\phi}, \qquad H^2 = \left(\frac{\dot{a}}{a}\right)^2 \sim \frac{8\pi V(\phi)}{3}. \tag{3.41}$$

We can integrate the second equation, obtaining directly that $a(t) \propto e^{\sqrt{8\pi V/3}\,t}$, being a exponential rapid expansion of the universe. For that reason, this stage is related with the normal inflation that is widely studied, during around 10^{-35} seconds in realistic models.

$V(\phi)$ will decrease its value until $\dot{\phi}^2 < V(\phi)$ no longer hold and inflation comes to an end. If $V(\phi)$ has a minimum V_0, the field will oscillate around it because of the friction term, $3H\dot{\phi}$, see Fig. 14. The released potential energy could be transferred to the universe, and through the mass-energy equivalence principle ($E = mc^2$), this energy facilitated particle creation and provided them kinetic energy, resulting in a hot, dense state more closely resembling our conventional conception of the Big Bang [81].

At the end of inflation, particles were created and provided with energy, and the universe became so flat that the curvature of the spatial hypersurfaces seems to be nowadays $L \approx 0$ [59].

To conclude this section, several models have been proposed and studied to describe the inflation phase. One notable example is chaotic inflation, which utilizes a different type of potential, $V(\phi) = m^2\phi^2/2$ [70]. Additionally, many other models precede this one, each varying the form of the potential [82, 83].

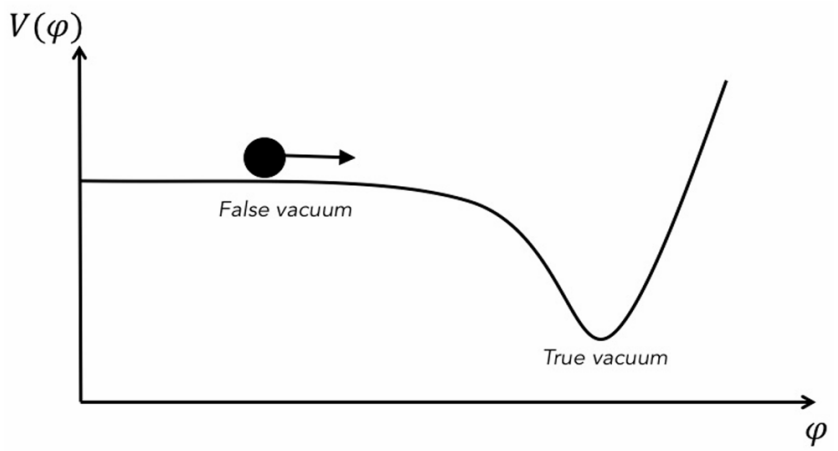

Figure 14: For $\varphi = \phi$ the inflaton field, it is represented the potential associated to the slow-roll regime in the case it has a minimum value V_0. Around it, the released potential energy is transfered to the Universe, allowing the formation of new particles, and providing them with kinetic energy. This potential will decrease its value slowly because of the friction term $3H\dot{\phi}$. Image extracted from [80].

4 Quantum Inflation

4.1 Relationship Between the Wheeler-DeWitt Equation and the Friedmann Equations

A natural question at this point would be: what is the relationship between the Wheeler-DeWitt equation and the equations for a Friedmann universe? At first view, the equations (2.26) and (3.5), (3.6), and (3.8) appear to be entirely different. Let us develop the Wheeler-DeWitt equation for the metric (3.3), taking into account that the Ricci scalar R, which appears explicitly, is the 3-dimensional Ricci scalar associated with the metric induced on the spatial hypersurface:

$$\gamma_{ij} = \begin{pmatrix} a^2(t)\frac{1}{1-Qr^2} & 0 & 0 \\ 0 & a^2(t)r^2 & 0 \\ 0 & 0 & a^2(t)r^2\sin^2\theta \end{pmatrix} = a^2(t)\begin{pmatrix} \frac{1}{1-Qr^2} & 0 & 0 \\ 0 & r^2 & 0 \\ 0 & 0 & r^2\sin^2\theta \end{pmatrix} = a^2(t)P_{ij}(r,\theta). \tag{4.1}$$

Here, the matrix $P_{ij}(r,\theta)$ has been defined for simplicity. Using the code presented in Appendix E.3, we find that:

$$R = -\frac{6Q}{a^2}. \tag{4.2}$$

Additionally, we need the expression for the extrinsic curvature tensor K_{ij} on the hypersurface, derived from (2.19). Considering that, due to the form of the metric, the shift vector is zero ($\beta_i = 0$), and that we can adopt adapted coordinates where $\mathscr{L}_{\vec{t}} = t^\mu\partial_\mu = \partial_t$, the spatial components satisfy the evolution equation (see Appendix B.1):

$$\partial_t\gamma_{ij} - \mathscr{L}_{\vec{\beta}}\gamma_{ij} = -2\alpha K_{ij} \rightarrow K_{ij} = -\frac{1}{2}\partial_t\gamma_{ij} = -\frac{1}{2}2a\dot{a}P_{ij} = -\frac{\dot{a}}{a}\gamma_{ij}. \tag{4.3}$$

With this simple expression, it becomes straightforward to compute the other components of the Wheeler-DeWitt equation.

The second term, K^2, is given by:

$$K = \gamma^{ij}K_{ij} = -\frac{\dot{a}}{a}\gamma^{ij}\gamma_{ij} = -3\frac{\dot{a}}{a}, \tag{4.4}$$

and then $K^2 = 9(\dot{a}/a)^2 = 9H^2$, while the third term, $K_{ij}K^{ij}$, is:

$$K_{ij}K^{ij} = H^2\gamma_{ij}\gamma^{ij} = 3H^2. \tag{4.5}$$

Thus, the equation (2.26), also known as the Hamiltonian constraint, becomes in this case (recall that $1/(8\pi) = M_{\text{pl}}^2$):

$$H^0 = 0 = \frac{6Q}{a^2} + 6H^2 - \frac{2}{M_{\text{pl}}^2}\rho - 2\Lambda, \tag{4.6}$$

where, in our case, $\Lambda = 0$, $Q = 1$, and ρ is given by (3.17). It is evident that this equation is equivalent to the Friedmann equation:

$$H^2 = \frac{\dot{a}^2}{a^2} = \frac{1}{3M_{\text{pl}}^2}\left(V\big(\phi(t)\big) + \frac{1}{2}\dot{\phi}^2\right) - \frac{1}{a^2(t)}, \tag{4.7}$$

which, when multiplied by $6M_{pl}^2 a^3$, yields:

$$6M_{\text{pl}}^2 a\dot{a}^2 - a^3\dot{\phi}^2 + 6M_{\text{pl}}^2\left(a - \frac{V(\phi)}{3M_{\text{pl}}^2}a^3\right) = 0. \tag{4.8}$$

The goal of this section is to obtain approximate solutions to the previous equation by employing the WKB method. To quantize it and finally explore the quantum realm, we will use the Hamiltonian formulation to introduce the conjugate momenta.

4.2 WDW Equation for a Closed Universe

First, starting from the action (3.2), let us write down the expression for the Lagrangian:

$$L = \frac{{}^{(4)}R - 2\Lambda}{16\pi} - \frac{1}{2}\dot{\phi}^2 - V(\phi). \tag{4.9}$$

Again, we can calculate the 4-dimensional Ricci scalar (using the code from Appendix E.1), obtaining:

$${}^{(4)}R = \frac{6}{a^2}(Q + \dot{a}^2 + a\ddot{a}). \tag{4.10}$$

This shows that our Lagrangian depends on $\dot{a}$ and $\dot{\phi}$. As in Hamiltonian mechanics, we can calculate the associated canonical momentum densities for the different configuration variables [84]:

$$\overline{p}_a = \frac{\partial L}{\partial \dot{a}} = \frac{12\dot{a}}{a^2}\frac{1}{16\pi} = \frac{6M_{\text{pl}}^2\dot{a}}{a^2}, \tag{4.11}$$

$$\overline{p}_\phi = \frac{\partial L}{\partial \dot{\phi}} = -\dot{\phi}. \tag{4.12}$$

To simplify equation (4.8), we will redefine the recently obtained momentums by introducing a variable multiplied by the scale factor. This is possible in our theory because the constraints exhibit an invariance [85]. That is, it does not matter whether we have $H^0 = 0$ or $-2\pi^2 a^3 H^0 = 0$; both are exactly zero. Thus, we redefine our conjugate momenta as:

$$p_\phi = -2\pi^2 a^3 \overline{p}_\phi = 2\pi^2 a^3 \dot{\phi}, \tag{4.13}$$

$$p_a = -2\pi^2 a^3 \overline{p}_a = -12\pi^2 M_{\text{pl}}^2 a\dot{a}. \tag{4.14}$$

Note that, compared to what was obtained in Section 2.4.3, instead of having γ_{ij} as the dynamical variable, we now have $a(t)$, the scale factor, which encodes the information of the induced metric since $\gamma_{ij} = a^2(t)P_{ij}(r,\theta)$. It should not be surprising that we now have another dynamical variable, the scalar field $\phi(t)$, as it was introduced after the treatment in Section 2. This scalar field encodes the inflaton field we are studying, which is of vital importance in the theory.

Once we have the dynamical variables of our theory along with their conjugate momenta, (a, p_a) and (ϕ, p_ϕ), we can rewrite equation (4.8) as a function of these variables:

$$6M_{\text{pl}}^2 a \frac{p_a^2}{12^2\pi^4 M_{\text{pl}}^4 a^2} - a^3 \frac{p_\phi^2}{2^2\pi^4 a^6} + 6M_{\text{pl}}^2 \left(a - \frac{V(\phi)}{3M_{\text{pl}}^2} a^3 \right) = 0, \tag{4.15}$$

which can be further simplified by multiplying by $24\pi^4 M_{\text{pl}}^2 a$. Defining the constant $\lambda = 1/(12\pi^2 M_{\text{pl}}^2)$, we arrive at the final classical expression for the Friedmann equation:

$$p_a^2 - \frac{6M_{\text{pl}}^2}{a^2} p_\phi^2 + \frac{1}{\lambda^2} \left(a^2 - \frac{V(\phi)}{3M_{\text{pl}}^2} a^4 \right) = 0 = p_a^2 - \frac{6M_{\text{pl}}^2}{a^2} p_\phi^2 + \overline{U}(a,\phi). \tag{4.16}$$

The last term, $\overline{U}(a,\phi) = \left(a^2 - V(\phi)a^4/(3M_{\text{pl}}^2) \right)/\lambda^2$, is known as the superpotential function [86, 87].

4.2.1 Quantisation rules

As performed in Section 2.4.3, once we have the canonical variables and their conjugate momenta - which are independent and thus satisfy the following Poisson brackets [88, 89, 90]:

$$\{a, \phi\} = 0 = \{p_a, p_\phi\}, \tag{4.17}$$

$$\{a, p_a\} = 1 = \{\phi, p_\phi\}, \tag{4.18}$$

we can proceed to quantize the system by promoting the canonical variables to their corresponding quantum operators: $\hat{a}$, $\hat{\phi}$, $\hat{p}_a$, and $\hat{p}_\phi$. These operators satisfy the commutation relations:

$$[\hat{a}, \hat{p}_a] = i\hbar = [\hat{\phi}, \hat{p}_\phi], \quad [\hat{a}, \hat{\phi}] = 0 = [\hat{p}_a, \hat{p}_\phi], \tag{4.19}$$

in complete analogy with the discussion in Appendix D.

Defining a wave functional $\Psi[a, \phi]$ on the space of field configurations a and ϕ [50], the operators act as follows:

$$\hat{a}\Psi[a,\phi] = a\Psi[a,\phi], \quad \hat{\phi}\Psi[a,\phi] = \phi\Psi[a,\phi], \tag{4.20}$$

$$\hat{p}_a\Psi[a,\phi] = -i\hbar\frac{\partial}{\partial a}\Psi[a,\phi], \quad \hat{p}_\phi\Psi[a,\phi] = -i\hbar\frac{\partial}{\partial \phi}\Psi[a,\phi]. \tag{4.21}$$

However, in the equation of interest (4.16), we encounter squares of the classical operators, which implies that their quantum counterparts will be applied twice. At this point, an important subtlety arises, one that Stephen Hawking first realized [23]. When computing the action of our system, the integrand contains $\sqrt{-g} \propto a^3$ in the FRW metric, making it crucial that $\hat{p}_a^2$ properly encodes the non-commutativity between $\hat{a}$ and $\hat{p}_a$, $[\hat{a}, \hat{p}_a] = i\hbar$. If we fail to account for this crucial property, we risk obtaining incorrect actions, Lagrangians, and equations of motion. This is because the expressions $a\partial_a\sqrt{-g}$ and $\partial_a(a\sqrt{-g})$ are fundamentally distinct due to the non-commutativity of the operators.

For instance, if we take $\hat{p}_a^2\Psi[a,\phi] = -\hbar^2(\partial^2/\partial a^2)\Psi[a,\phi]$, it would fail to capture this essential property. A more appropriate expression would be:

$$\hat{p}_a^2\Psi[a,\phi] = -\frac{\hbar^2}{2a}\left(\frac{\partial}{\partial a} + \frac{\partial}{\partial a}\left(a\frac{\partial}{\partial a}\right) + a\frac{\partial^2}{\partial a^2}\right)\Psi[a,\phi] = -\hbar^2\left(\frac{\partial^2}{\partial a^2} + \frac{1}{a}\frac{\partial}{\partial a}\right)\Psi[a,\phi], \tag{4.22}$$

which takes a non-trivial form that better encodes this property.

The most comprehensive approach to this problem is to adopt a general form that encompasses, in the simplest way, various possible orderings, including the two cases mentioned above:

$$\hat{p}_a^2\Psi[a,\phi] = -\hbar^2\frac{1}{a^{\overline{p}}}\frac{\partial}{\partial a}\left(a^{\overline{p}}\frac{\partial}{\partial a}\right)\Psi[a,\phi], \tag{4.23}$$

with $\overline{p}$ an arbitrary parameter. Note that for $\overline{p} = 0$, we recover $\hat{p}_a^2\Psi[a,\phi] = -\hbar^2(\partial^2/\partial a^2)\Psi[a,\phi]$, while for $\overline{p} = 1$, we obtain equation (4.22).

Regarding the momentum operator associated with ϕ, this issue does not arise because $\sqrt{-g}$ is independent of ϕ. Thus, in this case, we can simply take:

$$\hat{p}_\phi^2\Psi[a,\phi] = -\hbar^2\frac{\partial^2}{\partial \phi^2}\Psi[a,\phi]. \tag{4.24}$$

4.2.2 WDW equation and WKB solutions

Therefore, we can substitute the expressions for $\hat{p}_a^2$ and $\hat{p}_\phi^2$ obtained in (4.23) and (4.24) into the WDW equation (4.16) by applying it to the wave function $\Psi[a,\phi]$ and multiplying by $-1/\hbar^2$ to obtain the quantum (and modern) version of this famous equation [26, 22]:

$$\left(\frac{\partial^2}{\partial a^2}+\frac{\overline{p}}{a}\frac{\partial}{\partial a}-\frac{6M_{\rm pl}^2}{a^2}\frac{\partial^2}{\partial\phi^2}-\frac{1}{\hbar^2}U(a,\phi)\right)\Psi[a,\phi]=0. \tag{4.25}$$

In this is convenient to introduce a function that also depends on the independent variables, $\mathbb{S}(a,\phi)$, proposed as a solution [91, 92]:

$$\Psi[a,\phi]:=\exp\left(i\frac{\mathbb{S}(a,\phi)}{\hbar}\right), \tag{4.26}$$

where $\mathbb{S}$ is the classical action (a real function). Due to $\mathbb{S}$ and $\hbar$, this approximation has a semiclassical character [67]. A solution of this form is known as a WKB solution, widely used in quantum mechanics to approximate the Schrödinger equation.

By supporting this approximation, we will be able to obtain analytical expressions to investigate the physical-mathematical meaning hidden behind our Universe at the beginning of time, allowing us to gain insight into it [93]. The WKB method is particularly interesting because it will yield a wave function describing properties and regions that would be classically forbidden [94]. The only restriction of this method is that the classical quantities associated with the action must be larger than the Planck constant [95].

In this context, we expand $\mathbb{S}$ as a series in $\hbar$ such that:

$$\mathbb{S}=\mathbb{S}_0+\frac{\hbar}{i}\mathbb{S}_1+\left(\frac{\hbar}{i}\right)^2\mathbb{S}_2+\cdots \tag{4.27}$$

In the formulation used, $\hbar\ll 1$. To better appreciate its value, let us consider the International System of Units, where $\hbar=h/2\pi$, with $h=6.626\times10^{-34}\,\mathrm{J\cdot s}$ being the Planck constant [96]. Consequently, the successive contributions to $\mathbb{S}$ become progressively smaller as they involve higher orders of $\hbar$.

Being a semiclassical approximation, such that in the classical limit where $\hbar\to 0$, we recover the classical solution associated with classical cosmology. Naturally, in the literature, $\hbar\to 0$ indicates that terms containing this constant will be negligible compared to terms independent of it. This limits the validity of the approximation when dealing with purely quantum systems at sufficiently small scales where the action becomes smaller than the Planck constant.

Let us substitute our WKB solutions (4.27) and (4.26) into the WDW equation given by (4.25). First, we note that:

$$\frac{\partial^2\Psi}{\partial a^2} = \frac{\partial}{\partial a}\left(\frac{\partial}{\partial a}e^{i\mathbb{S}/\hbar}\right) = \frac{\partial}{\partial a}\left(e^{i\mathbb{S}/\hbar}\frac{i}{\hbar}\frac{\partial\mathbb{S}}{\partial a}\right) = e^{i\mathbb{S}/\hbar}\left(\frac{i}{\hbar}\frac{\partial^2\mathbb{S}}{\partial a^2} + \left(\frac{i}{\hbar}\frac{\partial\mathbb{S}}{\partial a}\right)^2\right), \tag{4.28}$$

where $\partial\Psi/\partial a$ has been calculated in the second equality. Similar expressions hold for $\partial^2\Psi/\partial\phi^2$ and $\partial\Psi/\partial\phi$, simply by replacing a with ϕ in the above expression.

Considering terms up to $\hbar^1$ order, we obtain:

$$\begin{aligned} &e^{i\mathbb{S}/\hbar}\left[\left(\frac{i}{\hbar}\frac{\partial\mathbb{S}_0}{\partial a}\right)^2 + \frac{i}{\hbar}\frac{\partial^2\mathbb{S}_0}{\partial a^2} + \frac{\overline{p}}{a}\frac{i}{\hbar}\frac{\partial\mathbb{S}_0}{\partial a} - \frac{6M_{\rm pl}^2}{a^2}\left(\left\{\frac{i}{\hbar}\frac{\partial\mathbb{S}_0}{\partial\phi}\right\}^2 + \frac{i}{\hbar}\frac{\partial^2\mathbb{S}_0}{\partial\phi^2}\right) - \frac{1}{\hbar^2}U\right] \\ &+ e^{i\mathbb{S}/\hbar}\frac{\hbar}{i}\left(\frac{i}{\hbar}\right)^2\left[\left(\frac{\partial\mathbb{S}_0}{\partial a}\frac{\partial\mathbb{S}_1}{\partial a} + \frac{\partial\mathbb{S}_1}{\partial a}\frac{\partial\mathbb{S}_0}{\partial a}\right) - \frac{6M_{\rm pl}^2}{a^2}\left(\frac{\partial\mathbb{S}_0}{\partial\phi}\frac{\partial\mathbb{S}_1}{\partial\phi} + \frac{\partial\mathbb{S}_1}{\partial\phi}\frac{\partial\mathbb{S}_0}{\partial\phi}\right)\right] + \ldots = 0 \end{aligned} \tag{4.29}$$

Multiplying by $\hbar^2$ and separating by orders of $\hbar$, we obtain for $\hbar^0 = 1$:

$$\hbar^0 : -\left(\frac{\partial\mathbb{S}_0}{\partial a}\right)^2 + \frac{6M_{\rm pl}^2}{a^2}\left(\frac{\partial\mathbb{S}_0}{\partial\phi}\right)^2 - U(a,\phi) = 0, \tag{4.30}$$

and for $\hbar^1$, factoring out i:

$$\hbar^1 : \frac{\partial^2\mathbb{S}_0}{\partial a^2} - \frac{6M_{\rm pl}^2}{a^2}\frac{\partial^2\mathbb{S}_0}{\partial\phi^2} + 2\frac{\partial\mathbb{S}_0}{\partial a}\frac{\partial\mathbb{S}_1}{\partial a} - \frac{12M_{\rm pl}^2}{a^2}\frac{\partial\mathbb{S}_0}{\partial\phi}\frac{\partial\mathbb{S}_1}{\partial\phi} + \frac{\overline{p}}{a}\frac{\partial\mathbb{S}_0}{\partial a} = 0. \tag{4.31}$$

Higher-order terms will not be considered in this work. Note that the $\overline{p}$-parameter we introduced affects only the second equation, not the first.

4.2.3 Semiclassical Analysis: Consistency with Classical Mechanics

Before proceeding with the approximation, we must verify that we recover the classical equations in the classical limit. In this limit, only equation (4.30) remains from the WKB approximation. Substituting (4.27) into (4.21), we obtain the classical operators associated with the system (recalling (4.13) and (4.14)):

$$\hat{p}_a\Psi = \left(\frac{\partial\mathbb{S}_0}{\partial a} + \mathcal{O}(\hbar)\right)\Psi, \quad \hat{p}_\phi\Psi = \left(\frac{\partial\mathbb{S}_0}{\partial\phi} + \mathcal{O}(\hbar)\right)\Psi, \tag{4.32}$$

that is, the classical momenta are:

$$p_a = \frac{\partial\mathbb{S}_0}{\partial a} = -12\pi^2 M_{\rm pl}^2 a\dot{a}, \tag{4.33}$$

$$p_\phi = \frac{\partial \mathbb{S}_0}{\partial \phi} = 2\pi^2 a^3 \dot{\phi}. \tag{4.34}$$

Note that in the classical limit, time serves as the independent variable, whereas in the quantum description, a and ϕ are the independent variables. Then, it will be more convenient to write down their derivatives obtained via (4.33) and (4.34):

$$\dot{a} = -\frac{\lambda}{a}\frac{\partial \mathbb{S}_0}{\partial a}, \qquad \dot{\phi} = \frac{1}{2\pi^2 a^3}\frac{\partial \mathbb{S}_0}{\partial \phi}. \tag{4.35}$$

This set of equations will play a fundamental role in our quantum description, as their solutions automatically satisfy Eqs. (3.9) and (3.11) (but the converse is not guaranteed). Let us verify this explicitly.

Using (4.33) and (4.34), we can derive equations that coincide with (3.9) and (3.11), the classical equations describing the closed universe.

To obtain (3.9), H^2, we use $\dot{a}$ from (4.33) and (4.30):

$$\begin{aligned} H^2 = \left(\frac{\dot{a}}{a}\right)^2 &= \frac{p_a^2}{(12\pi^2 M_{\rm pl}^2 a^2)^2} = \frac{1}{(12\pi^2 M_{\rm pl}^2 a^2)^2}\left(\frac{6M_{\rm pl}^2}{a^2}\left(\frac{\partial \mathbb{S}_0}{\partial \phi}\right)^2 - U(a,\phi)\right) \\ &= \frac{1}{(12\pi^2 M_{\rm pl}^2 a^2)^2}\left(\frac{6M_{\rm pl}^2}{a^2}\left(2\pi^2 a^3 \dot{\phi}\right)^2 - \left(12\pi^2 M_{\rm pl}^2\right)^2\left(a^2 - \frac{V(\phi)}{3M_{\rm pl}^2}a^4\right)\right) \\ &= \frac{1}{3M_{\rm pl}^2}\left(\frac{1}{2}\dot{\phi} + V(\phi)\right) - \frac{1}{a^2}. \end{aligned} \tag{4.36}$$

This result yields the Friedmann equation (3.9). Next, using (4.34):

$$\ddot{\phi} = \frac{\partial}{\partial t}\left(\frac{1}{2\pi^2 a^3}\frac{\partial \mathbb{S}_0}{\partial \phi}\right) = \frac{1}{2\pi^2 a^3}\left[-\frac{3\dot{a}}{a}\frac{\partial \mathbb{S}_0}{\partial \phi} + \frac{\partial}{\partial t}\left(\frac{\partial \mathbb{S}_0(a,\phi)}{\partial \phi}\right)\right] \tag{4.37}$$

$$= -3H\dot{\phi} + \frac{1}{2\pi^2 a^3}\frac{\partial}{\partial t}\left(\frac{\partial \mathbb{S}_0(a,\phi)}{\partial \phi}\right). \tag{4.38}$$

To evaluate the last term, we employ the chain rule:

$$\frac{\partial}{\partial t}\left(\frac{\partial \mathbb{S}_0(a,\phi)}{\partial \phi}\right) = \dot{a}\frac{\partial^2 \mathbb{S}_0}{\partial a \partial \phi} + \dot{\phi}\frac{\partial^2 \mathbb{S}_0}{\partial \phi^2} = \dot{a}\frac{\partial p_a}{\partial \phi} + \dot{\phi}\frac{\partial p_\phi}{\partial \phi}. \tag{4.39}$$

Since we cannot directly compute this value, we utilize the fact that the Friedmann equation is already satisfied and can be expressed in terms of p_a and p_ϕ as in (4.16). Differentiating it with respect to ϕ yields:

$$\begin{aligned} 0 = \frac{\partial p_a^2}{\partial \phi} - \frac{6M_{\rm pl}^2}{a^2}\frac{\partial p_\phi^2}{\partial \phi} - \frac{a^4}{3M_{\rm pl}^2\lambda^2}V'(\phi) &= 2p_a\frac{\partial p_a}{\partial \phi} - \frac{6M_{\rm pl}^2}{a^2}2p_\phi\frac{\partial p_\phi}{\partial \phi} - \frac{a^4}{3M_{\rm pl}^2\lambda^2}V'(\phi) \\ = -2\cdot 12\pi^2 M_{\rm pl}^2 a\dot{a}\frac{\partial p_a}{\partial \phi} - \frac{12M_{\rm pl}^2}{a^2}2\pi^2 a^3\dot{\phi}\frac{\partial p_\phi}{\partial \phi} - \frac{12^2\pi^4 M_{\rm pl}^4 a^4}{3M_{\rm pl}^2}V'(\phi), \end{aligned} \tag{4.40}$$

which can be expressed equivalently as:

$$\dot{a}\frac{\partial p_a}{\partial \phi} + \dot{\phi}\frac{\partial p_\phi}{\partial \phi} = -2\pi^2 a^3 V'(\phi) = \frac{\partial}{\partial t}\left(\frac{\partial \mathbb{S}_0(a,\phi)}{\partial \phi}\right). \tag{4.41}$$

Thus, equation (4.38) becomes:

$$\ddot{\phi} + 3H\dot{\phi} + V'(\phi) = 0, \tag{4.42}$$

which is the acceleration equation (3.11). This demonstrates how the WKB approximation to the WDW solutions connects with the classical Friedmann and acceleration equations. The quantum-to-classical transition reveals that every quantum solution describes a universe whose classical limit follows these standard cosmological equations. This is particularly noteworthy because our quantum description will be centered on the system governed by equations (4.35).

5 Case of Study: Constant Potential

In this final section, we examine the Wheeler-DeWitt equation for a constant potential scenario. Recalling the superpotential function defined in (4.16) and considering $V(\phi) = V_0 \in \mathbb{R}^+$, we can express it as:

$$\overline{U}(a,\phi) = \frac{1}{\lambda^2}\left(a^2 - \frac{V_0}{3M_{\text{pl}}^2}a^4\right) = \frac{a^2}{\lambda^2}\left(1 - \frac{a^2}{p^2}\right) = \overline{U}_0(a), \tag{5.1}$$

where $p^2 = 3M_{\text{pl}}^2/V_0$, as previously defined.

For our analysis, we will employ the following ansatz to seek solutions of the form:

$$\mathbb{S}_0(a,\phi) = S_0(a) + k\phi, \quad k \in \mathbb{R}, \tag{5.2}$$

$$\mathbb{S}_n(a,\phi) = S_n(a), \qquad n \in \mathbb{N} - \{0\}. \tag{5.3}$$

This demonstrates how solution (4.26) connects to our new solutions. By adopting this approach, we effectively separate the $\mathbb{S}$ dependence between the independent variables a and ϕ, at the cost of introducing a new variable k.

Thus, the first equation (4.30) that we already obtained with the WKB approximation becomes, in this particular case:

$$\left(\frac{dS_0}{da}\right)^2 - \frac{k^2}{2\pi^2\lambda}\cdot\frac{1}{a^2} + \overline{U}_0(a) = 0 = \left(\frac{dS_0}{da}\right)^2 + U(k,a), \tag{5.4}$$

where we have redefined:

$$U(k,a) := \overline{U}_0(a) - \frac{k^2}{2\pi^2\lambda a^2} = \frac{a^2}{\lambda^2}\left(1 - \frac{a^2}{p^2} - \frac{k^2\lambda}{2\pi^2 a^4}\right). \tag{5.5}$$

And the second equation obtained with the WKB approximation, (4.31), will simplify to, noting that $\partial_\phi \mathbb{S}_1 = 0 = \partial_\phi^2 \mathbb{S}_0$:

$$\frac{d^2S_0}{da^2} + 2\frac{dS_0}{da}\frac{dS_1}{da} + \frac{\overline{p}}{a}\frac{dS_0}{da} = 0. \tag{5.6}$$

Our new system of equations are (5.4) and (5.6). We can solve the first one directly:

$$S_0(k,a) = \pm\int_{a_0}^{a}\sqrt{-U(k,a')}\,da' = \pm\int_{a_0}^{a} r(k,a')\,da', \tag{5.7}$$

with a_0 as a reference point. Note that S_0 is a real valued function only if $U(k,a) \leq 0$, and otherwise, i.e. $U(k,a) > 0$, it will be a complex valued function. With S_0, let us substitute it into (5.6) to obtain the next term of the WKB approximation S_1:

$$\frac{dr}{da} + 2r\frac{dS_1}{da} + \frac{\overline{p}}{a}r = 0, \tag{5.8}$$

which can be reduced by imposing $r(k,a) \neq 0$, such that:

$$\frac{dS_1}{da} = -\frac{1}{2}\left(\frac{\overline{p}}{a} + \frac{1}{r(k,a)}\frac{d}{da}r(k,a)\right), \tag{5.9}$$

with the straightforward solution:

$$S_1(a) = c_1 - \frac{\overline{p}}{2}\ln(a) - \frac{1}{2}\ln(r(k,a)) = c_1 - \ln\sqrt{a^{\overline{p}}\, r(k,a)}. \tag{5.10}$$

Consequently, the wave function of the whole Universe $\Psi[a,\phi] = e^{i\mathbb{S}/\hbar}$ is given by:

$$\Psi_\pm[k,a,\phi] = e^{i\mathbb{S}_0/\hbar}e^{\mathbb{S}_1} = \frac{1}{\sqrt{a^{\overline{p}}\, r(k,a)}}\exp\left(\pm\frac{i}{\hbar}\int_{a_0}^{a} r(k,a')\,da'\right)e^{ik\phi/\hbar}. \tag{5.11}$$

We could normalize this wave function, but doing so would require verifying that it is square-integrable such that $\int da\, d\phi \overline{\Psi}_\pm \Psi_\pm < +\infty$ [23]. While we will not explicitly normalize it here, the condition above will be satisfied if and only if $\overline{p} \leq 1$ (demonstrated in the following sections). Then, $U > 0$ and $U < 0$ divides our problem in two regions [67] (in total analogy to what happen to a particle inside a box with barriers $V > E$ described by the Schrödinger equation, i.e., with a value of the potential in the barriers higher than the energy of the particle [97]):

- If $U(k,a) > 0$, we have a classically forbidden region where Ψ is oscillating combined with an exponential decrease due to the fact that r is an imaginary valued function. Therefore, the first exponent of $\Psi_\pm$ is of the form:

$$\pm\frac{i}{\hbar}\int_{a_0}^{a} i\sqrt{|U(k,a')|}\,da' = \mp\frac{1}{\hbar}\int_{a_0}^{a}\sqrt{|U(k,a')|}\,da' \in \mathbb{R}, \tag{5.12}$$

  that is, a real number.

- And if $U(k,a) < 0$, there is a classically allowed region where Ψ is oscillatory because $e^{ix} = \cos(x) + i\sin(x)$.

The boundary between both regions is $U = 0$.

Once we have obtained the wave function of the universe, we may ask ourselves which are the classical allowed regions. This wave function is strongly peaked around the solutions of equations (4.35), which in our case are:

$$\dot{a} = \mp \frac{\lambda}{a} r(k,a), \qquad \dot{\phi} = \frac{k}{2\pi^2 a^3}. \tag{5.13}$$

This system reduces to the set of equations (3.37) and (3.38). By comparing boths $\dot{a}$ expression, we can discuss the different classical universes that may emerge for a constant potential.

This study can be simplified and generalized for the quantum regime for low and high values of a, for which the superpotential (5.5) may reduce its form.

5.1 Asymptotic behaviour of the wave functions as $a \to +\infty$

In this case, far away from the singularity in which all of our solutions will be in the inflation phase, our superpotential (5.5) will be reduce to:

$$U_{a\to\infty}(k,a) = \frac{a^2}{\lambda^2}\left(1 - \frac{a^2}{p^2}\right) = U_{a\to\infty}(a). \tag{5.14}$$

This superpotential is the same that we have for $k = 0$, and that has been represented in Fig. 16. It can be seen that there is a classically forbiden region in $a \in (0,p)$, and an allowed one in $a > p$.

The Wheeler-DeWitt equation associated to this case, from (4.25), is:

$$\left(\frac{d^2}{da^2} + \frac{\overline{p}}{a}\frac{d}{da} - \frac{1}{\hbar^2}U_{a\to\infty}(a)\right)\Psi^{(\infty)}(a) = 0. \tag{5.15}$$

This form was presented in [67], and this equation have an expression of the wave function (5.11) that we can obtain. To obtain it, we can compute its form using the WKB approximation of the solutions given by Equations (5.7) and (5.10).

Like the classically allowed region is $a > p$, we can it take as the reference point for integration, which is reasonable because it is the unique positive zero of $U_{a\to\infty}$. Thus, (5.7) will be given by:

$$S_0(k,a)|_{a\to\infty} = \pm\int_p^a \frac{a'}{\lambda}\sqrt{-\left(1 - \frac{a'^2}{p^2}\right)}\,da' = \frac{p^2}{3\lambda}\left(\frac{a^2}{p^2} - 1\right)^{3/2} = \frac{M_{\rm pl}^2}{\lambda V_0}\left(\frac{a^2}{p^2} - 1\right)^{3/2}. \tag{5.16}$$

With it, the wave function for $a \to \infty$, that is, at large scale factor, is:

$$\Psi_{\pm}^{(\infty)}(a) = \lambda^{1/2} a^{-(\overline{p}+1)/2}\left(\frac{a^2}{p^2} - 1\right)^{-1/4} \times \exp\left[\pm\frac{i}{\hbar}\frac{M_{\rm pl}^2}{\lambda V_0}\left(\frac{a^2}{p^2} - 1\right)^{3/2}\right] \cdot e^{ik\phi/\hbar}. \tag{5.17}$$

$\Psi_+^{(\infty)}$ is associated with a contracting universe ($\dot{a} < 0$), and $\Psi_-^{(\infty)}$ with an expanding one, both in the inflatianory phase, see Fig. 10.

It must be verfied that $V_0 \ll M_{\rm pl}^4$ in the classical limit because the energy density $\rho < M_{\rm pl}^4$ and the kinetic energy $K_e \in \mathbb{R}^+$ is positive by definition, such that $\rho = V_0 + K_e < M_{\rm pl}^4$. Then via (3.21),

$$p = \frac{\sqrt{3} M_{\rm pl}}{\sqrt{V_0}} \gg \frac{\sqrt{3}}{M_{\rm pl}}, \tag{5.18}$$

because $1/V_o \gg 1/M_{\rm pl}^4$. Therefore, a takes values much higher than the classical limit allowed, and remembering that the condition for the inflationary regime was (3.23), we can combine all this results in:

$$a > \sqrt{\frac{2}{V_0}} M_{\rm pl} = \sqrt{\frac{2}{3}} p \gg \frac{\sqrt{2}}{M_{\rm pl}}, \tag{5.19}$$

verifying a the necessary condition for the model to be in the classical limit given by (3.21). In conclusion, the classical solution emerges in the classical limit in the inflationary regime for $a \to \infty$, in which is verified that $a > \sqrt{2/3}\, p$, and for that reason p is an appropiate lower limit.

Just to relate this solution with some obtained by Vilenkin and Hartle-Hawking in previous works:

1. **Vilenkin tunneling wave function** [98, 24]: Their wave function is defined as:
$$\Psi_T(k, a, \phi) = e^{i\pi/4} e^{-M_{\rm pl}^2/(\lambda\hbar V_0)} e^{ik\phi/\hbar} \Psi_-^{(\infty)}(a) \tag{5.20}$$
in the region where $a > p$. That is, they described an expanding universe, which is of great interest because it is associated (theoretically) with a more realistic model.

2. **Hartle-Hawking wave function** [23, 99]: And this second wave function was taking as a superposition of wave functions associated to contracting and expanding universes given by:
$$\Psi_{NB}(k, a, \phi) = e^{M_{\rm pl}^2/(\lambda\hbar V_0)} \left(e^{-i\pi/4} \Psi_+^{(\infty)}(a) + e^{i\pi/4} \Psi_-^{(\infty)}(a) \right) e^{ik\phi/\hbar}. \tag{5.21}$$

5.2 Asymptotic behaviour of the wave functions as $a \to 0^+$

Now, let us evaluate how is our problem described when $a \to 0^+$, i.e. near the singularity that is at $a = 0^+$.

In this case, the superpotential (5.5) reduce to:

$$U_{a\to o^+}(k,a) = \frac{a^2}{\lambda^2}\left(1 - \frac{k^2\lambda}{2\pi^2 a^4}\right) = \frac{a^2}{\lambda^2}\left(1 - \frac{y(k)^4}{a^4}\right), \tag{5.22}$$

where we have defined $y(k) := (k^2\lambda/(2\pi^2))^{1/4} = (\sqrt{6}M_{\rm pl}\lambda|k|)^{1/2}$, in total analogy to the p we had in the last section.

This superpotential only have a positive zero at $y(k)$, being now the classically allowed region that near the origin (at the left of $y(k)$), and the forbiden one classically for $a > y(k)$, see Fig. 15. Note that the $k-$parameter can not take all values. If it is lower, $y(k)$ will move nearest $a = 0$, while if it is higher, it will move to the left, to higher values of a. This will limitate our classical region, but it can not be null because of (3.21). That is, this condition will impose a minimum value of k via $y(k)$, that can not be lower than this limit. Therefore, combining the classical limit condition (3.21) and the expression of $y(k)$:

$$y(k)^2 = \frac{|k|\sqrt{6}M_{\rm pl}}{12\pi^2 M_{\rm pl}^2} > a^2 > \frac{3}{M_{\rm pl}^2}, \tag{5.23}$$

from which we can derive the minimum value of k:

$$|k| > \frac{6\sqrt{6}\pi^2}{M_{\rm pl}}. \tag{5.24}$$

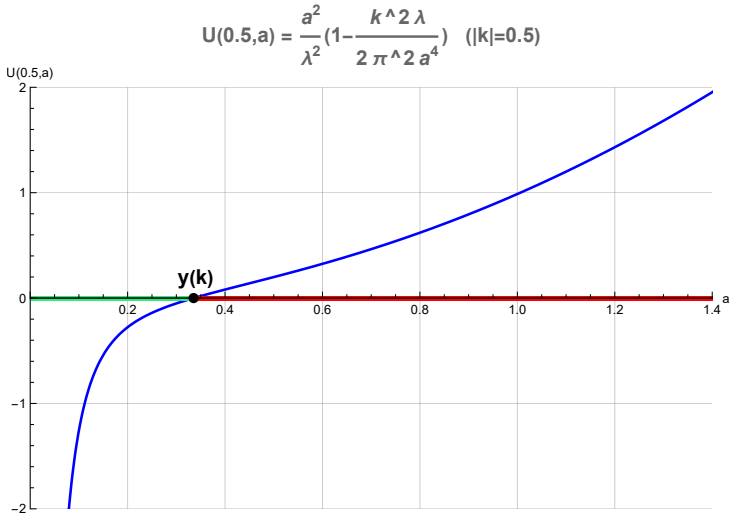

Figure 15: For parameters $k = 0.5$ and $\lambda = 1$, we show the superpotential function $U(k,a)$ (5.22) ($U(k,a) < 0$, green region, and otherwise red). The point is $y(k) = (k^2\lambda/(2\pi^2))^{1/4}$.

Thus, the WDW equation in this case is:

$$\left(\frac{d}{da^2} + \frac{\overline{p}}{a}\frac{d}{da} - \frac{1}{\hbar^2}U_{a\to 0}(a)\right)\Psi^{(0)}(a) = 0. \tag{5.25}$$

We want to evaluate it near the origin, so we can obtain the wave function (5.11) using this time as the reference point $y(k)$, and by taking $y(k) > a$, we can obtain the wave function in the classical region allowed that is where all our assumptions make sense. First, let us calculate (5.7):

$$\begin{aligned} S_0(k,a)|_{a\to 0} &= \mp\int_a^{y(k)} \frac{1}{\lambda}\frac{\sqrt{y(k)^4 - a'^4}}{a'}da' \\ &= \pm\frac{1}{2\lambda}\left[\sqrt{y(k)^4 - a^4} - y(k)^2\ln\left(y(k)^2 + \sqrt{y(k)^4 - a^4}\right) + y(k)^2\ln(a^2)\right]. \end{aligned} \tag{5.26}$$

In the limit in which $a \to 0^+$, the last term is the dominant, because $\lim_{a\to 0^+}\ln a = -\infty$, and because of this it will be the only term that we will keep:

$$S_0(k,a)|_{a\to 0^+} \sim \pm\frac{y(k)^2}{\lambda}\ln(a) = \pm\sqrt{6}M_{\rm pl}|k|\ln(a). \tag{5.27}$$

Second, the denominator of the wave function (5.11) now it is not trivial:

$$(a^{\overline{p}}r(k,a))^{-1/2} = \left[\frac{a^{\overline{p}-1}}{\lambda}\sqrt{y(k)^4 - a^4}\right]^{-1/2} \sim \frac{\lambda^{1/2}}{y(k)}a^{(1-\overline{p})/2} \tag{5.28}$$

as $a \to 0^+$. If we want our wave function to be regular at $a = 0$, then we can not have a term as $1/a$, which can be avoid by taking $\overline{p} \leq 1$.

Then, the wave function associated to this particular case is:

$$\Psi^{(0)}_{\pm}(k,a,\phi) \sim \frac{\lambda^{1/2}}{y(k)}a^{(1-\overline{p})/2}\exp\left[\pm\frac{i}{\hbar}\left(\sqrt{6}M_{\rm pl}|k|\ln(a)\right)\right]\cdot e^{ik\phi/\hbar}. \tag{5.29}$$

They will describe the universe near $a \to 0^+$, i.e., in the kinetic dominance phase, such that $\Psi^{(0)}_+$ will be associated with a contrancting universe, and $\Psi^{(0)}_-$ with an expanding one. To justify that these equations describe the kinetic dominance phase, we substitute $S_0(k,a)|_{a\to 0}$ from (5.27) into the first equation from (4.35):

$$\dot{a} = \frac{da}{dt} = -\frac{\lambda}{a}\frac{\partial\mathbb{S}_0}{\partial a} \sim \mp\lambda\sqrt{6}M_{\rm pl}|k|\frac{1}{a^2} = \mp\frac{y(k)}{a^2}. \tag{5.30}$$

This equation can be solved by separating variables:

$$a^2\,da \sim \mp y(k)\,dt, \tag{5.31}$$

whose solutions are:

$$a^3 \sim \overline{a}_0^3 \mp 3y(k)\cdot(t-\overline{t}_0) = 3y(k)\cdot\left[\mp t \pm \overline{t}_0\left(1-\frac{\overline{a}_0^3}{3\overline{t}_0 y(k)}\right)\right] \equiv a_0^3(\mp t \pm t_0), \quad (5.32)$$

where we have defined $a_0 = 3y(k)$ and $t_0 = \overline{t}_0(1-\overline{a}_0^3/(3\overline{t}_0 y(k)))$, with $\overline{t}_0$ being a reference integration time such that $a(\overline{t}_0) := \overline{a}_0$. Thus, it is obtained associated to $\Psi_+^{(0)}$ that $a \sim a_0(t_0 - t)$, representing a contracting universe in the kinetic dominance phase, consistent with (3.34); and associated to $\Psi_-^{(0)}$ is $a \sim a_0(t - t_0)$, describing an expanding universe in the same phase, now consistent with (3.31).

This last wave function can be related with the classical universes that are represented in Fig. 11 and 17 for $a \to 0^+$, that is, it describes the solutions that are in the kinetic dominance regime in the classically allowed region that is at the left of p_1.

But we pointed out that the most relevant universe that emerges are that with an inflationaty and kinetic dominance phases, that are the ones associated to Fig. 13 and 19 for $k > \sqrt{8\pi^2 p^4/(27\lambda)}$. If this condition is satified, given the general wave function:

$$\begin{aligned}\Psi_\pm(k,a,\phi) &= \frac{e^{ik\phi/\hbar}}{a^{\overline{p}} r(k,a)} \exp\left[\mp\frac{i}{\hbar}\int_a^{y(k)} r(k,a')da' \mp \frac{i}{\hbar}\int_{y(k)}^{p} r(k,a')da'\right] \\ &\sim \Psi_\pm^{(0)}(k,a,\phi)\exp\left[\mp\frac{i}{\hbar}\int_{y(k)}^{p} r(k,a')da'\right] \end{aligned} \quad (5.33)$$

if $a \to 0^+$, $\Psi_-(k,a,\phi)$ would be the one that represents our expanding universe, one that started (theoretically) with a kinetic dominance phase that was preceed by a inflationary regime.

5.3 Connection between quantum and classical solutions

This section will be in total analogy with the one we study in-deepth in Section 3.5. For that, we can compare both expressions we have for $\dot{a}$ obtained from the classical,

$$\dot{a}^2 = \frac{q}{a^4} + \frac{a^2}{p^2} - 1, \quad (5.34)$$

and the WKB approach,

$$\dot{a}^2 = \frac{k^2\lambda}{2\pi^2 a^4} + \frac{a^2}{p^2} - 1. \quad (5.35)$$

such that we identify $q = k^2\lambda/(2\pi^2)$, which was evaluated for different values. The key point is the one that makes the right-hand side of (5.34) equal to zero, which was associated to $q = 4p^4/27$. That is, in our case we will have four

different scenarios. All these behaviours can be related with the form of the superpotential (5.5) via k, such that the classically allowed region will be that associated with a negative superpotential. Let us explain in more detail the relation for the different values of k:

1. $k=0$: If $q=0$, then $k=0$. This scenario is basically the same that we got in Section 3.5.1. $U(0,a)$ will be negative from the point $a=p$, see Fig. 16, which is in total analogy with what we plot on Fig. 10, with the allowed region for $P(A)>0$, and an associated contracting and expanding universe described by the classical inflation without kinetic dominance.

   Even more, as $U(0,a)<0$, via (5.13), $\dot{a}$ will be a real valued function, such that the negative solution, $\dot{a}<0$, is related with a contracting universe in the inflation phase, described by the wave function Ψ_+ from (5.11); and $\dot{a}>0$ is related with an expanding universe described by Ψ_-.

2. $|k| \in \left(0, \sqrt{8\pi^2 p^4/(27\lambda)}\right)$**:** If $q \in (0, 4p^4/27)$, that means that in the upper limit, $q = 4p^4/27 = k^2\lambda/(2\pi^2) = 4M_{\rm pl}^4/(3V_0^2)$, from where we can obtain the upper limit of k, $k^2 = 8\pi^2 p^4/(27\lambda)$ and $|k| = \sqrt{8\pi^2 p^4/(27\lambda)} = 4\sqrt{2}\pi^2 M_{\rm pl}^3/V_0$. This was studied in Section 3.5.2.

   In this second case, $U(|k|=1,a)$ becomes only positive in an inner region between p_1 and p_2, and negative in the rest of the domain, see Fig. 17, i.e., there are two disconnected regions with negative superpotential that are associated with the classical allowed regions.

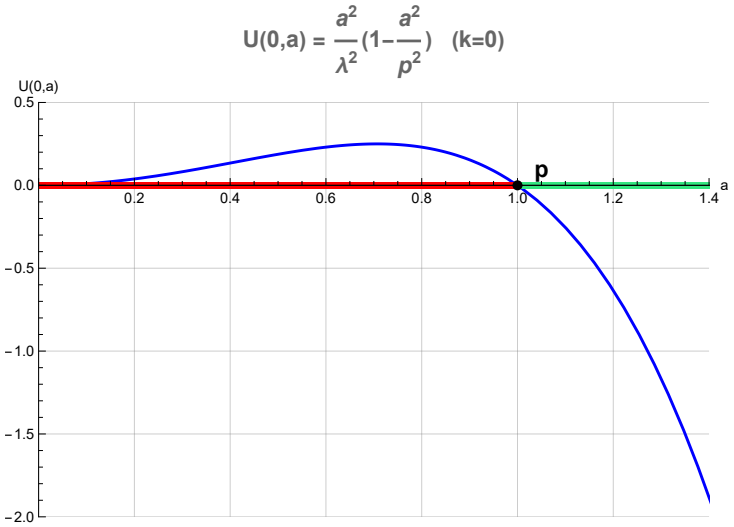

Figure 16: For parameters $k=0$, $\lambda=1$ and $p=1$, we show the superpotential function $U(0,a)$ (5.5) ($U(0,a)<0$, green region, and otherwise red).

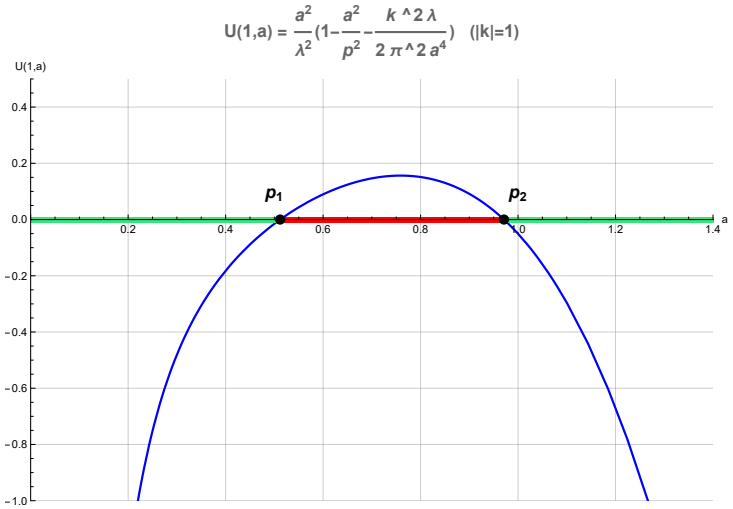

Figure 17: For parameters $|k| = 1$, $\lambda = 1$ and $p = 1$, we show the superpotential function $U(1,a)$ (5.5) ($U(1,a) < 0$, green region, and otherwise red).

This behaviour can be clearly in Fig. 11, with two different solutions: in the range $(0, p_1)$, there is an expanding universe associated with $\dot{a} > 0$ and Ψ_- that reaches its maximum size at $a = p_1$, and it starts to collapse towards the initial singularity $a = 0$ with $\dot{a} < 0$ describded by Ψ_+, both in the kinetic dominance phase because they undergoes and depart from $a = 0$ as described in Section 5.2. That is, they describe the dynamic of the universe near the Big Crunch and the Big Bang, respectively.

And in the range $(p_2, +\infty)$, again we have the universe described for $k = 0$ in the inflation phase but with p_2 instead of p.

In this study, k must satisfy the classical condition given by (5.24), which is satisfied when:

$$\frac{4\sqrt{2}\pi^2 M_{\rm pl}^3}{V_0} > |k| \gg \frac{4\sqrt{2}\pi^2}{M_{\rm pl}} > 0, \tag{5.36}$$

where we have used $V_0 \ll M_{\rm pl}^4$. Consequently, $|k| > 6\sqrt{6}\pi^2/M_{\rm pl}$ will be verified. While we have chosen the plot parameters of Fig. 17 for simplicity, their values must be carefully selected to satisfy all these conditions. For $k = 4\sqrt{2}\pi^2 M_{\rm pl}^3/V_0 = 1$, we have $M_{\rm pl}^3 = V_0/(4\sqrt{2}\pi^2)$, from where we conclude that $M_{\rm pl}^4 \gg V_0$, being in the classical limit.

3. $|k| = \sqrt{8\pi^2 p^4/(27\lambda)} = 4\sqrt{2}\pi^2 M_{\rm pl}^3/V_0$: If $q = 4p^4/27$, it is straight to obtain this value of k. This was studied in Section 3.5.3.

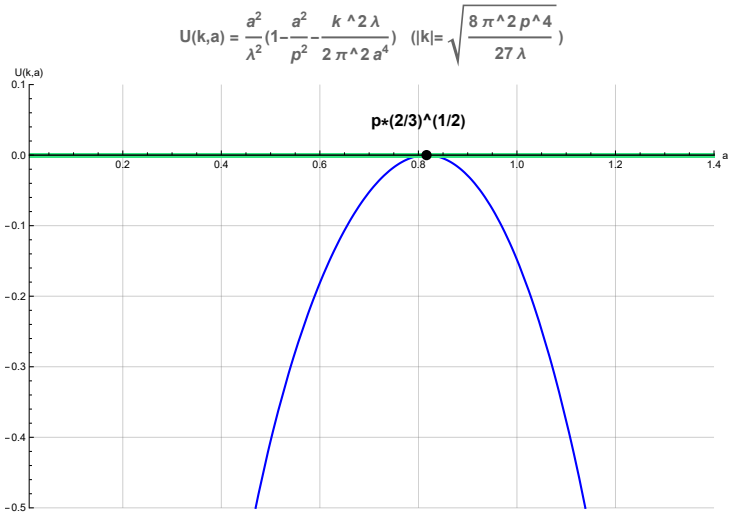

Figure 18: For parameters $|k| = \sqrt{8\pi^2/27} \approx 1.71$, $\lambda = 1$ and $p = 1$, we show the superpotential function $U(k,a)$ (5.5) ($U(k,a) < 0$, green region).

In this case, $U(|k|,a)$ will only be non-negative in one point where $a = \sqrt{2}p/\sqrt{3}$, and in the rest it will be negative, see Fig. 18.

This can be seen in Fig. 12, where the four solutions that we have already defined for $|k| \in \left(0, \sqrt{8\pi^2 p^4/(27\lambda)}\right)$ tend asympotically in one of their extremes to the solution associated with $\dot{a} = 0$. Thus, these solutions are separated, but we can describe them with $\Psi_\pm$ for a contracting and an expanding universe, respectively.

Now, $|k| = 2\sqrt{2}\pi/\sqrt{27} = 4\sqrt{2}\pi^2 M_{\rm pl}^3/V_0$ for $p = 1$ and $\lambda = 1$, so $M_{\rm pl}^3 = V_0/(2\sqrt{27}\pi)$, satisfying again the classical behaviour in the classically allowed regions.

4. $|k| > \sqrt{8\pi^2 p^4/(27\lambda)}$: this last case is associated with $q > 4p^4/27$, which was studied in Section 3.5.4.

   Finally, all the superpotential in this regime verify $U(|2|,a) < 0$, for $a > 0$, see Fig. 19. This will bring up two new scenarios, in which if $\dot{a} > 0$, an expanding universe will be describe by Ψ_- with a kinetic dominance phase for low values of a, that later on enters an inflation phase for high values of a, in total analogy with what is represented in Fig. 13; and if $\dot{a} < 0$, a contracting universe described by Ψ_+ emerges, with an initial inflation phase and a following kinetic dominance phase during the contraction towards the singularity at $a = 0$.

Note that $\Psi_\pm$ are oscillatory functions on the whole classically allowed region

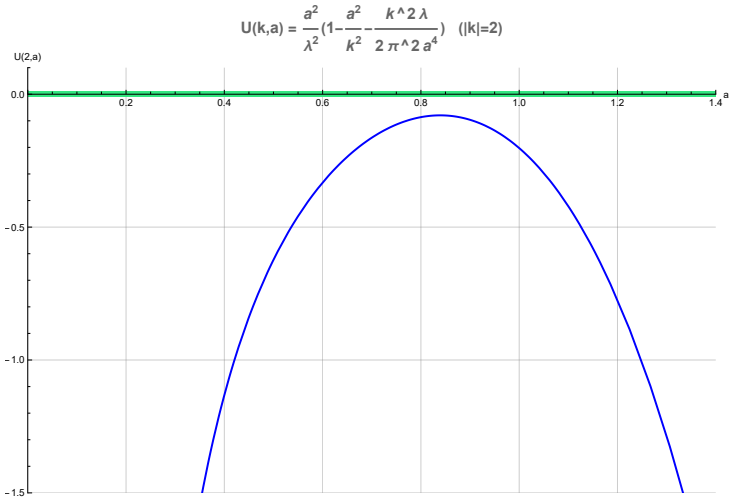

Figure 19: For parameters $|k| = 2$, $\lambda = 1$ and $p = 1$, we show the superpotential function $U(2,a)$ (5.5) ($U(2,a) < 0$, green region).

with $a > 0$.

5.4 General wave function of the Universe for different $k-$values

In this final section, we will focus on representing the wave function (5.11) for different values of k, which will lead us to various behaviors and reveal classically allowed and forbidden regions when plotted as a function of a.

Moreover, another observable that is particularly interesting in quantum mechanics is the probability density, given by [100, 101]:

$$\sigma(k,a,\phi) = |\Psi_{\pm}(k,a,\phi)|^2. \tag{5.37}$$

Note that from the definition of our wave function, the probability density as a function of a is identical for both expanding and contracting universes. This quantity is actually the relevant one because it represents what we can measure, at least in laboratory experiments. Although we cannot measure it for the entire Universe, it gives us an idea of which values and regions of a are most significant. Furthermore, it might even explicitly show us that there is some non-zero probability of the Universe existing in the forbidden regions.

Thus, in the following plots we will represent both the real and imaginary parts of $\Psi_{\pm}$, as well as its squared magnitude $|\Psi_{\pm}|^2$ (obtained by multiplying the wave function by its complex conjugate), which is a real valued function.

In this section we will study the wave functions for $\overline{p} = 0$. In Appendix F we have performed the same analysis for $\overline{p} = 1$, which requires no additional

comments because the results are essentially identical for both cases. The slight differences between them will be discussed in the appendix.

5.4.1 $k = 0$

First, for $k = 0$, we have classically forbidden and allowed regions for $a \leq p$ and $a > p$, respectively, as shown in Fig. 16. As previously explained, in the forbidden region ($U < 0$), the wave function behaves as a decaying exponential, while in the allowed region ($U > 0$), it exhibits oscillatory decay towards zero. This exact behavior is represented in the first panel of Fig. 20, where the forbidden region ($a < p$) is shown in red, the classically allowed region ($a > p$) in green, and p is marked as a single point.

Note that both components (real and imaginary parts) of our wave function displays two peaks: one at $a = 0$ (with a finite maximum value of 1565.2), and another near $a = p$ (with a value of $\sim 4 \ll 1565.2$), corresponding to the transition between regions. In the classically forbidden region, the wave function behaves as a decaying exponential (it will not oscillate in any forbidden region of this entire section because we have taken $\phi = 0$ in the wave function (5.11), such that $e^{ik\phi} = 1$, $\forall\, |k|$), while in the green region it shows oscillatory behavior combined with exponential decay.

On the other hand, the second panel of Fig. 20 shows $|\Psi_{\pm}|^2$, representing the probability density for the Universe's initial conditions as a function of a. At $a = 0$, the probability density reaches $\sim 10^6$ (a remarkably high value), then decays to $\sim 10^1$ at the second peak, and continues decreasing below 1 in the classically allowed region. This verifies that $\lim_{a\to\infty} \Psi_+ = 0$, demonstrating good behavior for a normalizable wave function (though we have not normalized it here, which would only require a multiplicative constant).

Thus, in this case there is a high probability for the Universe to begin in the forbidden region ($a = 0$ and nearby values), and a much lower probability for initial conditions with $a > p$ (where we recover the classical solutions described earlier). That is, the classical solution associated with this quantum description is less likely but not impossible. Therefore, this model with purely inflationary classical behavior does not represent the most probable scenario, suggesting the Universe most likely began at $a = 0$. We emphasize that we have successfully recovered the classical solution through this semiclassical analysis.

This concentration of probability near $a = 0$ may reflect quantum gravitational effects dominating at small scales, where classical notions of spacetime break down. The sharp peak suggests a quantum preference for initial conditions near the singularity, despite its classical forbidden nature.

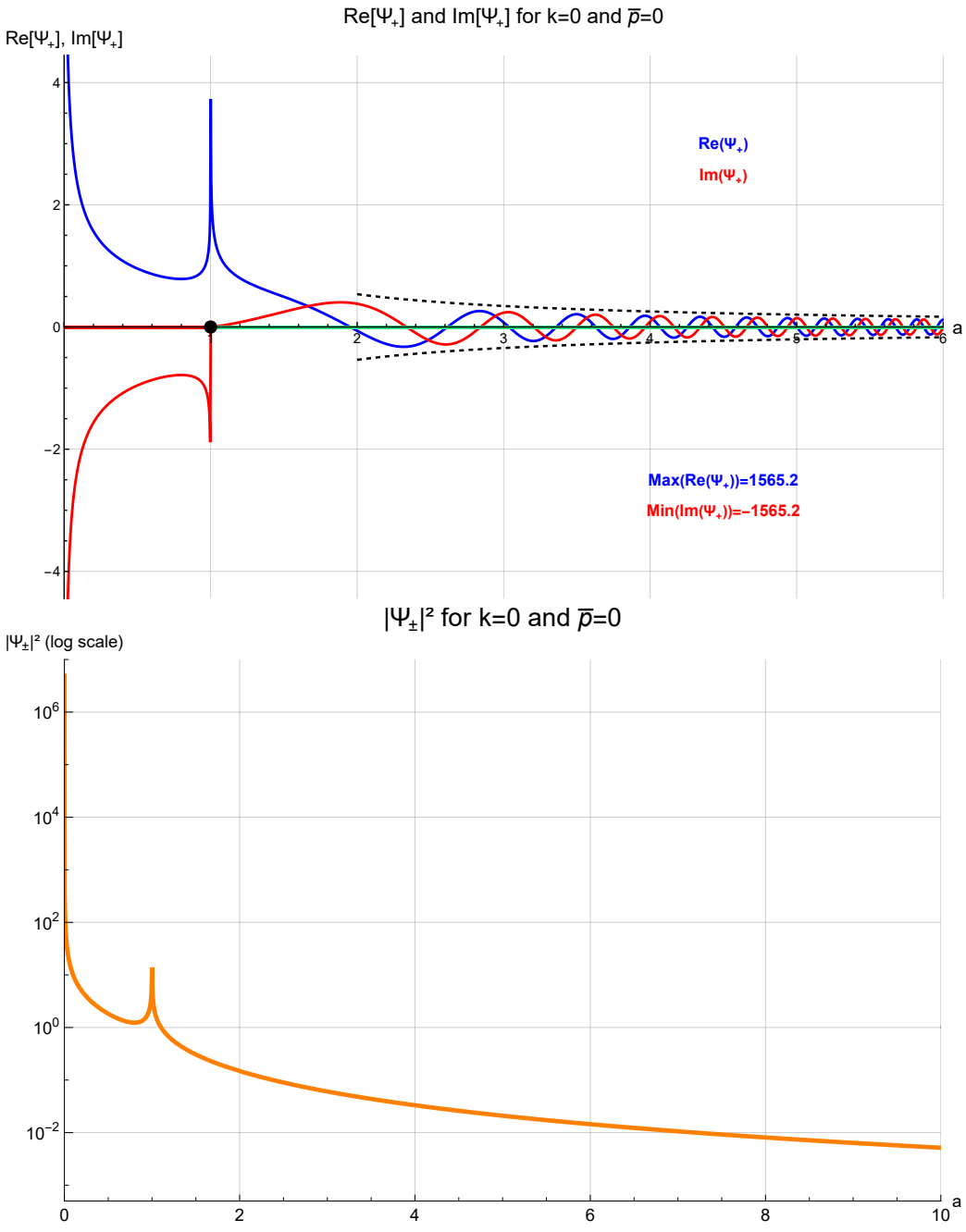

Figure 20: For $k = 0$, $\overline{p} = 0$, $\phi = 0$, $\lambda = 1$, $p = 1$ and $\hbar = 1$: (Top) Real and imaginary parts of the general wave function (5.11) for an expanding universe (Ψ_+) (blue and red curves, respectively), with the forbidden classical region ($a < p$) shown in red and the allowed region ($a > p$) in green; (Bottom) $|\Psi_\pm|^2$ (5.37) as a function of a.

5.4.2 $|k| = 1$

Second, for $|k| = 1$, the forbidden region corresponds to $a \in (p_1, p_2)$ (see Fig. 17), while for other values of a we have classically allowed regions where classical solutions may emerge.

In the upper panel of Fig. 21, we have plotted the real and imaginary parts of Ψ_+. The oscillatory portion of Ψ_+ now extends beyond the classical region $a < p_1$, and neither component actually oscillates but rather rapidly approaches the boundary at $a = p_1$, where there is the transition between classical and forbidden regions. Between p_1 and p_2 (both indicated by dotted points in the plot, with the region between shown in red), the function simply decays in absolute value before reaching another peak at $a = p_2$. Beyond this point, the solutions again exhibit oscillatory behavior with exponential decay.

The lower panel of Fig. 21 shows the probability density. In this case, the density reaches exactly zero at $a = 0$, making it impossible for the universe to begin at this point. The density increases to its first maximum at $a = p_1$, decreases, and then increases again to a second peak at $a = p_2$. Beyond this point, it decays asymptotically to zero as $a \to \infty$.

This behavior suggests an interesting physical interpretation: the double-peaked structure in the probability density indicates two prefered metastable solutions where quantum effects are particularly significant, while the vanishing probability at $a = 0$ indicates a quantum suppression of the initial singularity.

Therefore, in this scenario, the universe is likely to exist in either classical region, but with higher probability in the forbidden region. The most probable configurations are those associated with $a = p_1$ and $a = p_2$. This allows both purely kinetic-dominated universes and purely inflationary universes as possible outcomes.

This result has important cosmological implications. The presence of significant probability density in the classically forbidden region suggests that quantum tunneling effects may play a crucial role in the very early universe. Furthermore, the equal prominence of both peaks at p_1 and p_2 indicates that neither the kinetic-dominated phase nor the inflationary phase is inherently preferred in this quantum description - both emerge as equally probable from the fundamental quantum description.

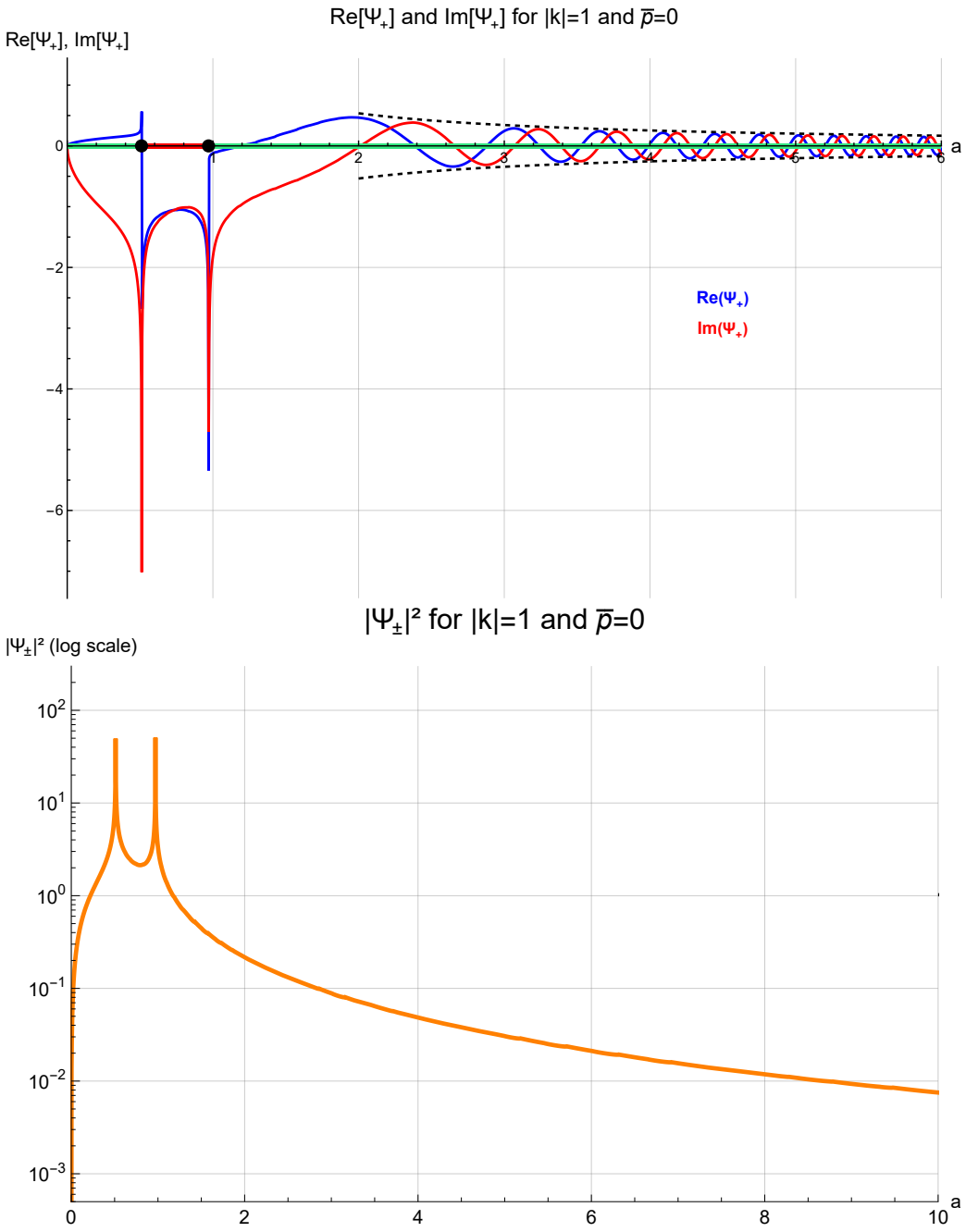

Figure 21: For $|k| = 1$, $\overline{p} = 0$, $\phi = 0$, $\lambda = 1$, $p = 1$ and $\hbar = 1$: (Top) Real and imaginary parts of the general wave function (5.11) for an expanding universe (Ψ_+) (blue and red curves, respectively), with the forbidden classical region ($p_1 < a < p_2$) shown in red and the allowed region ($a < p_1$ and $a > p_2$) in green; (Bottom) $|\Psi_\pm|^2$ (5.37) as a function of a.

5.4.3 $|k| = \sqrt{8\pi^2 p^2/(27\lambda)}$

Third, for $|k| = \sqrt{8\pi^2 p^2/(27\lambda)}$, the potential vanishes ($U = 0$) at $a = a_0 = (2p^2/3)^{1/2}$ (see Fig. 18), while all other values of a correspond to classically allowed regions.

From the first panel of Fig. 22, we observe that the oscillatory behaviour in the region below a_0 extends beyond the region itself. While this might suggest non-oscillatory behavior, we know oscillations do occur (this could be made explicitily by adjusting parameter values). Both the real and imaginary components reach their respective maximum and minimum values at a_0, beyond which they exhibit exponentially decaying oscillations.

The lower panel of Fig. 22 shows the probability density reaching its maximum at $a = a_0$, while approaching zero both at infinity and at $a = 0$. This indicates that the Universe is most likely to begin near (but not exactly at) a_0, with the highest probability concentrated at a_0.

This behavior suggests that a_0 represents a preferred quantum state for the early Universe, serving as an effective "quantum threshold" before classical inflation dominates. The vanishing probability at exact $a = 0$ implies quantum avoidance of the initial singularity.

In this scenario, we have successfully recovered all possible classical solutions across the entire a-space.

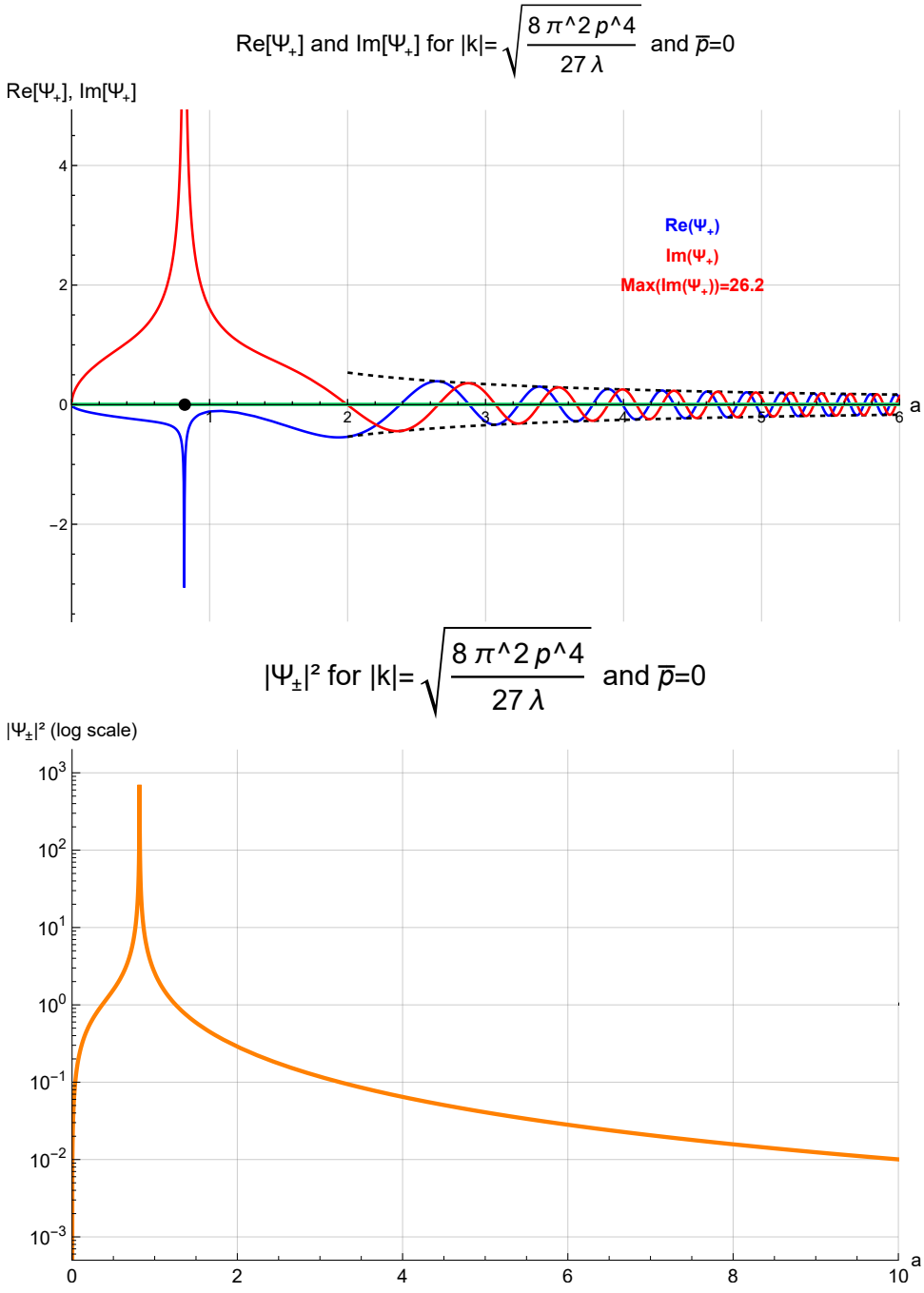

Figure 22: For $|k| = \sqrt{8\pi^2 p^2/(27\lambda)}$, $\overline{p} = 0$, $\phi = 0$, $\lambda = 1$, $p = 1$ and $\hbar = 1$: (Top) Real and imaginary parts of the general wave function (5.11) for an expanding universe (Ψ_+) (blue and red curves, respectively), with the forbidden classical region ($a < p$) shown in red and the allowed region ($a > p$) in green; (Bottom) $|\Psi_\pm|^2$ (5.37) as a function of a.

5.4.4 $|k| = 2$

Finally, in this last subsection we consider $|k| = 2$, corresponding to Fig. 19 where, for $a \geq 0$, $U > 0$, making the entire space classically allowed.

The first panel of Fig. 23 shows that both the real and imaginary parts oscillate while decaying throughout the space $a > 0$, though they exhibit non-trivial behavior near $a = 0$ where the description becomes particularly complex. Note again that both components vanish at $a = 0$.

The second panel of Fig. 23 displays the probability density, which reaches zero both at $a = 0$ and at infinity, reaching its maximum at an intermediate value of a. This maximum probability occurs below the threshold where inflation would begin (for an expanding universe) or end (for a contracting universe), as can be seen by comparison with Fig. 13. Therefore, this classical universe configuration is the most likely one and it occurs during the kinetic domain phase, which is a key finding of this thesis.

This result strongly supports the quantum mechanical preference for kinetic-dominated initial conditions over inflationary ones in this model. The vanishing probability at both extremes ($a = 0$ and $a \to \infty$) with a well-defined peak at finite a suggests the existence of a preferred quantum state for the early universe.

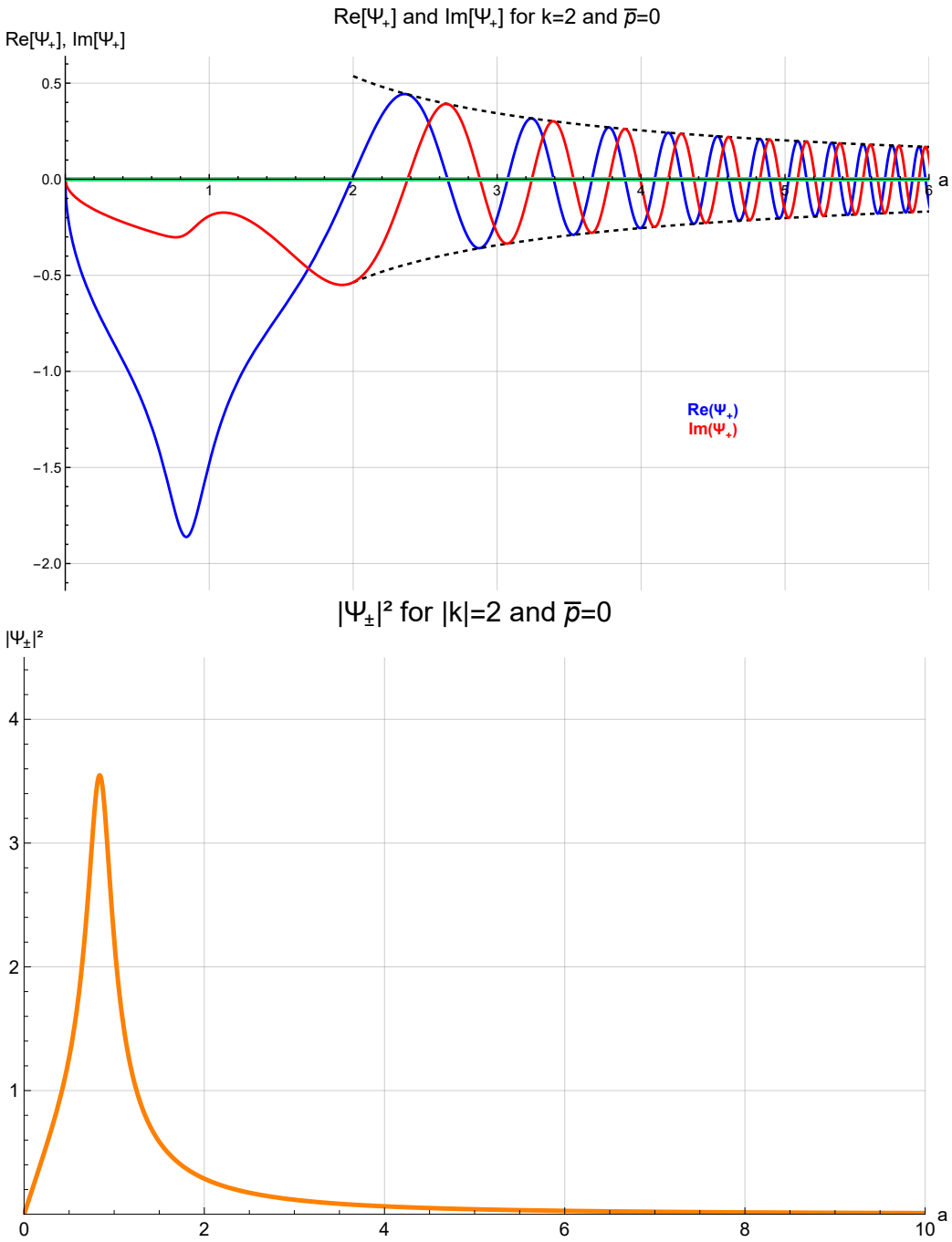

Figure 23: For $|k| = 2$, $\overline{p} = 0$, $\phi = 0$, $\lambda = 1$, $p = 1$ and $\hbar = 1$: (Top) Real and imaginary parts of the general wave function (5.11) for an expanding universe (Ψ_+) (blue and red curves, respectively), with the forbidden classical region ($a < p$) shown in red and the allowed region ($a > p$) in green; (Bottom) $|\Psi_\pm|^2$ (5.37) as a function of a.

5.5 Connection with the asymptotic behaviours

As a final point, we examine whether the previous solutions align with the asymptotic behaviors presented earlier. For simplicity, we have plotted the comparison for two particular cases: for $k = 0$ at large a-values, and for $k = 1$ near $a = 0$. The only constraint is that for comparing both solutions, they must lie in classically allowed regions, as our asymptotic analysis is limited to these zones. For $k = 0$, there is only one allowed region when $a > p$, preventing comparison near $a = 0$ but allowing us to compare in the region $a > p$ (note from eq. 5.17 that if we take $a = p$, $\Psi_{\pm}$ diverges; for that reason we are limitated to $a > p$); however, for $|k| > 0$, a classical zone emerges in the desired region.

The asymptotic solutions presented here have been multiplied by a constant factor. This adjustment accounts for the non-normalized wave functions we have studied and the different integration limits required to satisfy normalization conditions in each regime.

For $a \to 0^+$, the upper panel of Fig. 24, where we consider $|k| = 1$ and $\overline{p} = 0$, both solutions almost coincide at $a \sim 10^{-8}$ but begin to split up by $a \sim 10^{-7}$. This indicates that our asymptotic approximation remains valid only for extremely small values of a. As we have already examined this in previous sections, we will not explore it further here.

Conversely, for $k = 0$ with $a > p$, the asymptotic solution shows better agreement with the exact solution, see the lower panel of Fig. 24. Both the imaginary and real parts align almost perfectly beyond the forbidden region. That is, this asymptotic behaviour can be better studied and applied to investigate how the Universe will behave far away from $a = 0$.

These results correctly connect the asymptotic solutions that were already studien in deep in [26] with the exact wave functions solutions.

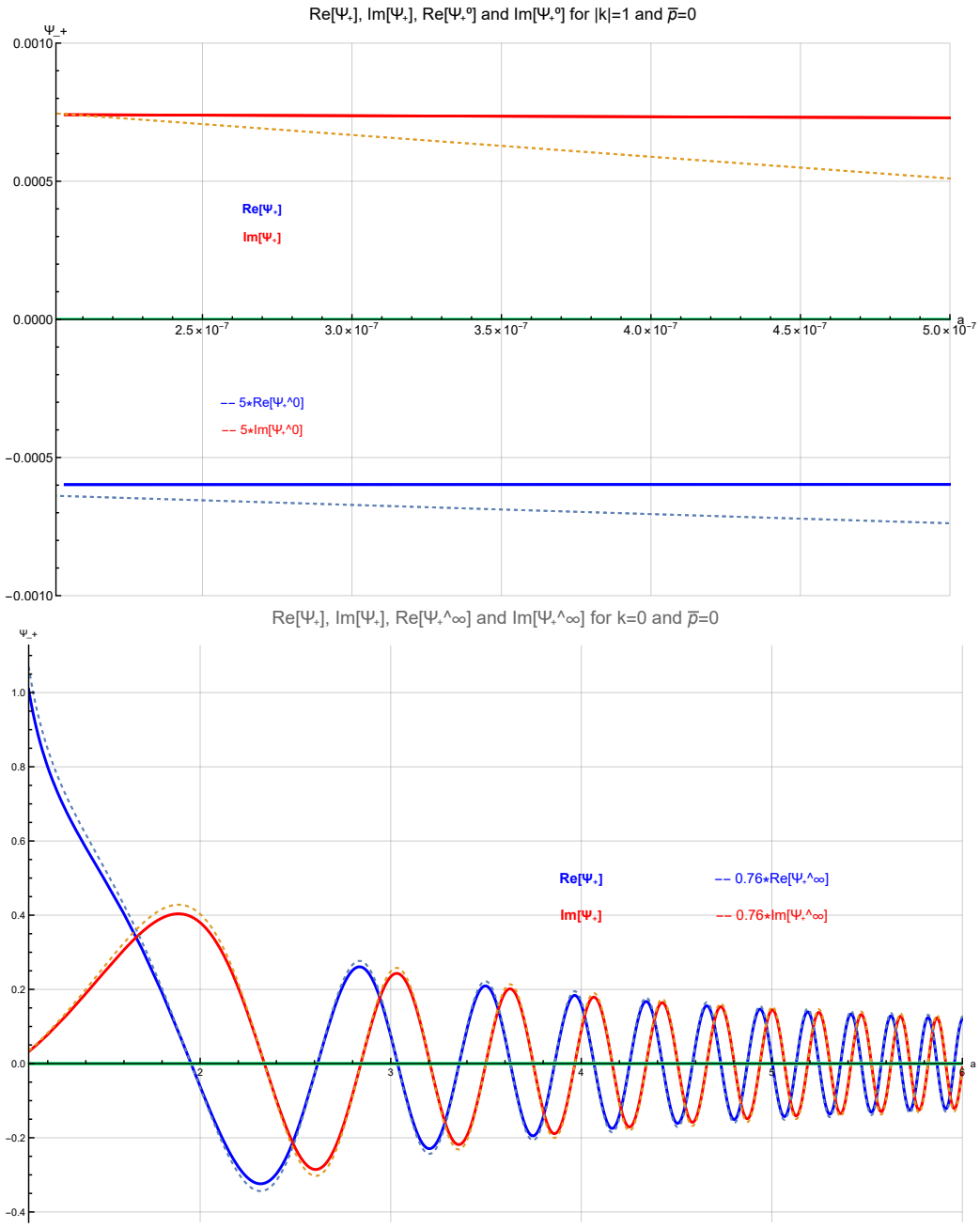

Figure 24: For $\overline{p} = 0$, $\phi = 0$, $\lambda = 1$, $p = 1$ and $\hbar = 1$: (Top) for $|k| = 1$, real and imaginary parts of the general wave function (5.11) and its asymptotic behaviour (5.29) for an expanding universe (Ψ_+) in the allowed region ($a < p_1$) in green; (Bottom) for $|k| = 0$, real and imaginary parts of the general wave function (5.11) and its asymptotic behaviour (5.17) for an expanding universe (Ψ_+) in the allowed region ($a > p$) in green (note that this second plot starts at $a = 1.1p = 1.1$).

6 Conclusion

In this Master's Thesis, we have theoretically and numerically studied the WDW equation to reveal a kinetic dominance regime after the Big Bang, specifically for a closed Friedmann universe with a constant inflaton potential. The aim of this work was to use the WKB approximation to obtain the Universe's wave function, describing both classically allowed and forbidden regions through this semiclassical approximation. We have satisfactorily shown that for different values of $|k|$, there exist classically allowed regions where classical solutions emerge, all defined by the wave function of the entire Universe near the well-known initial singularity. In our study, quantum effects have suppressed this singularity at $a = 0$ for $\overline{p} \leq 1$. Moreover, there are no singularities, and $\Psi_{\pm}$ is consequently square-integrable and normalizable because $\sigma = |\Psi_{\pm}|^2$ is finite and positive for all k-values and for $a \geq 0$, if and only if $\overline{p} \leq 1$.

The wave function of the universe is represented with the scale factor acting as a time variable, contributing to a dynamic picture of the universe despite the time-independent nature of both the wave function itself and the WDW equation [102].

Our results demonstrate how quantum effects can naturally resolve cosmological singularities while maintaining consistency with classical solutions in the appropriate limits. This provides a concrete example of quantum gravity effects in a cosmological context.

The role of quantum cosmology is to determine the probability distribution for the initial states of the universe, and this study shown here may represent one step towards achieving this goal. Furthermore, this same approach can be applied to other cosmological scenarios such as gravitational collapse [56], in which the central singularity appearing in black holes might similarly disappear.

This study has several limitations that could be addressed in future work:

- The semiclassical WKB approximation (4.26).
- The use of only two terms in the WKB approximation ($\mathbb{S}_0$ and $\mathbb{S}_1$).
- The restriction to a closed universe rather than general spatial curvature.
- The exclusion of dark energy via the cosmological constant Λ, which may be important.

- The use of a positive constant potential rather than a more generic one.
- The assumption of perfect homogeneity and isotropy.

Two natural extensions for future research would be the study of inhomogeneities in the early Universe, specifically the cosmological perturbations generated during the kinetic dominance and/or inflation phases. There are two approaches to study them:

1. We could decompose the inflation field into $\phi = \phi_0(t) + \delta\phi(x,t)$, where ϕ_0 is a homogeneous component and $\delta\phi$ represents small quantum fluctuations about ϕ_0. These perturbations would lead to a perturbed energy-momentum tensor, and via the Einstein equations (2.1), the curvature of the spacetime would also be perturbed, describing a perturbed space-time [79].

   It would be interesting to investigate these perturbations, and to compare them with the microwave cosmic background, to determine whether we can predict these inhomogeneities from early-universe perturbations.

2. Perturbations of the metric itself, where we decompose the metric as:

$$g_{\mu\nu} = \overline{g}_{\mu\nu} + \delta g_{\mu\nu}, \tag{6.1}$$

   with $\overline{g}_{\mu\nu}$ the metric we have studied during this thesis, the FLRW metric, and $\delta g_{\mu\nu}$ representing a perturbation.

   The behavior of these perturbations differs from scalar perturbations as they contain a tensor component rather than a scalar one. These perturbations would produce gravitational waves [27, 103], i.e., space-time perturbations propagating at light speed that were experimentally detected in 2015 [104].

   These perturbations could have been produced in the early Universe, potentially generating a stochastic gravitational wave background [105], similar to the cosmic microwave fluctuation but of gravitational waves. Studying and, more importantly, detecting these spacetime ripples remains a challenge that we might overcome in the future.

With them, we could test the first moments of the universe, and to prove whether our models are correct and sufficient to describe our universe, or whether we need new physics and mathematics.

A Mathematical Foundations

This appendix presents the fundamental mathematical framework required to fully comprehend the theoretical background of our work [27, 60, 106, 107, 108, 109, 110].

A.1 Manifolds and Differentiable Structures

Definition A.1 *A topological space M satisfies the **Hausdorff property** if for any two distinct points $p_1, p_2 \in M$, there exist two open sets $\Omega_1, \Omega_2 \in \mathcal{O}$ (family of subsets of M) containing $p_1 \in \Omega_1$ and $p_2 \in \Omega_2$, $\Omega_1 \cap \Omega_2 = \emptyset$.*

Definition A.2 *M is **paracompact** if every open covering admits a locally finite open refinement. Specifically, for any open covering $\{\Omega_\alpha\}_{\alpha \in A}$ (being A an arbritary index set), there exists another locally finite open covering $\{\Omega'_\beta\}_{\beta \in B}$ such that $\exists \alpha \in A : \Omega'_\beta \subset \Omega_\alpha$.*

Definition A.3 *A **d-dimensional manifold** is a connected, paracompact Hausdorff space where every point has a neighborhood U homeomorphic (continous bujective map in both dimensions) to an open subset of $\mathbb{R}^d$. A (coordinate) chart is the homeomorphism $x : U \to \Omega \subset \mathbb{R}^d$.*

In other words, a manifold is a space consisting of neighbourhoods that are locally homeomorphic to and open subset of $\mathbb{R}^d$ and that can be glued together through continuous transition maps.

Definition A.4 *For a point $p \in U_\alpha$, its local coordinates are given by the components of $x_\alpha(p) \in \mathbb{R}^d$.*

Throughout our work, we assume all manifolds are **differentiable** (of class C^∞, where we can define a scalar field for all points of the manifold that can be differentiated) unless stated otherwise. That is, every time you see M, think of it as a differentiable manifold.

Definition A.5 *A **differentiable atlas** $\mathscr{A}$ on M is a collection of charts $\{(U_\alpha, x_\alpha)\}_{\alpha \in I}$ where:*

1. *$\bigcup_{\alpha \in I} U_\alpha = M$, that is, $\{U_\alpha\}_{\alpha \in I}$ forms an open cover of M*
2. *If $U_\alpha \cap U_\beta \neq \emptyset$, the transition maps $x_\beta \circ x_\alpha^{-1} : x_\alpha(U_\alpha \cap U_\beta) \to x_\beta(U_\alpha \cap U_\beta)$ are smooth (C^∞) diffeomorphisms*

From now on, all our atlas will be assumed differentiable.

Definition A.6 *An atlas is **oriented** if all transition maps have positive Jacobian determinant. A manifold admitting such an atlas is called **orientable**.*

A.2 Tangent Spaces and Vector Fields

Definition A.7 *The **tangent space** T_pM to M at $p \in M$ is the space of equivalence classes of curves through p.*

In local coordinates x, a tangent vector field of M at some point p has the form $V(x) \overset{(\text{loc})}{=} v^i(x)\frac{\partial}{\partial x^i}$. The collection of all differentiable vector fields at p forms the tangent space T_pM, with basis $\{\frac{\partial}{\partial x^i}\} = \{\partial_i\}$, see Fig. 25.

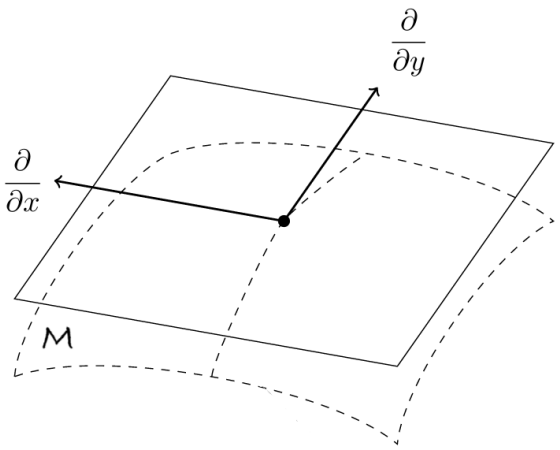

Figure 25: Tangent space to M at a point of it, with basis $\{\partial/\partial x, \partial/\partial y\}$. Image extracted from [111].

A.3 Riemannian and Lorentzian Geometry

Definition A.8 *A **Riemannian metric** on M is a smoothly varying inner product $\langle\cdot,\cdot\rangle_p$ (depends on the point p) on each tangent space T_pM.*

In local coordinates $x = (x^1, ..., x^d)$, the metric is represented by a positive definite symmetric matrix $(g_{ij}(x))$, allowing us to compute the product of two tangent vectors $v, w \in T_pM$, $v \overset{(\text{loc})}{=} v^i\partial_i$ and $w \overset{(\text{loc})}{=} w^j\partial_j$:

$$\langle v, w\rangle = g_{ij}(x(p))\, v^i\, w^j,$$

where, $g_{ij} = \langle\partial_i, \partial_j\rangle$ has d real positive eigenvalues.

Definition A.9 *A **Riemannian manifold** is a differentiable manifold equipped with a Riemannian metric.*

Definition A.10 *A **Lorentzian metric** on a $(d+1)$-dimensional manifold has signature $(1,d)$ on each tangent space T_pM, with one negative and d positive eigenvalues. They are also known as **pseudo-Riemannian metrics**, where the negative eigenvalue is associated with the time coordinate. A **Lorentzian manifold** is a differentiable manifold with such a metric.*

In physical applications, for example for the Minkowski case with the metric $diag(\eta_{ij}) = (-1,+1,+1,+1)$, we can calculate $||V||^2 = \langle V,V\rangle$:

- **Timelike** vectors ($\langle V,V\rangle < 0$) represent massive particle trajectories.
- **Null** vectors ($\langle V,V\rangle = 0$) represent lightlike paths.
- **Spacelike** vectors ($\langle V,V\rangle > 0$) are unphysical (superluminical speeds, greater than the speed of light).

The unphysical vectors will lie outside the so-called **light cones**, see Fig. 26.

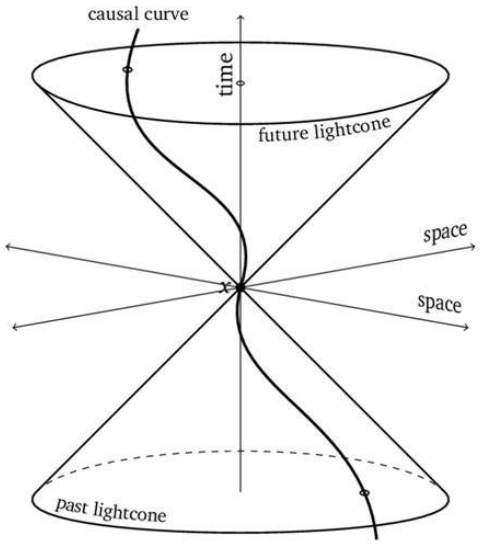

Figure 26: Light cone representing, for a point $x \in M$, the future and past lightcone whose border is formed by null vectors, and the physical vectors lie inside it, such that they will be causally connected. Image extracted from [112].

A.4 Vector Bundles and Tensors

Definition A.11 *A (differentiable)* ***vector bundle*** *of rank n consists of:*

- *A total space E and a base M (both differentiable manifold).*
- *A projection $\pi : E \to M$ (differentiable map).*

such that:

1. *Each fiber $E_x := \pi^{-1}(x)$ for $x \in M$ has the structure of an n-dimensional real vector space.*
2. *For each $x \in M$, there exists a neighborhood $U \subset M$ and a diffeomorphism $\varphi : \pi^{-1}(U) \to U \times \mathbb{R}^n$ (called a local trivialization) that preserves the lineal structure on each fiber.*

Definition A.12 *The* ***cotangent space*** *T_x^*M is the dual space to T_xM, for $x \in M$. Its cotangent bundle T^*M is the vector bundle over M whose fibers are the cotangent spaces of M, such that it has sections called* ***1-forms****, and elements called* ***cotangent vectors****.*

Given a basis $(e_i)_{i=1,\dots,d}$ ($d = \dim(M)$) for T_xM, the dual basis $(w^j)_{j=1,\dots,d}$ satisfies $w^j(e_i) = \delta^j{}_i$, that is = 1 if $i = j$, and = 0 otherwise. Transformation properties distinguish:

- **Contravariant** vectors: $V = v^i \frac{\partial y^k}{\partial x^i} \frac{\partial}{\partial y^k}$
- **Covariant** vectors: $w_i dx^i = w_i \frac{\partial x^i}{\partial y^j} dy^j$

Definition A.13 *A (p,q)-****tensor*** *(p times contravariant and q times covariant) on M is a section of $TM \otimes \dots \otimes TM$ p times multiplied tensorially by $\otimes T^*M \otimes \dots \otimes T^*M$ q times.*

Definition A.14 *A Riemannian metric on M is a symmetric, positive definite (0,2)-tensor, a section of $T^*M \otimes T^*M$, locally expressible as $g_{ij} dx^i \otimes dx^j$.*

Thus, the volume form is given by:

$$d\mathrm{vol}_g = \sqrt{\det(g_{ij})}\; dx^1 \wedge \dots \wedge dx^d,$$

with $\wedge$ the exterior product.

Finally, we can obtain the components of a 1-form or vector by using the metric tensor to lower or raise indices, respectively:

$$u_i = g_{ij} u^j, \quad u^i = g^{ij} u_j, \tag{A.1}$$

where:

- u^i are the contravariant components of the vector.
- u_i are the covariant components of the 1-form.
- g_{ij} is the metric tensor.
- g^{ij} is the inverse metric tensor.

A.5 Lie Derivatives

Definition A.15 *A **local 1-parameter group of diffeomorphisms** is a family $(\varphi_t)_{t\in I}$, with I an open interval, of diffeomorphisms from M to M that satisfy:*

$$\varphi_t \circ \varphi_s = \varphi_{t+s}$$

if $s, t, s+t \in I_q$, and maps U diffeomorphically onto its image if φ_t is defined on $U \subset M$.

Definition A.16 *For a vector field X with a local 1-parameter group $(\psi_t)_{t\in I}$ of local diffeomorphisms, and S a tensor field on M, the **Lie derivative** of S in the X-direction is:*

$$\mathscr{L}_X S = \frac{d}{dt}(\psi_t^* S)\big|_{t=0}.$$

Theorem A.1 *Lie Derivative Properties:*

1. *For differentiable functions $f : M \to \mathbb{R}$,*

$$\mathscr{L}_X(f) = df(X) = X(f), \tag{A.2}$$

such that in local coordinates is:

$$\mathscr{L}_X(f) \overset{(loc)}{=} X^i \frac{\partial}{\partial x^i}(f). \tag{A.3}$$

2. *For vector fields Y, in general and local coordinates will be:*

$$\mathscr{L}_X Y = [X, Y] \overset{(loc)}{=} \left(X^k \frac{\partial Y^j}{\partial x^k} - Y^k \frac{\partial X^j}{\partial x^k} \right) \frac{\partial}{\partial x^j}. \tag{A.4}$$

3. *For 1-forms $w = w_j dx^j$, in local coordinates:*

$$\mathscr{L}_X w \overset{(loc)}{=} \left(\frac{\partial w_j}{\partial x^i} X^i + \frac{\partial X^i}{\partial x^j} w_i \right) dx^j. \tag{A.5}$$

4. *For (0,2)-tensors $h = h_{ij} dx^i \otimes dx^j$, in local coordinates:*

$$\mathscr{L}_X h \overset{(loc)}{=} \left(\frac{\partial h_{ij}}{\partial x^k} X^k + h_{kj} \frac{\partial X^k}{\partial x^i} + h_{ik} \frac{\partial X^k}{\partial x^j} \right) dx^i \otimes dx^j. \tag{A.6}$$

A.6 Connections and Curvature

Definition A.17 *A **covariant derivative** (linear connecion) on a vector bundle $E \to M$ is a map:*

$$D : \Gamma(E) \to \Gamma(E) \otimes \Gamma(T^*M)$$

where $\Gamma(E)$ is the space of vector bundles on M, $\Gamma(TM)$ such that D is tensorial in the first argument,

$$D_{V+W}\sigma = D_V\sigma + D_W\sigma, \quad \text{for } V, W \in T_xM, \sigma \in \Gamma(E),$$

$$D_{fV}\sigma = fD_V\sigma \quad \text{for } f \in C^\infty(M,\mathbb{R}),\ V \in \Gamma(TM),$$

and D is $\mathbb{R}-$linear in the second term,

$$D_V(\sigma+\tau) = D_V\sigma + D_V\tau \quad \text{for } V \in T_xM, \sigma, \tau \in \Gamma(E),$$

that satisfies the product rule

$$D_V(f\sigma) = V(f)\cdot\sigma + fD_V\sigma \quad \text{for } f \in C^\infty(M,\mathbb{R}).$$

Analogously, it can be defined for our manifold M and for $\Gamma(TM)$, as the linear map

$$D : \Gamma(TM) \otimes_{\mathbb{R}} \Gamma(TM) \to \Gamma(TM), \tag{A.7}$$

$$(V, W) \to D_V W, \tag{A.8}$$

that satisfy the same conditions than before. $D_V W$ is called the covariant derivative of W in the direction V.

Definition A.18 *Let U be a coordinate chart in M, with local coordinates x and coordinate vector field $\partial_1 = \partial/\partial x^1, ..., \partial_d$, with $d = dim(M)$. Then, we can define the **Christoffel symbols** of the connection D via*

$$D_{\partial_i}\partial_j \overset{(loc)}{=} \Gamma^k{}_{ij}\partial_k. \tag{A.9}$$

Thus,

$$D_V W \overset{(loc)}{=} V^i \frac{\partial W^j}{\partial x^i}\frac{\partial}{\partial x^j} + V^i W^j \Gamma^k_{ij}\partial_k. \tag{A.10}$$

Definition A.19 ***Parallel transport** along a smooth curve $c(t)$ in M is the unique solution to:*

$$D_{\dot{c}(t)}W(t) = 0 \tag{A.11}$$

with given initial condition $W(0)$, where $\dot{c}(t) = \frac{dc(t)}{dt}$ is the tangent vector fild of c, and $W(t) \in T_{c(t)}M$ for all t another vector field.

Theorem A.2 *The **curvature tensor** R of a connection D satisfies:*

$$R(X,Y)\mu = D_X D_Y \mu - D_Y D_X \mu - D_{[X,Y]}\mu$$

for all vector fields X, Y on M, and all $\mu \in \Gamma(E)$. In local coordinates,

$$R\left(\frac{\partial}{\partial x^i},\frac{\partial}{\partial x^i}\right)\frac{\partial}{\partial x^l} \overset{(loc)}{=} R^k{}_{lij}\frac{\partial}{\partial x^k} = \left(\frac{\partial \Gamma^k{}_{jl}}{\partial x^i} - \frac{\partial \Gamma^k{}_{il}}{\partial x^j} + \Gamma^k{}_{im}\Gamma^m{}_{jl} - \Gamma^k{}_{jm}\Gamma^m{}_{il}\right)\frac{\partial}{\partial x^k}. \tag{A.12}$$

That is, the multilinear operator R is a tensor field of rank $(1,3)$, which maps three vector fields to a vector field.

Definition A.20 *The **torsion tensor** is [113]:*

$$Tor(X,Y) = D_X Y - D_Y X - [X,Y]$$

for any two vector fields X, Y on M, that in local coordinates is given by $Tor^k_{ij} \overset{(loc)}{=} \Gamma^k_{ij} - \Gamma^k_{ji}$. It causes a "twisting" of vectors when they are parallel-transported.

Lemma A.1 *The connection ∇ on TM is torsion free if and only if $\Gamma^k{}_{ij} = \Gamma^k{}_{ji}$, $\forall i,j,k$.*

Since the torsion is a tensor field, it must be equal to zero everywhere to hold the torsion free condition.

In general relativity is usual to work with a torsion free connection.

A.7 Levi-Civita Connection

Let M be a Riemann manifold with metric $\langle\cdot,\cdot\rangle$.

Definition A.21 *The **Levi-Civita connection** is the unique metric and torsion-free connection ∇ determined by:*

$$\langle D_X Y, Z\rangle = \frac{1}{2}\big(X\langle Y,Z\rangle + Y\langle Z,X\rangle - Z\langle X,Y\rangle - \langle X,[Y,Z]\rangle + \langle Y,[Z,X]\rangle + \langle Z,[X,Y]\rangle\big)$$

Corollary A.1 ***The Christoffel symbols** for the Levi-Civita are given in local coordinates by:*

$$\Gamma^k{}_{ij} \overset{(loc)}{=} \frac{1}{2}g^{kl}(\partial_j g_{il} + \partial_i g_{jl} - \partial_l g_{ij}). \tag{A.13}$$

Definition A.22 *The **Ricci curvature** in direction $X = \xi^i\partial_i \in T_xM$ is:*

$$Ric(X,X) = g^{jl}\left\langle R\left(X,\frac{\partial}{\partial x^j}\right)\frac{\partial}{\partial x^l},X\right\rangle. \tag{A.14}$$

The Ricci tensor in local coordinates is $R_{ik} \overset{(\text{loc})}{=} g^{jl} R_{ijkl}$, and the scalar curvature or Ricci scalar is $R \overset{(\text{loc})}{=} g^{ik} R_{ik}$.

Lemma A.2 *For any metric tensor, we can consider a **locally intertial frame** (LIF) at an arbritary point $\mathscr{P}$ such that $g_{ij}(\mathscr{P}) = \eta_{ij}$, $\forall i, j$, with $diag(\eta_{ij}) = (-1, +1, +1, +1)$ the Minkowskian metric, and $\partial_k \eta_{ij} = 0$, $\forall i, j, k$. Thus, via (A.13), all the Christoffel symbols are zero. Therefore, the **Ricci's lemma** holds:*

$$\nabla_k g_{ij} \overset{(loc)}{=} 0, \tag{A.15}$$

with ∇ the Levi-Civita connection. This holds in any LIF, and because it is a tensor equation, it will hold in any other reference frame.

Theorem A.3 *The fundamental theorem of (pseudo-)Riemannian geometry: There exists a unique torsion-free connection compatible with a given metric - the **Levi-Civita connection.***

This theorem is the basis of general relativity, in which is taken $\Gamma^k{}_{ij} = \Gamma^k{}_{ji}$ and $\nabla_k g_{ij} = 0$.

From now on, ∇ will denote the Levi-Civita connection.

A.8 Foliation of Spacetime

Definition A.23 *A smooth curve $\gamma : [a, b] \to M$ that satisfies in local coordinates*

$$\ddot{x}^i(t) + \Gamma^i{}_{jk}(x(t)) \dot{x}^j(t) \dot{x}^k(t) = 0, \text{ for } i = 1, ..., d$$

*is called a **geodesic**. Geodesics represent the critical points of the energy functional.*

Definition A.24 ***Future-directed condition**: For any future-directed timelike vector field t^a in a neighborhood of a curve γ, the inner product satisfies:*

$$g_{ab} t^a \dot{\gamma}^b < 0 \tag{A.16}$$

at every point along the curve.

Definition A.25 *The **chronological future** of $p \in M$, denoted $I^+(p)$, is the set of events reachable by future-directed timelike curves starting from p,*

$I^+(p) = \{q \in M \,/\, \exists$ *a future-directed timelike curve $\lambda(t)$ with $\lambda(0) = p$ and $\lambda(1) = q\}$.*

*An analogous definition applies to the **chronological past** $I^-(p)$.*

Definition A.26 *A subset $S \subset M$ is **achronal** if there exist no $p, q \in S$ such that $q \in I^+(p)$, i.e., if $I^+(p) \cap S = \emptyset$.*

Theorem A.4 *If Σ is a closed and achronal set, then Σ is a **Cauchy surface** if and only if every inextendible null geodesic intersects Σ and enters both $I^+(\Sigma)$ and $I^-(\Sigma)$.*

Definition A.27 *A spacetime (M, g_{ab}) possessing a Cauchy surface Σ is called **globally hyperbolic**.*

Theorem A.5 *A spacetime (M, g_{ab}) is **stably causal** if and only if there exists a differentiable function f on M such that $\nabla^a f$ is a past-directed timelike vector field.*

Theorem A.6 *Let (M, g_{ab}) be a globally hyperbolic spacetime that is stably causal. Then, a global time function f can be chosen such that each surface of constant f is a Cauchy surface. Consequently, M can be foliated by Cauchy surfaces, and the spacetime topology becomes $\Sigma \times \mathbb{R}$, where Σ denotes any Cauchy surface.*

Theorem A.7 *Let Σ be a three-dimensional C^∞ manifold with a smooth Riemannian metric γ_{ij} and a smooth symmetric tensor field K_{ab}. If γ_{ij} and K_{ij} satisfy the constraint equations (2.26) and (2.27), then there exists a unique C^∞ spacetime (M, g_{ij}), called the **maximal Cauchy development** of $(\Sigma, \gamma_{ij}, K_{ij})$, satisfying:*

1. *(M, g_{ij}) is a solution to Einstein's equations.*
2. *(M, g_{ij}) is globally hyperbolic with Cauchy surface Σ.*
3. *The induced metric and extrinsic curvature of Σ are γ_{ij} and K_{ij}, respectively.*
4. *Any other spacetime satisfying these conditions can be isometrically embedded into (M, g_{ij}).*

B Derivation of the ADM equations

Here we present the derivation of the ADM equations, (2.24), (2.25), (2.26), and (2.27), from Einstein's equations, using the definitions provided by the $3+1$ formalism: the extrinsic curvature K_{ij} and the spatial metric $\gamma_{\mu\nu}$.

B.1 First Equation: Time Evolution of the Spatial Metric

We begin by introducing the fundamental concept of the Lie derivative, which provides a coordinate-independent generalization of partial derivatives. The Lie derivative $\mathscr{L}_{\vec{u}}$ measures the change of a tensor field along the flow of a vector field $\vec{u}$. When coordinates can be aligned with a congruence, this derivative reduces to a simple partial derivative, making it particularly useful in differential geometry.

For various tensor types, the Lie derivative takes the forms that are in Definition A.16 and Theorem A.1. Applying this operator to the spatial metric $\gamma_{\mu\nu}$ induced on the hypersurface Σ_t, see equation (A.6), yields a crucial equation governing its temporal evolution:

$$\mathscr{L}_{\vec{n}}\gamma_{\mu\nu} = n^\alpha \nabla_\alpha \gamma_{\mu\nu} + \gamma_{\mu\alpha}\nabla_\nu n^\alpha + \gamma_{\nu\alpha}\nabla_\mu n^\alpha \tag{B.1}$$

The simplification of this expression relies on several key observations:

- The metric compatibility of the Levi-Civita connection implies $\nabla_\alpha g_{\mu\nu} = 0$ (Lemma A.2), which consequently gives $\nabla_\alpha \gamma_{\mu\nu} = \nabla_\alpha g_{\mu\nu} + \nabla_\alpha(n_\mu n_\nu) = \nabla_\alpha(n_\mu n_\nu)$.
- For unit normal vectors following geodesic paths, their gradient maintains orthogonality: $n^\alpha \nabla_\beta n_\alpha = 0$.
- From the spatial metric definition (2.2), we derive the relation $n^\alpha n_\mu = \gamma^\alpha{}_\mu - g^\alpha{}_\mu$.
- The spacetime metric $g_{\mu\nu}$ serves as the fundamental index raising/lowering operator.

These properties allow us to simplify (B.1) significantly:

$$\begin{aligned}\mathscr{L}_{\vec{n}}\gamma_{\mu\nu} &= \\ &= n^\alpha \nabla_\alpha (n_\mu n_\nu) + g_{\mu\alpha}\nabla_\nu n^\alpha + g_{\nu\alpha}\nabla_\mu n^\alpha \\ &= n^\alpha n_\mu \nabla_\alpha n_\nu + n^\alpha n_\nu \nabla_\alpha n_\mu + \nabla_\nu n_\mu + \nabla_\mu n_\nu \\ &= (\gamma^\alpha{}_\mu - g^\alpha{}_\mu)\nabla_\alpha n_\nu + (\gamma^\alpha{}_\nu - g^\alpha{}_\nu)\nabla_\alpha n_\mu + \nabla_\nu n_\mu + \nabla_\mu n_\nu \\ &= \gamma^\alpha{}_\mu \nabla_\alpha n_\nu + \gamma^\alpha{}_\nu \nabla_\alpha n_\mu = -2K_{\mu\nu}.\end{aligned}$$

This elegant result demonstrates how the extrinsic curvature tensor $K_{\mu\nu}$ emerges naturally from the hypersurface-normal behavior of $\vec{n}$, representing an intrinsic geometric property of the hypersurface itself. The equation fundamentally relates temporal changes in the spatial metric to the extrinsic curvature.

For any scalar field ζ, given the normal vector's orthogonality to the hypersurfaces, we obtain the scaling relation:

$$\mathscr{L}_{\vec{n}}\gamma_{\mu\nu} = \frac{1}{\zeta}\mathscr{L}_{\zeta\vec{n}}\gamma_{\mu\nu}. \tag{B.2}$$

Rescaling by the lapse function and introducing the time vector $\vec{t}$ from (2.5) yields:

$$K_{\mu\nu} = -\frac{1}{2\alpha}\mathscr{L}_{\alpha\vec{n}}\gamma_{\mu\nu} = -\frac{1}{2\alpha}\big(\mathscr{L}_{\vec{t}} - \mathscr{L}_{\vec{\beta}}\big)\gamma_{\mu\nu}, \tag{B.3}$$

which leads to:

$$\big(\mathscr{L}_{\vec{t}} - \mathscr{L}_{\vec{\beta}}\big)\gamma_{\mu\nu} = -2\alpha K_{\mu\nu}. \tag{B.4}$$

In adapted coordinates where $\mathscr{L}_{\vec{t}} = t^\mu \partial_\mu = \partial_t$, the spatial components satisfy the evolution equation:

$$\partial_t \gamma_{ij} - \mathscr{L}_{\vec{\beta}}\gamma_{ij} = -2\alpha K_{ij}. \tag{B.5}$$

The second term in (B.5) can be expanded using the Lie derivative definition, with several simplifying conditions:

- We can select coordinates where Christoffel symbols vanish, making $\nabla_\mu g_{ij} = \partial_\mu g_{ij} = 0$, see Lemma A.2.
- The shift vector β^μ maintains orthogonality to $\partial_\mu n_i$.
- The 3-dimensional covariant derivative D_i emerges as the projection of the 4-dimensional derivative: $D_\mu \equiv P^\alpha{}_\mu \nabla_\alpha$.

The Lie derivative term then expands as:

$$\mathscr{L}_{\vec{\beta}}\gamma_{ij} = \beta^{\mu}\partial_{\mu}\gamma_{ij} + \gamma_{ik}\partial_j\beta^k + \gamma_{kj}\partial_i u^k = \beta^{\mu}(\partial_{\mu}g_{ij} + \partial_{\mu}(n_i n_j)) + D_j\beta_i + D_i\beta_j. \tag{B.6}$$

Only the last two terms survive and therefore contribute to the evolution.

Thus, (B.5) simplifies to the fundamental evolution equation:

$$\boxed{\partial_t\gamma_{ij} = -2\alpha K_{ij} + D_i\beta_j + D_j\beta_i}. \tag{B.7}$$

This equation represents one quarter of our Cauchy formulation, providing the evolution dynamics for γ_{ij}. To complete the system, we require evolution equations for K_{ij} plus the constraint equations (energy and momentum conservation). Remarkably, this derivation relies solely on geometric constructs without invoking Einstein's field equations, which will subsequently provide the remaining constraints and evolution equations.

B.2 Gauss-Codazzi and Codazzi-Mainardi Equations

These two fundamental equations form the backbone of the 3+1 formalism, yielding the remaining three equations when contracted with the spatial metric. Their derivation requires careful consideration of both the spatial Riemann tensor and its four-dimensional counterpart.

B.2.1 Spatial Covariant Derivative and Extrinsic Curvature

The spatial covariant derivative D_α projects all indices of the 4D derivative ∇_α onto Σ_t:

$$D_\alpha T^{\nu_1\nu_2\mu_3\cdots}{}_{\mu_1\mu_2\mu_3\ldots} = \gamma^{\beta}{}_{\alpha}\gamma^{\sigma_1}{}_{\mu_1}\gamma^{\sigma_2}{}_{\mu_2}\cdots\gamma^{\nu_1}{}_{\rho_1}\gamma^{\nu_2}{}_{\rho_2}\cdots\nabla_\beta T^{\rho_1\rho_2\cdots}{}_{\sigma_1\sigma_2\ldots} \tag{B.8}$$

for any hypersurface tensor $T^{\nu_1\nu_2\mu_3\cdots}{}_{\mu_1\mu_2\mu_3\ldots}$. This construction ensures the spatial metric's covariant derivative vanishes:

$$\begin{aligned} D_\mu\gamma_{\alpha\beta} &= \gamma^{\nu}{}_{\mu}\gamma^{\sigma}{}_{\alpha}\gamma^{\rho}{}_{\beta}\nabla_\nu(g_{\sigma\rho} + n_\sigma n_\rho) \\ &= \gamma^{\nu}{}_{\mu}\gamma^{\sigma}{}_{\alpha}\gamma^{\rho}{}_{\beta}(n_\sigma\nabla_\nu n_\rho + n_\rho\nabla_\nu n_\sigma) = 0. \end{aligned}$$

Here we've utilized both metric compatibility ($\nabla_\nu g_{\sigma\rho} = 0$) and orthogonality between a temporal vector and a spatial tensor ($n_\sigma\gamma^{\sigma}{}_{\alpha} = 0$). This result mirrors the four-dimensional condition $\nabla_\mu g_{\alpha\beta} = 0$, facilitating the adaptation of four-dimensional equations to the hypersurface context.

The spatial Riemann tensor is defined analogously to its 4D counterpart:

$$R^{\nu}{}_{\alpha\beta\mu}\omega_\nu = (D_\alpha D_\beta - D_\beta D_\alpha)\omega_\mu \quad \text{with} \quad R^{\nu}{}_{\alpha\beta\mu}n_\nu = 0, \tag{B.9}$$

for any spatial vector $\omega_\mu \in T_pM$. The 3D Ricci tensor and scalar follow as $R_{\alpha\beta} = R^{\mu}{}_{\alpha\mu\beta} = \gamma^{\mu\nu}R_{\alpha\mu\beta\nu}$ and $R = \gamma^{\alpha\beta}R_{\alpha\beta} = R^{\alpha}{}_{\alpha}$.

From the extrinsic curvature definition ($P_{\mu\nu} = \gamma_{\mu\nu}$):

$$K_{\mu\nu} = -\gamma^{\alpha}{}_{\mu}\nabla_\alpha n_\nu \tag{B.10}$$

we derive:

$$K_{\mu\nu} = -(n^\alpha n_\mu \nabla_\alpha n_\nu + \nabla_\mu n_\nu) = -n_\mu a_\nu - \nabla_\mu n_\nu, \tag{B.11}$$

where the spatial acceleration vector is:

$$a_\nu \equiv n^\alpha \nabla_\alpha n_\nu = D_\nu \ln\alpha. \tag{B.12}$$

Thus we obtain:

$$\nabla_\mu n_\nu = -K_{\mu\nu} - n_\mu D_\nu \ln\alpha. \tag{B.13}$$

B.2.2 Gauss-Codazzi Equation

Beginning with (B.9) for a spatial vector satisfying $\omega_\alpha n^\alpha = 0$, we examine the double spatial covariant derivative:

$$\begin{aligned} D_aD_b\omega_c &= \gamma^f{}_a\gamma^g{}_b\gamma^h{}_c\nabla_f(D_g\omega_h) = \gamma^f{}_a\gamma^g{}_b\gamma^h{}_c\nabla_f(\gamma^d{}_g\gamma^e{}_h\nabla_d\omega_e) \\ &= \gamma^f{}_a\gamma^d{}_b\gamma^e{}_c\nabla_f\nabla_d\omega_e + \gamma^f{}_a\gamma^d{}_b\gamma^h{}_c(\nabla_f\gamma^e_h)(\nabla_d\omega_e) + \gamma^f{}_a\gamma^g{}_b\gamma^e{}_c(\nabla_f\gamma^d_g)(\nabla_d\omega_e). \end{aligned} \tag{B.14}$$

The last two terms simplify through careful analysis:

- Second term: Using $\gamma^e{}_h = g^e{}_h + n^e n_h$:

  $$\gamma^f{}_a\gamma^h{}_c(\nabla_f\gamma^e{}_h) = \gamma^f{}_a\gamma^h{}_c(n_h\nabla_f n^e + n^e\nabla_f n_h) = \gamma^f{}_a\gamma^h{}_c n^e\nabla_f n_h = -n^e K_{ac}. \tag{B.15}$$

  We've employed both metric compatibility ($\nabla_f g^e{}_h = 0$) and the projector definition (2.16), $K_{\mu\nu} \equiv -\gamma^{\alpha}{}_{\mu}\nabla_\alpha n_\nu$.

  This leads to:

  $$\gamma^f{}_a\gamma^d{}_b\gamma^h{}_c(\nabla_f\gamma^e{}_h)(\nabla_d\omega_e) = -\gamma^d{}_b n^e K_{ac}(\nabla_d\omega_e), \tag{B.16}$$

  where we can rewrite $\nabla_d(n^e\omega_e) = 0 = n^e\nabla_d\omega_e + (\nabla_d n^e)\omega_e$ due to $\omega_d n^d = 0$, yielding:

  $$\gamma^f{}_a\gamma^d{}_b\gamma^h{}_c(\nabla_f\gamma^e{}_h)(\nabla_d\omega_e) = -K_{ac}\gamma^d{}_b(\nabla_d n^e)\omega_e = -K_{ac}K^e_b\omega_e. \tag{B.17}$$

- Third term:

  $$\gamma^f{}_a\gamma^g{}_b(\nabla_f\gamma^d{}_g) = -n^d K_{ab}. \tag{B.18}$$

Thus, (B.14) becomes:

$$D_a D_b \omega_c = \gamma^f{}_a \gamma^d{}_b \gamma^e{}_c \nabla_f \nabla_d \omega_e - K_{ac} K^d_b \omega_d - n^d (\nabla_d \omega_e) \gamma^e{}_c K_{ab}. \tag{B.19}$$

Combining terms in (B.9):

$$\begin{aligned} R^d{}_{abc} \omega_d = (D_a D_b - D_b D_a)\omega_c &= \gamma^f{}_a \gamma^g{}_b \gamma^e{}_c (\nabla_f \nabla_g - \nabla_g \nabla_f)\omega_e + (K_{bc} K^d{}_a - K_{ac} K^d{}_b)\omega_d \\ &= (\gamma^f{}_a \gamma^g{}_b \gamma^e{}_c {}^{(4)}R^d{}_{fge} + K_{bc} K^d{}_a - K_{ac} K^d{}_b)\omega_d. \end{aligned}$$

Here we've utilized the four-dimensional Riemann tensor definition.

Since this holds for any spatial tensor ω^d, we obtain the Gauss-Codazzi equation:

$$\boxed{\gamma^e{}_a \gamma^f{}_b \gamma^g{}_c \gamma^h{}_d \, {}^{(4)}R_{efgh} = R_{abcd} - K_{ac} K_{bd} + K_{ad} K_{bc}}. \tag{B.20}$$

B.2.3 Codazzi-Mainardi Equation

From the 4D Riemann tensor identity (definition of the Riemann tensor (B.9) now 4-dimensional):

$$v_d \, {}^{(4)}R^d{}_{mbc} = (\nabla_m \nabla_b - \nabla_b \nabla_m) v_c. \tag{B.21}$$

for any vector v_d. Projecting with $\gamma^d{}_m \gamma^e{}_b \gamma^f{}_c$ for n^f:

$$\gamma^d{}_m \gamma^e{}_b \gamma^f{}_c (\nabla_c \nabla_d - \nabla_d \nabla_e) n^f = \gamma^d{}_m \gamma^e{}_b \gamma^f{}_c n^g \, {}^{(4)}R^f{}_{deg}. \tag{B.22}$$

Using $\nabla_c n^b = -K_c{}^b - n_c a^b$, $\gamma^d{}_m n_d = 0$, and $\nabla_d n_e = -K_{de} - n_d a_e$, the second term becomes:

$$\begin{aligned} \gamma^d{}_m \gamma^e{}_b \gamma^f{}_c \nabla_d \nabla_e n^f &= -\gamma^d{}_m \gamma^e{}_b \gamma^f{}_c \nabla_d (K_e{}^f + n_e a^f) = -D_m K_b{}^c - \gamma^d{}_m \gamma^e{}_b a^c \nabla_d n_e \\ &= -D_m K_b{}^c + a^c K_{mb}. \end{aligned}$$

Thus (B.22) yields the Codazzi-Mainardi equation:

$$\boxed{D_b K_{mc} - D_m K_{bc} = \gamma^d{}_m \gamma^e{}_b \gamma^f{}_c n^g \, {}^{(4)}R_{defg}}. \tag{B.23}$$

B.3 Second Equation: Hamiltonian Constraint

Contracting the Gauss-Codazzi equation (B.20) twice yields the Hamiltonian constraint—a scalar equation governing energy conservation. The first contraction with γ^{bd} gives:

$$\begin{aligned} R_{ac} = \gamma^{bd} R_{abcd} &= \gamma^e{}_a \gamma^{bd} \gamma^g{}_c \, {}^{(4)}R_{ebgd} + K_{ab} K_c{}^b - K_{ac} K \\ &= \gamma^e{}_a \gamma^g{}_c ({}^{(4)}R_{eg} + n^b n^d \, {}^{(4)}R_{ebgd}) + K_{ab} K_c{}^b - K_{ac} K. \end{aligned} \tag{B.24}$$

Here we've used in the first term $\gamma^{bd} = g^{bd} + n^b n^d$, making $g^{bd\,(4)}R_{ebgd} = {}^{(4)}R_{eg}$.

The second contraction with γ^{ac}, using in the first two terms that $\gamma^{ac}\gamma^{e}{}_{a}\gamma^{g}{}_{c} = \gamma^{eg} = g^{eg} + n^e n^g$, such that $\gamma^{eg\,(4)}R_{eg} = {}^{(4)}R + n^e n^{g\,(4)}R_{eg}$, yields:

$$R = {}^{(4)}R + 2n^b n^{d\,(4)}R_{bd} + K_{ab}K^{ab} - K^2. \tag{B.25}$$

Using Einstein's equations (2.1) and $g_{ab}n^a n^b = -1$:

$$n^a n^b 2G_{ab} = 2n^a n^{b(4)}R_{ab} - n^a n^{b(4)}Rg_{ab} + 2\Lambda n^a n^b g_{ab} = 2n^a n^{b(4)}R_{ab} + {}^{(4)}R - 2\Lambda. \tag{B.26}$$

Thus (B.25) becomes:

$$R = 2n^a n^b G_{ab} + K_{ab}K^{ab} - K^2 + 2\Lambda. \tag{B.27}$$

Since $n^a n^b G_{ab} = 8\pi n^a n^b T_{ab} = 8\pi\rho$ by (2.21), we obtain the Hamiltonian constraint:

$$\boxed{H^0 = R - K_{ab}K^{ab} + K^2 - 16\pi\rho - 2\Lambda = 0}. \tag{B.28}$$

This constraint equation must hold at all times, governing the energy conservation in our spacetime foliation.

B.4 Third Equation: Momentum Constraints

The momentum constraints emerge from the Codazzi-Mainardi equation through careful projection and contraction. Using:

$$\gamma^{e}{}_{b}n^{g\,(4)}R_{eg} = \gamma^{e}{}_{b}n^{g}\left(8\pi T_{eg} - \Lambda g_{eg} + \frac{1}{2}g_{eg}{}^{(4)}R\right) = 8\pi\gamma^{e}{}_{b}n^{g}T_{eg}, \tag{B.29}$$

since $\gamma^{e}_{b}n_e = 0$.

Contracting (B.23) with γ^{ac} yields:

$$D_b K - D_a K^a_b = \gamma^{e}{}_{b}(g^{df} + n^d n^f)n^{g\,(4)}R_{defg} = \gamma^{e}{}_{b}n^{g\,(4)}R_{eg} = 8\pi\gamma^{e}{}_{b}n^{g}T_{eg}, \tag{B.30}$$

which, via (2.22), becomes the momentum constraints:

$$\boxed{H^b = D_a(K^{ab} - \gamma^{ab}K) - 8\pi J^b = 0}. \tag{B.31}$$

These three constraint equations ($b = 1,2,3$) govern momentum conservation in our foliation.

B.5 Fourth Equation: Extrinsic Curvature Evolution

The evolution equation for K_{ab} derives from examining:

$$\gamma^e{}_a\gamma^h{}_c n^b n^{d\,(4)}R_{ebhd}. \tag{B.32}$$

Beginning with (B.21) for n_d:

$$n_d{}^{(4)}R^d{}_{abc} = (\nabla_a\nabla_b - \nabla_b\nabla_a)n_c. \tag{B.33}$$

Expanding the first term using (B.13):

$$\begin{aligned}\nabla_a\nabla_b n_c &= -\nabla_a(K_{bc} + n_b D_c \ln\alpha) = -\nabla_a K_{bc} - (\nabla_a n_b)D_c\ln\alpha - n_b\nabla_a D_c\ln\alpha \\ &= -\nabla_a K_{bc} + (K_{ab} + n_a D_b\ln\alpha)D_c\ln\alpha - n_b\nabla_a D_c\ln\alpha.\end{aligned}$$

Thus (B.33) becomes:

$$\begin{aligned}&\gamma^e{}_a\gamma^h{}_c n^b n^{d\,(4)}R_{ebhd} = \gamma^e{}_a\gamma^h{}_c n^d(\nabla_e\nabla_d - \nabla_d\nabla_e)n_h \\ &= \gamma^e{}_a\gamma^h{}_c n^d[-\nabla_e K_{dh} + \nabla_d K_{eh} + 0 + (n_e D_d\ln\alpha - n_d D_e\ln\alpha)D_h\ln\alpha \\ &\qquad - (n_d\nabla_e - n_e\nabla_d)D_h\ln\alpha].\end{aligned}$$

Several terms vanish identically because $n^d D_d\ln\alpha = n^d\gamma^z{}_d\nabla_z\ln\alpha = 0$ ($n^d\gamma^z{}_d = 0 = \gamma_a{}^e n_e$). The remaining terms includind $\ln\alpha$ that are not trivial simplify to:

$$\gamma^e{}_a\gamma^h{}_c(-n^d n_d)(D_e\ln\alpha + \nabla_e)D_h\ln\alpha = \left(\frac{1}{\alpha}D_a\alpha + D_a\right)\frac{1}{\alpha}D_c\alpha = \frac{1}{\alpha}D_aD_c\alpha. \tag{B.34}$$

This leads (B.33) to:

$$\gamma^e{}_a\gamma^h{}_c n^b n^{d\,(4)}R_{ebhd} = \gamma^e{}_a\gamma^h{}_c n^d(\nabla_d K_{eh} - \nabla_e K_{dh}) + \frac{1}{\alpha}D_aD_c\alpha. \tag{B.35}$$

- First term: Using (B.1), the Lie derivative definition:

$$\gamma^e{}_a\gamma^h{}_c n^d\nabla_d K_{eh} = \gamma^e{}_a\gamma^h{}_c(\mathcal{L}_n K_{eh} - K_{eb}\nabla_h n^b - K_{bh}\nabla_e n^b). \tag{B.36}$$

  The second term becomes $\gamma^e{}_a\gamma^h{}_c K_{eb}\nabla_h n^b = (\gamma^e{}_a K_{eb})(\gamma^h{}_c\nabla_h n^b) = K_{ab}(-K_c{}^b)$, using $K_{\mu\nu} = -\gamma^\alpha{}_\mu\nabla_\alpha n_\nu$. Similarly, $\gamma^e{}_a\gamma^h{}_c K_{bh}\nabla_e n^b = K_{bc}(-K^b{}_a)$. Thus, those two terms are equal and:

$$\gamma^e{}_a\gamma^h{}_c n^d\nabla_d K_{eh} = \mathcal{L}_n K_{ac} + 2K_{ab}K^b{}_c \tag{B.37}$$

- Second term: From $\nabla_e(n^d K_{dh}) = 0 = (\nabla_e n^d)K_{dh} + n^d(\nabla_e K_{dh})$, we obtain:

$$-\gamma^e{}_a\gamma^h{}_c n^d\nabla_e K_{dh} = \gamma^e{}_a K_{cd}\nabla_e n^d = -K_{cd}K^d{}_a. \tag{B.38}$$

Thus:

$$\gamma^e{}_a\gamma^h{}_c n^b n^{d\,(4)}R_{ebhd} = \mathscr{L}_n K_{ac} + K_{ab}K^b{}_c + \frac{1}{\alpha}D_a D_c\alpha. \tag{B.39}$$

Substituting (B.39) into (B.24) and isolating the Lie derivative:

$$\mathscr{L}_n K_{ac} = R_{ac} - \gamma^e{}_a\gamma^h{}_c\,{}^{(4)}R_{eh} - 2K_{ab}K^b_c + KK_{ac} - \frac{1}{\alpha}D_a D_c\alpha. \tag{B.40}$$

- Second term: Contracting Einstein's equations with g^{ab}:

$${}^{(4)}R - \frac{1}{2}4^{(4)}R + 4\Lambda = 8\pi T_b{}^b \rightarrow {}^{(4)}R = 4\Lambda - 8\pi T_b{}^b, \tag{B.41}$$

  allowing us to rewrite (2.1) as:

$${}^{(4)}R_{ab} - \frac{1}{2}g_{ab}(4\Lambda - 8\pi T_b{}^b) + \Lambda g_{ab} = 8\pi T_{ab}, \tag{B.42}$$

$${}^{(4)}R_{ab} = 8\pi\left(T_{ab} - \frac{1}{2}T_b{}^b\right) + \Lambda g_{ab}. \tag{B.43}$$

  Therefore:

$$\begin{aligned}\gamma^e{}_a\gamma^h{}_c\,{}^{(4)}R_{eh} &= 8\pi\gamma^e{}_a\gamma^h{}_c\left(T_{eh} - \frac{1}{2}g_{eh}T_b{}^b\right) + \gamma^e{}_a\gamma^h{}_c\Lambda g_{eh}\\ &= 8\pi\left(S_{ac} - \frac{1}{2}\gamma_{ac}T_b{}^b\right) + \Lambda\gamma_{ac},\end{aligned} \tag{B.44}$$

  using definition (2.23).

- Left-hand side: Using (B.2):

$$\mathscr{L}_{\alpha n}K_{ac} = \alpha\mathscr{L}_n K_{ac} = \mathscr{L}_t K_{ac} - \mathscr{L}_{\vec{\beta}}K_{ac} = \partial_t K_{ac} - \mathscr{L}_{\vec{\beta}}K_{ac}, \tag{B.45}$$

  where the last term is given by the Lie derivative definition (B.1):

$$\mathscr{L}_{\vec{\beta}}K_{ac} = \beta^b D_b K_{ac} + K_{ab}D_c\beta^b + K_{bc}D_a\beta^b \tag{B.46}$$

Thus, from (B.45) we extract $\partial_t K_{ac}$, yielding the extrinsic curvature evolution equation:

$$\begin{aligned}\partial_t K_{ac} = {}&\beta^b D_b K_{ac} + K_{ab}D_c\beta^b + K_{bc}D_a\beta^b - D_a D_c\alpha +\\ &+ \alpha\left[R_{ac} - 2K_{ab}K_c{}^b + KK_{ac}\right] + 4\pi\alpha[\gamma_{ac}(S-\rho) - 2S_{ac}].\end{aligned} \tag{B.47}$$

This completes our formulation of Einstein's equations as a well-posed Cauchy problem.

C Lagrangian and Hamiltonian Formalisms

C.1 The Lagrangian Formalism

Our objective now transitions to deriving the Lagrangian formulation of the system, which will naturally lead to a Hamiltonian description. This approach will reveal the Hamiltonian constraint as a function of conjugate momenta, providing a pathway to quantum gravity.

We begin with the Einstein-Hilbert action [46]:

$$S_{EH} = \frac{1}{16\pi}\int_M \left({}^{(4)}R - 2\Lambda\right)\sqrt{-g}\, d^4x = \int_M \mathscr{L}\, d^4x, \tag{C.1}$$

where M represents the spacetime manifold and $\mathscr{L}$ the Lagrangian density.

To construct the Hamiltonian, we must identify the physical quantities and their conjugate momenta. Using (B.25), we rewrite the second term employing the Ricci tensor definition (B.33):

$$n^a n^{b\,(4)}R_{ab} = n^a[\nabla_b, \nabla_a]n^b = \Big[\nabla_b(n^a\nabla_a n^b) - (\nabla_b n^a)\nabla_a n^b\Big] - \Big[\nabla_b(n^b\nabla_a n^a) - (\nabla_a n^a)^2\Big]. \tag{C.2}$$

Using (B.13) and $n_\nu a^\nu = n_\nu(n^\alpha\nabla_\alpha n_\nu) = n^\alpha\frac{1}{2}\nabla_\alpha(n_\nu n^\nu) = 0$, we simplify:

- The second term of (C.2) becomes:

$$K_{mb}K^{mb} = (\nabla_m n_b + n_m a_b)K^{ab} = (\nabla_m n_b)K^{bm} = (\nabla_b n^m)(\nabla_m n^b), \tag{C.3}$$

  using $n^b K_{bm} = 0$ and $K_{mb} = K_{bm}$.

- The last term of (C.2) relates to:

$$\nabla_m n^m = -K_m{}^m - n_m a^m = -K_m{}^m \tag{C.4}$$

  making $(\nabla_a n^a)^2 = K^2$.

Substituting these into (C.2) and (C.1) via (B.25), with $\sqrt{-g} = \alpha\sqrt{\gamma}$, yields:

$$S_{EH} = \frac{1}{16\pi}\int_M \Big(R - K^2 + K_{ij}K^{ij} - 2\Lambda\Big)\alpha\sqrt{\gamma}\, d^4x - \frac{1}{8\pi}\int_M \alpha\sqrt{\gamma}\nabla_\alpha\left(n^\mu\nabla_\mu n^\alpha - n^\alpha\nabla_\mu n^\mu\right)d^4x. \tag{C.5}$$

The second integral represents a surface term via Stokes' theorem [114], which do not depend on any independent variable.

Indeed, we can calculate as we can do in Hamiltonian mechanichs the canonical momenta density Π associated to the different configuration variables q [84], such that:

$$\Pi_\alpha = \frac{\partial \mathscr{L}}{\partial \dot{\alpha}} = 0, \quad \Pi_{\beta^i} = 0, \quad \Pi^{ij} = \frac{\partial \mathscr{L}}{\partial \dot{\gamma}_{ij}} \neq 0 \tag{C.6}$$

due to the relation between K and $\dot{\gamma_{ij}} := \partial_t \gamma_{ij}$ via (B.7), and the absence of $\dot{\alpha}$, $\dot{\beta}^i$ in the action. This confirms α and β_i as non-dynamical Lagrange multipliers while γ_{ij} evolves dynamically. This will be more clear later on, when they appear as Lagrange multipliers in our description.

C.2 The Hamiltonian Formalism

We now drop the $1/16\pi$ factor for notational simplicity. The Hamiltonian density $\mathscr{H}$ emerges from the Legendre transform of $\mathscr{L}$, with Π as the dual variables [44]:

$$\mathscr{H} \doteq \sum_q \Pi \dot{q} - \mathscr{L}. \tag{C.7}$$

To find Π^{ij}, we note that the boundary term in (C.1) lacks $\dot{\gamma}_{ij}$ dependence. Thus we compute:

$$\frac{\partial (R - K^2 + K_{ij}K^{ij} - 2\Lambda)}{\partial \dot{\gamma}_{ij}} = \frac{\partial (K_{ij}K^{ij} - K^2)}{\partial \dot{\gamma}_{ij}}. \tag{C.8}$$

Let's do it by part. From (B.7):

$$K_{ij} = -\frac{1}{2\alpha}(D_i\beta_j + D_j\beta_i - \dot{\gamma}_{ij}) \;\rightarrow\; \frac{\partial K_{ij}}{\partial \dot{\gamma}_{kl}} = -\frac{1}{2\alpha}\delta_i^k \delta_j^l, \tag{C.9}$$

with δ_i^k the Kronecker delta, $\delta_i^k = 1$ if $i = k$ [115]. Including this result into Π^{ij}:

$$\begin{aligned}
\Pi^{kl} &= \alpha\sqrt{\gamma}\frac{\partial}{\partial \dot{\gamma}_{kl}}(K_{ij}K^{ij} - \gamma^{pn}K_{pn}\gamma^{ij}K_{ij}) \\
&= \alpha\sqrt{\gamma}\left(-\frac{1}{2\alpha}\right)(\delta_i{}^k\delta_j{}^l K^{ij} + K_{ij}\gamma^{ip}\gamma^{jn}\delta_p{}^k\delta_n{}^l - \gamma^{pn}\delta_p{}^k\delta_n{}^l K - K\gamma^{ij}\delta_i{}^k\delta_j{}^l) \\
&= -\frac{\sqrt{\gamma}}{2}(2K^{kl} - 2\gamma^{kl}K) = \sqrt{\gamma}(\gamma^{kl}K - K^{kl}).
\end{aligned} \tag{C.10}$$

It will be convenient to rewrite the variables that appear in the Lagrangian (C.5) as functions of γ_{ij} and Π^{ij}. To this end, let us compute the trace of Π^{ij}:

$$\Pi := \gamma_{ij}\Pi^{ij} = \sqrt{\gamma}(\gamma_{ij}\gamma^{ij}K - \gamma_{ij}K^{ij}) = 2\sqrt{\gamma}K. \tag{C.11}$$

We can introduce this expression into (C.10) to obtain K^{ij} as a function of Π^{ij} and Π:

$$K^{ij} = K\gamma^{ij} - \frac{\Pi^{ij}}{\sqrt{\gamma}} = \frac{1}{2\sqrt{\gamma}}(\Pi\gamma^{ij} - 2\Pi^{ij}). \tag{C.12}$$

The volume term of the Lagrangian density then becomes, as a function of the canonical variables:

$$\mathscr{L}_0 = \alpha\sqrt{\gamma}\left(R - K^2 + K_{ij}K^{ij} - 2\Lambda\right). \tag{C.13}$$

- $K^2 = \Pi^2/4\gamma$ from (C.11)
- $K_{ij}K^{ij}$ expands to:

$$\begin{aligned} K_{ij}K^{ij} &= \gamma_{ik}\gamma_{jl}\frac{1}{2\sqrt{\gamma}}(\Pi\gamma^{kl} - 2\Pi^{kl})\frac{1}{2\sqrt{\gamma}}(\Pi\gamma^{ij} - 2\Pi^{ij}) = \\ &= \frac{1}{4\gamma}\gamma_{ik}\gamma_{jl}(\Pi^2\gamma^{kl}\gamma^{ij} - 2\Pi\gamma^{kl}\Pi^{ij} - 2\Pi^{kl}\Pi\gamma^{ij} + 4\Pi^{kl}\Pi^{ij}) \\ &= \frac{1}{4\gamma}(\Pi^2\gamma_{ij}\gamma^{ij} - 2\Pi\gamma_{ij}\Pi^{ij} - 2\Pi_{ij}\Pi\gamma^{ij} + 4\Pi_{ij}\Pi^{ij}) \\ &= \frac{1}{\gamma}\left(\Pi_{ij}\Pi^{ij} - \frac{1}{4}\Pi^2\right) \end{aligned} \tag{C.14}$$

Thus the Lagrangian density finally becomes:

$$\mathscr{L}_0 = \alpha\sqrt{\gamma}\,(R - 2\Lambda) + \frac{\alpha}{\sqrt{\gamma}}\left(\Pi^{ij}\Pi_{ij} - \frac{1}{2}\Pi^2\right). \tag{C.15}$$

The Hamiltonian density corresponding to $\mathscr{L}_0$ then follows:

$$\mathscr{H}_0 \doteq \Pi^{ij}\dot{\gamma}_{ij} - \mathscr{L}_0. \tag{C.16}$$

Combining (B.7) and (C.10):

$$\begin{aligned} \Pi^{ij}\dot{\gamma}_{ij} &= -2\alpha\Pi^{ij}K_{ij} + \Pi^{ij}(D_i\beta_j + D_j\beta_i) \\ &= -2\alpha\sqrt{\gamma}(\gamma^{ij}KK_{ij} - K^{ij}K_{ij}) + 2D_i(\Pi^{ij}\beta_j) - 2(D_i\Pi^{ij})\beta_j. \end{aligned} \tag{C.17}$$

Simplifying:

- The third of (C.17) term is a surface term.
- The second term of (C.17) had been already calculated on (C.14).

- And the first term of (C.17) is given by:

$$\gamma^{ij}KK_{ij} = \gamma^{ij}\gamma_{in}\gamma_{jl}KK^{nl} = \gamma_{nl}\frac{\Pi}{2\sqrt{\gamma}}\frac{1}{2\sqrt{\gamma}}(\Pi\gamma^{nl} - 2\Pi^{nl}) = \frac{1}{4\gamma}(3\Pi^2 - 2\Pi^2)$$
$$= \frac{\Pi^2}{4\gamma}. \tag{C.18}$$

  He have used that $\gamma_{nl}\gamma^{nl} = 3$ for our 3-tridimensional hypersurface.

With all this calculus, we are in the position of showing the final expression of the Hamiltonian over the hypersurface Σ_t and over its boundary that we called surface $\partial\Sigma_t := S$. For that, we introduce (C.17) into the density Hamiltonian $\mathscr{H} = \Pi^{ij}\dot{\gamma}_{ij} - \mathscr{L}$, with $\mathscr{L}$ the density Lagrangian associated to the total action (C.5), and separating the volume and surface terms, we finally obtain the total Hamiltonian $H = H_\Sigma + H_S$:

$$H_\Sigma = \int_{\Sigma_t}\left[-2(D_i\Pi^{ij})\beta_j - \alpha\sqrt{\gamma}\,(R - 2\Lambda) + \frac{\alpha}{\sqrt{\gamma}}\left(\Pi_{ij}\Pi^{ij} - \frac{\Pi^2}{2}\right)\right]\mathrm{d}^3x, \tag{C.19}$$

$$H_S = 2\int_{\Sigma_t}\left[\alpha\sqrt{\gamma}\nabla_\alpha\left(n^\mu\nabla_\mu n^\alpha - n^\alpha\nabla_\mu n^\mu\right) + D_i(\Pi^{ij}\beta_j)\right]d^3x. \tag{C.20}$$

H_S can be converted into an integral over S using the Stokes theorem, so we will just keep its study out of this work (they do not alter the equations of motion).

D Brief review of quantum mechanics

Quantum mechanics describes the time evolution of particles at microscopic scales [88, 89, 90]. For a point $x \in M$ and time $t \in \mathbb{R}^+$, the system is characterized by a complex-valued wave function $\phi : M \to \mathbb{C}$. The probability distribution $|\phi(x)|^2$ represents the probability density for finding the particle at position x. The wave function is assumed to be square-integrable (L^2-function) with normalization $||\phi||^2_{L^2} = 1$ for all t.

In this framework, observables correspond to self-adjoint operators on the Hilbert space $\mathscr{H}_S := L^2(M, \mathbb{C})$, that is, a vector space supplied with a scalar product that is complete respect to the norm induced by the scalar product [116]. The eigenvalues associated with an operator's eigenstates represent the possible measurement outcomes.

Through canonical quantization, the classical momentum p_j becomes the operator $\frac{\hbar}{i}\partial_j$. The classical Poisson bracket relations:

$$\{x^i, x^j\} = 0 = \{p_i, p_j\} \quad \text{and} \quad \{x^i, p_j\} = \delta^i{}_j, \tag{D.1}$$

where $\{a, b\} := \frac{\partial a}{\partial x^i}\frac{\partial b}{\partial p_i} - \frac{\partial a}{\partial p_i}\frac{\partial b}{\partial x^i}$ is the Poisson bracket, translate to the quantum commutation relations:

$$[\hat{x}^i, \hat{x}^j] = 0 = [\hat{p}_i, \hat{p}_j] \quad \text{and} \quad [\hat{x}^j, \hat{p}_k] = i\hbar\delta^j{}_k, \tag{D.2}$$

where $[a, b] = ab - ba$.

The state of a particle is represented in Dirac's notation by $|\phi\rangle \in \mathscr{H}_S$, and its time evolution is governed by the Schrödinger equation [117]:

$$i\hbar\frac{\partial}{\partial t}|\phi(t)\rangle = \hat{H}|\phi(t)\rangle. \tag{D.3}$$

Here, $\hat{H}$ is the quantum operator corresponding to the classical Hamiltonian, which must be self-adjoint.

E Numerical implementations

E.1 Derivation of the Friedmann equations

E.1.1 Einstein Equations

Thanks to the metric in the (t, r, θ, φ) coordinates, equation (3.1):

$$g_{\mu\nu} = \begin{pmatrix} -\alpha(t)^2 & 0 & 0 & 0 \\ 0 & a^2(t)\frac{1}{1-Qr^2} & 0 & 0 \\ 0 & 0 & a^2(t)r^2 & 0 \\ 0 & 0 & 0 & a^2(t)r^2\sin^2\theta^2 \end{pmatrix}, \tag{E.1}$$

and to the Levi-Civita connection, we can calculate the Christoffel Symbols as (see Corollary A.1):

$$\Gamma^{\rho}{}_{\mu\nu} = \frac{1}{2}g^{\rho\sigma}\left(\partial_\mu g_{\nu\sigma} + \partial_\nu g_{\mu\sigma} - \partial_\sigma g_{\mu\nu}\right). \tag{E.2}$$

Thus, the Riemann tensor will be, in local coordinates (see Theorem A.2 and Definition A.22):

$$R^{\rho}_{\sigma\mu\nu} = \partial_\mu \Gamma^{\rho}{}_{\nu\sigma} - \partial_\nu \Gamma^{\rho}{}_{\mu\sigma} + \Gamma^{\rho}{}_{\mu\lambda}\Gamma^{\lambda}{}_{\nu\sigma} - \Gamma^{\rho}{}_{\nu\lambda}\Gamma^{\lambda}{}_{\mu\sigma}, \tag{E.3}$$

the Ricci tensor:

$$R_{\mu\nu} = R^{\lambda}_{\mu\lambda\nu} = \partial_\rho \Gamma^{\rho}{}_{\mu\nu} - \partial_\nu \Gamma^{\rho}{}_{\mu\rho} + \Gamma^{\rho}{}_{\mu\nu}\Gamma^{\sigma}{}_{\rho\sigma} - \Gamma^{\rho}{}_{\mu\sigma}\Gamma^{\sigma}{}_{\rho\nu}, \tag{E.4}$$

and the Ricci scalar:

$$R = g^{\mu\nu}R_{\mu\nu} \tag{E.5}$$

On the other hand, considering our action minimally coupled to the scalar field that we called inflaton, the energy-momentum tensor is given by (3.4):

$$T_{\mu\nu} = \partial_\mu\phi\,\partial_\nu\phi - g_{\mu\nu}\left(\frac{1}{2}g^{\rho\sigma}\partial_\rho\phi\,\partial_\sigma\phi + V(\phi)\right) \tag{E.6}$$

Then, we have all the ingredients to calculate the different components of the Einstein equations (2.1) with Λ a cosmological constant:

$$G_{\mu\nu} = R_{\mu\nu} - \frac{1}{2}g_{\mu\nu}R + \Lambda g_{\mu\nu} = 8\pi G T_{\mu\nu}. \tag{E.7}$$

In the following, you can see the code to calculate all this tensors:

```
from sympy import symbols, Function, diag, exp, diff, simplify, pi, sqrt, Eq, Matrix, Derivative, sin, cos,latex

# Define symbolic variables
t, r, theta, varphi, Q, Lambda = symbols('t r theta varphi Q Lambda', real=True)
# Time, radial, angular coordinates, curvature constant, and cosmological constant
a = Function('a')(t)  # Scale factor as a function of time
phi = Function('phi')(t)  # Scalar field as a function of time
alpha = Function('alpha')(t)  # Time-dependent function for the metric - Lapse function
V = Function('V')(phi)  # Potential of the scalar field

# Define the FLRW metric
g = diag(-alpha**2, a**2/(1-Q*r**2), a**2*r**2, a**2*r**2*sin(theta)**2)  # Metric tensor g_{mu nu}
g_inv = diag(-1/alpha**2, (1-Q*r**2)/a**2, 1/(a**2*r**2), 1/(a**2*r**2*sin(theta)**2))  # Inverse metric g^{mu nu}
det_g = g.det()  # Determinant of the metric tensor

# Function to calculate Christoffel symbols
def calculate_christoffel(g, g_inv, coords):
    dim = 4  # Number of dimensions (4D spacetime)
    Gamma = {}  # Dictionary to store Christoffel symbols
    for mu in range(dim):  # Loop over the first index of Christoffel symbols
        for nu in range(dim):  # Loop over the second index
            for rho in range(dim):  # Loop over the third index
                term = 0  # Initialize the Christoffel symbol to zero
                for sigma in range(dim):  # Sum over the metric indices
                    # Compute partial derivatives of the metric tensor
                    dg_sigma_nu = diff(g[sigma, nu], coords[rho])
                    dg_sigma_rho = diff(g[sigma, rho], coords[nu])
                    dg_nu_rho = diff(g[nu, rho], coords[sigma])
                    # Add the terms to compute the Christoffel symbol
                    term += (1/2)*g_inv[mu, sigma]*(dg_sigma_nu + dg_sigma_rho - dg_nu_rho)
                if term != 0:  # Store only non-zero Christoffel symbols
                    Gamma[(mu, nu, rho)] = term
```

```
    return Gamma

coords = [t, r, theta, varphi]  # Coordinates of the spacetime
Gamma = calculate_christoffel(g, g_inv, coords)  # Compute Christoffel symbols

# Function to calculate the Riemann tensor
def calculate_riemann(Gamma, coords):
    dim = 4  # Number of dimensions
    R = {}  # Dictionary to store Riemann tensor components
    for rho in range(dim):  # Loop over the first index
        for sigma in range(dim):  # Loop over the second index
            for mu in range(dim):  # Loop over the third index
                for nu in range(dim):  # Loop over the fourth index
                    # Compute partial derivatives of Christoffel symbols
                    term1 = diff(Gamma.get((rho, sigma, nu), 0), coords[mu])
                    term2 = diff(Gamma.get((rho, sigma, mu), 0), coords[nu])
                    # Compute products of Christoffel symbols
                    term3 = sum(Gamma.get((rho, mu, l), 0)*Gamma.get((l, sigma, nu), 0) for l in range(dim))
                    term4 = sum(Gamma.get((rho, nu, l), 0)*Gamma.get((l, sigma, mu), 0) for l in range(dim))
                    # Combine terms to compute the Riemann tensor
                    total = simplify(term1 - term2 + term3 - term4)
                    if total != 0:  # Store only non-zero components
                        R[(rho, sigma, mu, nu)] = total
    return R

Riemann = calculate_riemann(Gamma, coords)  # Compute the Riemann tensor

# Compute the Ricci tensor by contracting the Riemann tensor
Ricci = Matrix.zeros(4, 4)  # Initialize the Ricci tensor as a 4x4 zero matrix
for mu in range(4):  # Loop over the first index
    for nu in range(4):  # Loop over the second index
        Ricci[mu, nu] = simplify(sum(Riemann.get((rho, mu, rho, nu), 0) for rho in range(4)))

```

```
# Compute the Ricci scalar by contracting the Ricci tensor with the inverse metric
R_scalar = simplify(sum(g_inv[mu, nu] * Ricci[mu, nu] for mu in range(4) for nu in range(4)))

# Compute the Einstein tensor
G = Matrix.zeros(4, 4)  # Initialize the Einstein tensor as a 4x4 zero matrix
for mu in range(4):  # Loop over the first index
    for nu in range(4):  # Loop over the second index
        G[mu, nu] = simplify(Ricci[mu, nu] - (1/2)*g[mu, nu]*R_scalar + Lambda*g[mu, nu])

# Compute components of the energy-momentum tensor for the scalar field
T00 = simplify(diff(phi, t)**2 - g[0,0]*(0.5*g_inv[0,0]*diff(phi, t)**2 + V))  # T_{00} component
T11 = simplify(-g[1,1]*(0.5*g_inv[0,0]*diff(phi, t)**2 + V))  # T_{11} component

# Compare the Einstein tensor and energy-momentum tensor components
diff_00 = simplify(G[0,0] - 8*pi*T00)  # Difference for G_{00} - 8G T_{00}
diff_11 = simplify(G[1,1] - 8*pi*T11)  # Difference for G_{11} - 8G T_{11}
```

Let us evaluate the different components of the equations just obtained numerically. We will define $db(t)/dt = \dot{b}(t)$ to simplify. It can be checked that there are only two independent components, the $G_{00} - 8\pi T_{00} = 0$ given by:

$$\left(\frac{\dot{a}}{a}\right)^2 = \frac{8\pi}{3}\left(V(\phi(t)) \cdot \alpha^2 + \frac{1}{2}\dot{\phi}^2\right) + \frac{\Lambda}{3}\alpha^2 - \frac{Q}{a^2}\alpha^2, \tag{E.8}$$

and $G_{11} - 8\pi T_{11} = 0$,

$$\alpha\left(\frac{\ddot{a}}{a} + \frac{1}{2}\left(\frac{\dot{a}}{a}\right)^2\right) = \dot{\alpha}\frac{\dot{a}}{a} - 4\pi\left(\frac{1}{2}\dot{\phi}^2 - V(\phi)\right)\alpha - \frac{Q}{2a^2}\alpha^3 + \frac{\Lambda}{2}\alpha^3. \tag{E.9}$$

E.1.2 Lagrangian Formalism - Equations of motion

The lagrangian density associated to the action (3.2) is:

$$\mathscr{L} = \sqrt{-g}\left(\frac{R - 2\Lambda}{16\pi G} - \frac{1}{2}g^{\mu\nu}\partial_\mu\phi\partial_\nu\phi - V(\phi)\right), \tag{E.10}$$

and the general equation of motion for the scalar field (inflaton) is derived from the Euler-Lagrange equations in four dimensions:

$$\frac{\partial \mathscr{L}}{\partial \phi(x^\mu)} - \partial_\mu \left(\frac{\partial \mathscr{L}}{\partial(\partial_\mu \phi(x^\nu))} \right) = 0, \tag{E.11}$$

where μ, ν range over all spacetime coordinates. In our cosmological context, the inflaton field ϕ is spatially homogeneous, depending only on cosmic time t (i.e., $\phi = \phi(t)$). This symmetry reduces (E.11) to:

$$\frac{\partial \mathscr{L}}{\partial \phi(t)} - \frac{d}{dt} \left(\frac{\partial \mathscr{L}}{\partial \dot{\phi}(t)} \right) = 0, \tag{E.12}$$

where $\dot{\phi} \equiv d\phi/dt$.

We can implement it almost directly:

```
L = sqrt(-det_g) * ((R_scalar-2*Lambda)/(16 * pi ) - 0.5 * g_inv[0, 0] *
 ↪  diff(phi, t)**2 - V)
# Euler-Lagrange equations
eom = diff(L, phi) - diff(diff(L, diff(phi, t)), t)
```

The result is:

$$\ddot{\phi} + 3\dot{\phi}\frac{\dot{a}}{a} + \alpha^2 \frac{dV(\phi(t))}{d\phi} - \dot{\phi}\frac{\dot{\alpha}}{\alpha} = 0. \tag{E.13}$$

It is worth noting that this equation can alternatively be derived from the energy-momentum conservation law in general relativity, $\nabla_\mu T^{\mu\nu} = 0$. For the temporal component ($\nu = 0$), this yields [59]:

$$\dot{\rho} + 3H(\rho + P) = 0, \tag{E.14}$$

where ρ and P represent the energy density and pressure of the inflaton field, respectively, given by:

$$\rho = \frac{1}{2}\dot{\phi}^2 + V(\phi), \tag{E.15}$$

$$P = \frac{1}{2}\dot{\phi}^2 - V(\phi). \tag{E.16}$$

E.2 Derivation of the equations of the Kinetic Dominance

For an expanding universe in the kinetic dominance regime, the equations (3.27) were solved using Wolfram Mathematica:

$$\ddot{\phi} \sim -\sqrt{\frac{3}{2}}\frac{|\dot{\phi}|}{M_{\rm pl}}\dot{\phi}, \quad \frac{\dot{a}}{a} \sim \frac{|\dot{\phi}|}{\sqrt{6}M_{\rm pl}}. \tag{E.17}$$

```
(* First, we solve the evolution equation *)
eqn = D[\[Phi][t], {t, 2}] == -(Sqrt[3/2])*(1/Mpl)*D[\[Phi][t],
 ↪  t]*D[\[Phi][t], t];

(* Solve it numerically *)
sol = DSolve[{eqn}, \[Phi][t], t, Assumptions -> t >= 0 && Mpl > 0] //
 ↪  FullSimplify

(* Next, solve the Friedmann equation numerically *)
(* Introduce the simplified solution as shown in the main file *)
solnew = c2 + (Sqrt[2/3])*Mpl*Log[t - t0];
dsol = D[solnew, t];
eqa = D[a[t], t] == 1/(Sqrt[6]*Mpl)*dsol*a[t];
aSolution = DSolve[eqa, a[t], t, Assumptions -> t > t0 && t >= 0 && Mpl >
 ↪  0]
```

The first solution obtained is presented in equation (3.29),

$$\phi_+(t) \sim c_2 + \sqrt{\frac{2}{3}}M_{\rm pl}\log\left(\sqrt{6}t - 2M_{\rm pl}c_1\right), \tag{E.18}$$

which, as explained, can be simplified to obtain the solution for the second equation shown in (3.31),

$$a(t) \sim a_0(t-t_0)^{1/3}. \tag{E.19}$$

This solution corresponds to $\dot{\phi} > 0$. For $\dot{\phi} < 0$, the only change is the sign in front of $\sqrt{2/3}$ in (E.18) to satisfy the condition.

E.3 Derivation of the 3-D Ricci Scalar for a Closed Universe

We can derive the expression for R that appears in the Hamiltonian constraint (2.26),

$$H^0 = R + K^2 - K_{ij}K^{ij} - 16\pi\rho - 2\Lambda = 0, \tag{E.20}$$

for the case where the metric is given by (3.1),

$$ds^2 = -\alpha(t)^2 dt^2 + a^2(t)\left(\frac{dr^2}{1-Qr^2} + r^2(d\theta^2 + \sin^2\theta\, d\varphi^2)\right) = -\alpha(t)^2 dt^2 + \gamma_{ij} dx^i dx^j, \tag{E.21}$$

where γ_{ij} represents the metric induced on our hypersurface, which is a sphere in the case of interest with $Q = +1$.

To achieve this, we will use a code analogous to the one presented in Appendix E.1, but applied to our specific case. Here, the metric γ_{ij} will be used to compute the associated Christoffel symbols, the 3-dimensional Riemann tensor ${}^{(3)}R_{abcd}$, the Ricci tensor ${}^{(3)}R_{ab}$, and the desired Ricci scalar ${}^{(3)}R = R$. (The notation ${}^{(3)}$ is used to emphasize that this is a 3-dimensional quantity, but throughout the text, we do not explicitly use this notation because we have already defined the 4-dimensional quantities as ${}^{(4)}$. It is understood that if no subscript appears, the quantities are 3-dimensional).

```
from sympy import symbols, Function, diag, diff, simplify, sin

# Define symbolic variables
r, theta, varphi, Q = symbols('r theta varphi Q', real=True)  # Spatial coordinates and curvature
t = symbols('t', real=True)  # Time (not directly used in 3D)
a = Function('a')(t)  # Scale factor as a function of time

# Induced metric on the 3D spatial hypersurface (FLRW)
gamma = diag(a**2 / (1 - Q * r**2), a**2 * r**2, a**2 * r**2 * sin(theta)**2)  # 3D metric
gamma_inv = diag((1 - Q * r**2) / a**2, 1 / (a**2 * r**2), 1 / (a**2 * r**2 * sin(theta)**2))  # Inverse of the metric

# Function to calculate Christoffel symbols
def calculate_christoffel_3D(gamma, gamma_inv, coords):
    dim = 3  # Dimension of the metric (3D)
    Gamma = {}  # Dictionary to store Christoffel symbols
    for i in range(dim):  # Upper index
        for j in range(dim):  # First lower index
```

```
            for k in range(dim):  # Second lower index
                term = 0  # Initialize the Christoffel symbol
                for l in range(dim):  # Sum over indices
                    # Partial derivatives of the metric
                    dg_lj = diff(gamma[l, j], coords[k])
                    dg_lk = diff(gamma[l, k], coords[j])
                    dg_jk = diff(gamma[j, k], coords[l])
                    # Compute the Christoffel symbol
                    term += (1 / 2) * gamma_inv[i, l] * (dg_lj + dg_lk -
                     ↪ dg_jk)
                if term != 0:  # Store only non-zero Christoffel symbols
                    Gamma[(i, j, k)] = simplify(term)
    return Gamma

# Spatial coordinates
coords = [r, theta, varphi]

# Calculate Christoffel symbols for the 3D metric
Gamma_3D = calculate_christoffel_3D(gamma, gamma_inv, coords)

# Function to calculate the Riemann tensor
def calculate_riemann_3D(Gamma, coords):
    dim = 3  # Dimension of the metric (3D)
    R = {}  # Dictionary to store Riemann tensor components
    for i in range(dim):  # First index
        for j in range(dim):  # Second index
            for k in range(dim):  # Third index
                for l in range(dim):  # Fourth index
                    # Partial derivatives of Christoffel symbols
                    term1 = diff(Gamma.get((i, l, k), 0), coords[j])
                    term2 = diff(Gamma.get((i, l, j), 0), coords[k])
                    # Products of Christoffel symbols
                    term3 = sum(Gamma.get((i, j, m), 0) * Gamma.get((m,
                     ↪ l, k), 0) for m in range(dim))
                    term4 = sum(Gamma.get((i, k, m), 0) * Gamma.get((m,
                     ↪ l, j), 0) for m in range(dim))
                    # Compute the Riemann tensor
                    total = simplify(term1 - term2 + term3 - term4)
                    if total != 0:  # Store only non-zero components
                        R[(i, j, k, l)] = total
```

```
    return R

# Calculate the Riemann tensor for the 3D metric
Riemann_3D = calculate_riemann_3D(Gamma_3D, coords)

# Calculate the Ricci tensor by contracting the Riemann tensor
Ricci_3D = Matrix.zeros(3, 3)  # Initialize the Ricci tensor as a 3x3 zero matrix
for i in range(3):  # Upper index
    for j in range(3):  # Lower index
        Ricci_3D[i, j] = simplify(sum(Riemann_3D.get((k, i, k, j), 0) for k in range(3)))

# Calculate the Ricci scalar by contracting the Ricci tensor with the inverse metric
R_scalar_3D = simplify(sum(gamma_inv[i, j] * Ricci_3D[i, j] for i in range(3) for j in range(3)))

# Print the 3D Ricci scalar
print("3D Ricci Scalar:")
print(R_scalar_3D)
```

The result is:

$$R = \frac{6Q}{a^2}. \tag{E.22}$$

F Wave function for $\overline{p} = 1$

We present here an analogous study to the one performed in Section 5.4, but now for $\overline{p} = 1$ with the same $|k|$-values. The main differences are:

- For $k = 0$, see Fig. 27, the peak of both imaginary and real parts at $a = 0$ are three orders of magnitude higher than in Fig. 20 ($|3.46 \cdot 10^6| \gg |1565.2|$), indicating a greater probability of the Universe emerging at this point, with $|\Psi_\pm|^2(a = 0) \sim 10^{13}$. The first peak at $a = p$ has the same value for both cases, $\overline{p} = 0$ and $\overline{p} = 1$. The oscillatory part is narrower for $\overline{p} = 1$, resulting in lower values of $|\Psi_\pm|^2(a > p)$. This behavior occurs consistently across all cases, in the allowed region in which the functions are oscillatory.

- For $|k| = 1$, see Fig. 28, the real and imaginary parts approach a non-zero value as $a \to 0^+$. The first peak at $a = p_1$ is larger than for $\overline{p} = 0$, see Fig. 21 assocaited to $\overline{p} = 0$, leading to a higher value of $|\Psi_\pm|^2(a = p_1)$.

- For $|k| = \sqrt{8\pi^2 p^4/(27\lambda)}$, see Fig. 29, the value at $a = a_0$ is slightly greater than the peak for $\overline{p} = 0$, see Fig. 22, with $29 > 26.2$ for the imaginary part. Consequently, $|\Psi_\pm|^2(a = a_0)$ is greater for $\overline{p} = 1$, and again $|\Psi_\pm|^2(a = 0) \neq 0$.

- For $|k| = 2$, see Fig. 30, the behavior shows the same behaviour than in the previous cases: $|\Psi_\pm|^2(a = 0) \neq 0$; a larger peak compared to $\overline{p} = 0$, see Fig. 23; and a narrower oscillatory region for $a > 2$.

In summary, the key differences are: (1) the non-zero value of $|\Psi_\pm|^2(a = 0)$, (2) the increased peak height compared to $\overline{p} = 0$, and (3) the narrower oscillatory behavior for large a.

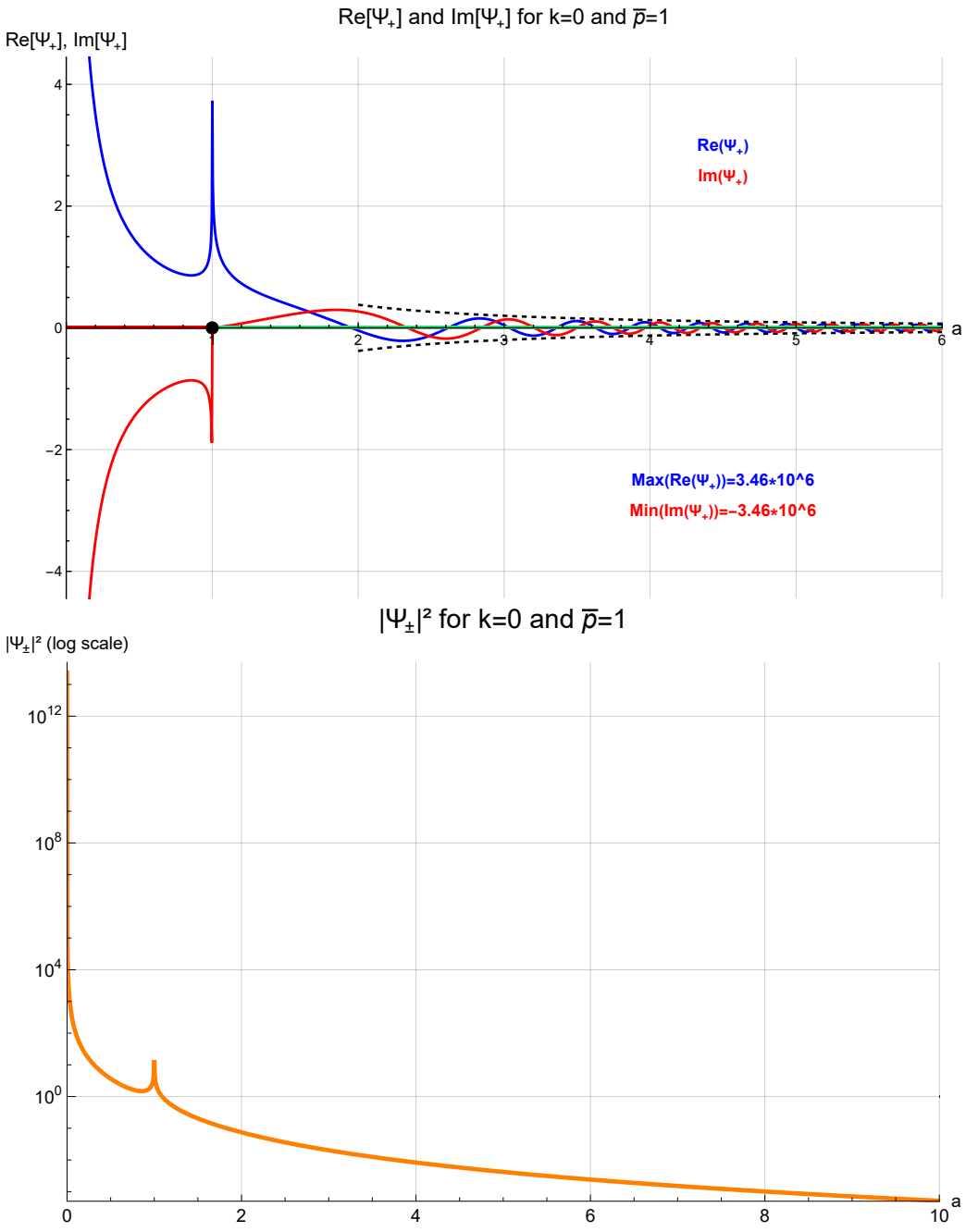

Figure 27: For $k = 0$, $\overline{p} = 1$, $\phi = 0$, $\lambda = 1$, $p = 1$ and $\hbar = 1$: (Top) Real and imaginary parts of the general wave function (5.11) for an expanding universe (Ψ_+) (blue and red curves, respectively), with the forbidden classical region ($a < p$) shown in red and the allowed region ($a > p$) in green; (Bottom) $|\Psi_\pm|^2$ (5.37) as a function of a.

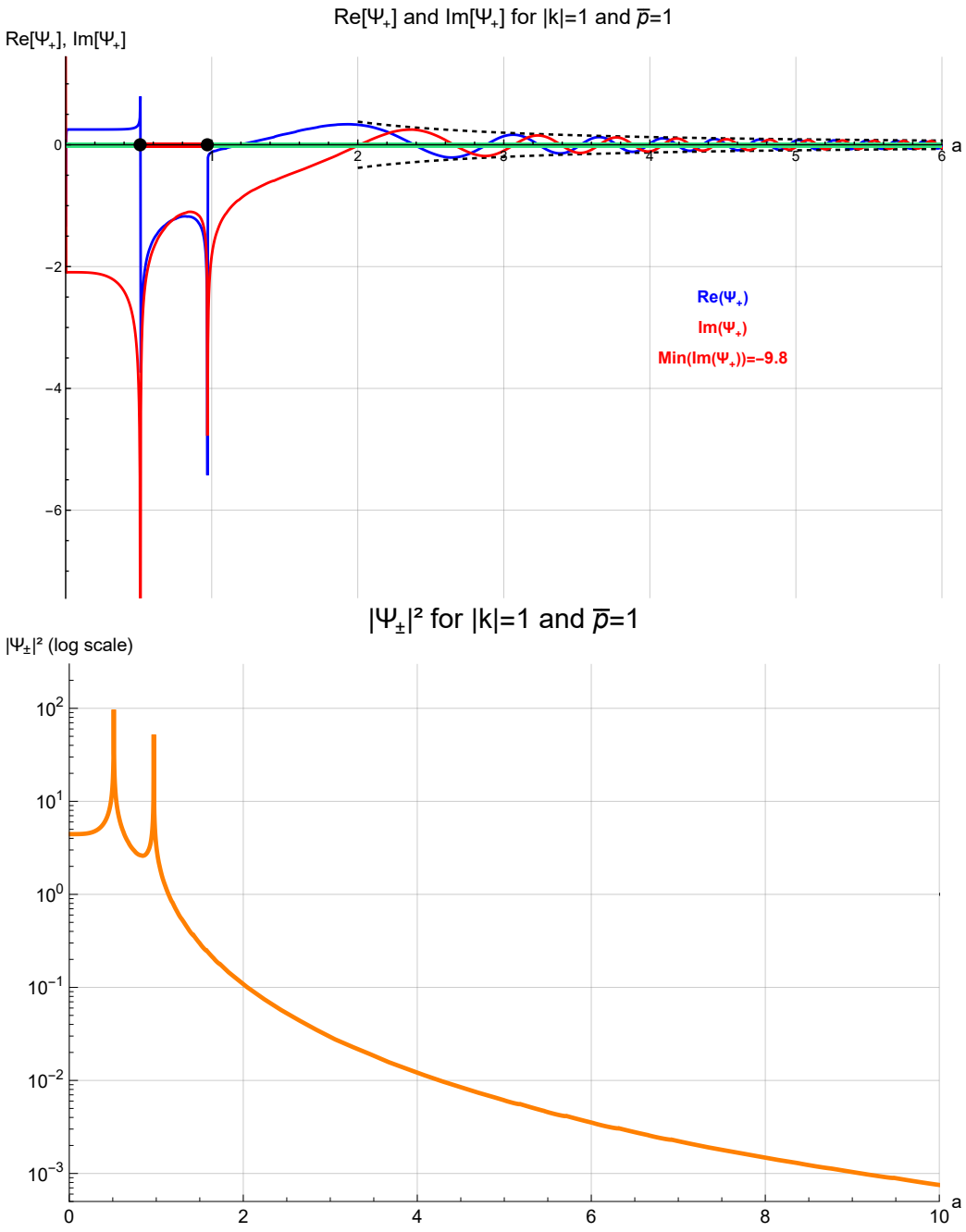

Figure 28: For $|k| = 1$, $\overline{p} = 1$, $\phi = 0$, $\lambda = 1$, $p = 1$ and $\hbar = 1$: (Top) Real and imaginary parts of the general wave function (5.11) for an expanding universe (Ψ_+) (blue and red curves, respectively), with the forbidden classical region ($p_1 < a < p_2$) shown in red and the allowed region ($a < p_1$ and $a > p_2$) in green; (Bottom) $|\Psi_\pm|^2$ (5.37) as a function of a.

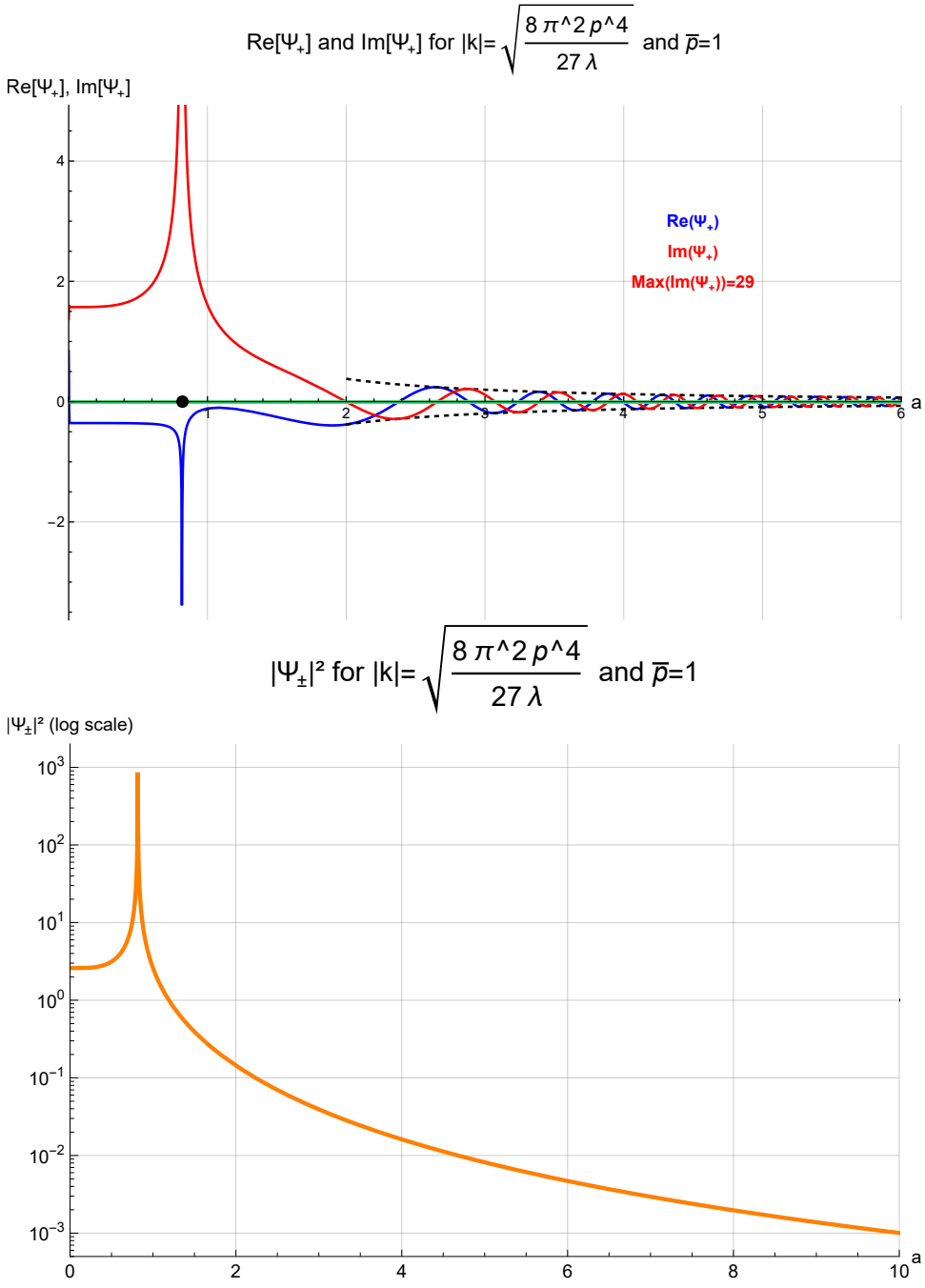

Figure 29: For $|k| = \sqrt{8\pi^2 p^2/(27\lambda)}$, $\overline{p} = 1$, $\phi = 0$, $\lambda = 1$, $p = 1$ and $\hbar = 1$: (Top) Real and imaginary parts of the general wave function (5.11) for an expanding universe (Ψ_+) (blue and red curves, respectively), with the forbidden classical region ($a < p$) shown in red and the allowed region ($a > p$) in green; (Bottom) $|\Psi_\pm|^2$ (5.37) as a function of a.

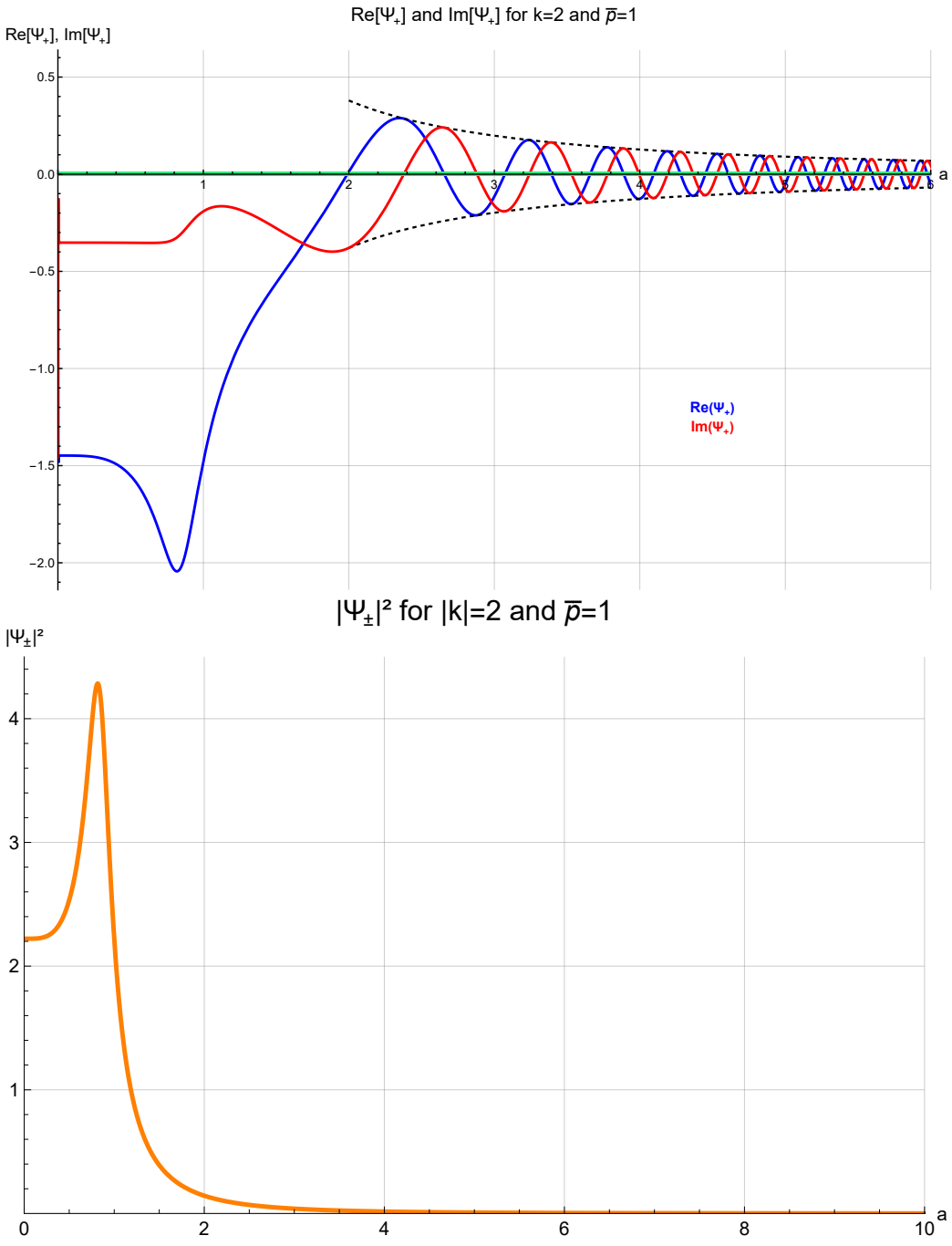

Figure 30: For $|k| = 2$, $\overline{p} = 1$, $\phi = 0$, $\lambda = 1$, $p = 1$ and $\hbar = 1$: (Top) Real and imaginary parts of the general wave function (5.11) for an expanding universe (Ψ_+) (blue and red curves, respectively), with the forbidden classical region ($a < p$) shown in red and the allowed region ($a > p$) in green; (Bottom) $|\Psi_\pm|^2$ (5.37) as a function of a.

Bibliography

[1] Edwin P Hubble. “Cepheids in spiral nebulae”. In: *Pop. Astr.; Vol. 33; Page 252-255* 33 (1925).

[2] Edwin Hubble. “A relation between distance and radial velocity among extra-galactic nebulae”. In: *Proceedings of the national academy of sciences* 15.3 (1929), pp. 168–173.

[3] Edwin Hubble and Milton L Humason. “The velocity-distance relation among extra-galactic nebulae”. In: *Astrophysical Journal, vol. 74, p. 43* 74 (1931), p. 43.

[4] Donald E Osterbrock, Joel A Gwinn, and Ronald S Brashear. “Edwin Hubble and the expanding universe”. In: *Scientific American* 269.1 (1993), pp. 84–89.

[5] Licia Verde, Tommaso Treu, and Adam G Riess. “Tensions between the early and late Universe”. In: *Nature Astronomy* 3.10 (2019), pp. 891–895.

[6] Wendy L Freedman. “Measurements of the Hubble constant: tensions in perspective”. In: *The Astrophysical Journal* 919.1 (2021), p. 16.

[7] Wendy L Freedman. “The Hubble constant and the expansion age of the Universe”. In: *Physics Reports* 333 (2000), pp. 13–31.

[8] Georges Lemaıtre. “Un Univers homogène de masse constante et de rayon croissant rendant compte de la vitesse radiale des nébuleuses extra-galactiques”. In: *Annales de la Société Scientifique de Bruxelles, A47, p. 49-59* 47 (1927), pp. 49–59.

[9] Phillip James Edwin Peebles. *Principles of physical cosmology*. Princeton university press, 2020.

[10] Cristi Stoica. “Big Bang singularity in the Friedmann-Lemaitre-Robertson-Walker spacetime”. In: *arXiv preprint arXiv:1112.4508* (2011).

[11] Stanislav R Kelner, A Yu Prosekin, and FA Aharonian. “Mechanics and kinetics in the Friedmann-Lemaıtre-Robertson-Walker space-times”. In: *Physical Review D—Particles, Fields, Gravitation, and Cosmology* 84.4 (2011), p. 044016.

[12] Miguel Ángel Sánchez Quintanilla. *El final del universo: ¿qué destino le espera al cosmos?* RBA Coleccionables, 2015.

[13] Weebly. *Bernhard Riemann: Mathematical Contributions/Legacy*. URL: https://bernhardriemann.weebly.com/mathematical-contributionslegacy.html.

[14] Alan H Guth. "Inflationary universe: A possible solution to the horizon and flatness problems". In: *Physical Review D* 23.2 (1981), p. 347.

[15] Andrei D Linde. "A new inflationary universe scenario: a possible solution of the horizon, flatness, homogeneity, isotropy and primordial monopole problems". In: *Physics Letters B* 108.6 (1982), pp. 389–393.

[16] *Astrofísica: del Big Bang a los agujeros negros*. Muy interesante, 2020.

[17] Arno A Penzias and Robert W Wilson. "A measurement of excess antenna temperature at 4080 MHz". In: *A Source Book in Astronomy and Astrophysics, 1900–1975*. Harvard University Press, 1979, pp. 873–876.

[18] Robert H Dicke et al. "Cosmic black-body radiation." In: *Astrophysical Journal, vol. 142, p. 414-419* 142 (1965), pp. 414–419.

[19] European Space Agency. *Planck's view of the cosmic microwave background*. Imagen publicada por la ESA. July 2018. URL: https://www.esa.int/ESA_Multimedia/Images/2018/07/Planck_s_view_of_the_cosmic_microwave_background (visited on 11/15/2023).

[20] Christiaan Huygens. *Traité de la lumiere; ou y sont expliquées les causes de ce qui luy arrive dans la reflexion et dans la refraction et particulierement dans l'étrange refraction du cristal d'islande*. Gressner & Schramm, 1885.

[21] Isaac Newton. *Opticks, or, a treatise of the reflections, refractions, inflections & colours of light*. Courier Corporation, 1952.

[22] Bryce S. DeWitt. "Quantum Theory of Gravity. I. The Canonical Theory". In: *Physical Review* 160.5 (1967). The foundational paper on canonical quantum gravity, pp. 1113–1148. DOI: 10.1103/PhysRev.160.1113.

[23] J. B. Hartle and S. W. Hawking. "Wave function of the universe". In: *Physical Review D* 28.12 (1983), pp. 2960–2975. DOI: 10.1103/PhysRevD.28.2960.

[24] Alexander Vilenkin. "Quantum cosmology and the initial state of the universe". In: *Physical Review D* 37.4 (1988), p. 888.

[25] José Rodríguez-Quientero and Mario Goméz Santamaría. *¿Por qué hay algo en lugar de nada?* RBA Coleccionables, 2017.

[26] Gabriel Álvarez, Luis Martínez Alonso, and Elena Medina. “Kinetic dominance and the wave function of the Universe”. In: *Physical Review D* 105.8 (2022), p. 083502.

[27] Charles W Misner, Kip S Thorne, and John Archibald Wheeler. *Gravitation*. Macmillan, 1973.

[28] Albert Einstein. *Sobre la teoría de la relatividad*. Neisa, 2024.

[29] Albert Einstein and Carlos E Prélat. “El significado de la relatividad”. In: *(No Title)* (1971).

[30] Kurt Gödel. “An example of a new type of cosmological solutions of Einstein’s field equations of gravitation”. In: *Reviews of modern physics* 21.3 (1949), p. 447.

[31] Olivier Sarbach and Manuel Tiglio. “Boundary conditions for Einstein’s field equations: mathematical and numerical analysis”. In: *Journal of Hyperbolic Differential Equations* 2.04 (2005), pp. 839–883.

[32] Thomas W Baumgarte and Stuart L Shapiro. “Numerical integration of Einstein’s field equations”. In: *Physical Review D* 59.2 (1998), p. 024007.

[33] Olivier Sarbach and Manuel Tiglio. “Continuum and discrete initial-boundary value problems and Einstein’s field equations”. In: *Living reviews in relativity* 15 (2012), pp. 1–194.

[34] Alma L Albujer, Jónatan Herrera, and Rafael M Rubio. “On complete trapped submanifolds in globally hyperbolic spacetimes”. In: *Journal of Physics A: Mathematical and Theoretical* 56.34 (2023), p. 345202.

[35] Eric Gourgoulhon. *3+ 1 formalism in general relativity: bases of numerical relativity*. Vol. 846. Springer Science & Business Media, 2012.

[36] Alejandro José Florido Tomé. *Formación dinámica y estabilidad de estrellas de bosones multi-estado*. University of Valencia, 2024.

[37] Miguel Alcubierre. *Introduction to 3+ 1 numerical relativity*. Vol. 140. OUP Oxford, 2008.

[38] FS Guzmán. “Introduction to numerical relativity through examples”. In: *Revista mexicana de física* 53 (2007), pp. 78–93.

[39] Carlos Palenzuela. “Introduction to numerical relativity”. In: *Frontiers in Astronomy and Space Sciences* 7 (2020), p. 58.

[40] Jonathan Gorard. “Computational General Relativity in the Wolfram Language using Gravitas II: ADM Formalism and Numerical Relativity”. In: *arXiv preprint arXiv:2401.14209* (2024).

[41] Alessandro Danieli and Luca Guido Molinari. “ADM formalism: a Hamiltonian approach to general relativity”. PhD thesis. Università degli Studi di Milano Milan, Italy, 2020.

[42] Bert Janssen. “Teorıa de la relatividad general”. In: *Granada: Universidad de Granada* (2013).

[43] Alejandro Corichi and Dario Núñez. “Introduction to the ADM formalism”. In: *arXiv preprint arXiv:2210.10103* (2022).

[44] Hiroaki Yoshimura and Jerrold E Marsden. “Dirac structures and the Legendre transformation for implicit Lagrangian and Hamiltonian systems”. In: *Lagrangian and Hamiltonian Methods for Nonlinear Control 2006: Proceedings from the 3rd IFAC Workshop, Nagoya, Japan, July 2006*. Springer. 2007, pp. 233–247.

[45] Peter Szekeres. “A Course in Modern Mathematical Physics”. In: ().

[46] Sumanta Chakraborty. “Boundary terms of the Einstein–Hilbert action”. In: *Gravity and the Quantum: Pedagogical Essays on Cosmology, Astrophysics, and Quantum Gravity*. Springer, 2017, pp. 43–59.

[47] Richard L Arnowitt, Stanley Deser, and Charles W Misner. “The dynamics of general relativity”. In: *Gen. Rel. Grav.* 40.arXiv: gr-qc/0405109 (2008), pp. 1997–2027.

[48] Andrei D Linde. “The inflationary universe”. In: *Reports on Progress in Physics* 47.8 (1984), p. 925.

[49] Alexander Polishchuk. “Algebraic geometry of Poisson brackets”. In: *Journal of Mathematical Sciences* 84.5 (1997), pp. 1413–1444.

[50] Matías Hersch. *The Wheeler-DeWitt equation*. 2017.

[51] Carlo Rovelli. *Quantum gravity*. Cambridge university press, 2004.

[52] Richard P Woodard. “Enforcing the Wheeler-DeWitt constraint the easy way”. In: *Classical and Quantum Gravity* 10.3 (1993), p. 483.

[53] Ali Kaya. “Schrödinger from Wheeler–DeWitt: The issues of time and inner product in canonical quantum gravity”. In: *Annals of Physics* 451 (2023), p. 169256.

[54] Np P Landsman. “Against the Wheeler-DeWitt equation”. In: *Classical and Quantum Gravity* 12.12 (1995), p. L119.

[55] Abhay Ashtekar and Vesselin Petkov. *Springer handbook of spacetime*. Springer, 2014.

[56] Davide Batic and Marek Nowakowski. “Gravitational collapse via Wheeler–DeWitt equation”. In: *Annals of Physics* 461 (2024), p. 169579.

[57] Martin Bojowald. *The universe: a view from classical and quantum gravity*. John Wiley & Sons, 2012.

[58] GK Goswami, Anirudh Pradhan, and A Beesham. "Friedmann–Robertson–Walker accelerating Universe with interactive dark energy". In: *Pramana* 93.6 (2019), p. 89.

[59] Patrick Peter and Jean-Philippe Uzan. *Primordial cosmology*. Oxford University Press, 2009.

[60] Robert M Wald. *General relativity*. University of Chicago press, 2010.

[61] Haradhan Mohajan. "Friedmann, Robertson-Walker (FRW) Models in Cosmology". In: (2013).

[62] Investigación y Ciencia. "El Universo Cuántico". In: *Investigación y Ciencia* 63 (2011).

[63] Samson HW Leong et al. "Gravitational-wave signatures of mirror (a) symmetry in binary black hole mergers: measurability and correlation to gravitational-wave recoil". In: *arXiv preprint arXiv:2501.11663* (2025).

[64] Hong-Yee Chiu. "Symmetry between particle and antiparticle populations in the universe". In: *Physical Review Letters* 17.13 (1966), p. 712.

[65] Ahmet M Öztaş, Emre Dil, and Michael L Smith. "The varying cosmological constant: A new approximation to the Friedmann equations and universe model". In: *Monthly Notices of the Royal Astronomical Society* 476.1 (2018), pp. 451–458.

[66] Alexander Friedman. "On the curvature of space". In: *General Relativity and Gravitation* 31.12 (1999), pp. 1991–2000.

[67] Alexander Vilenkin. "Interpretation of the wave function of the Universe". In: *Physical Review D* 39.4 (1989), p. 1116.

[68] Svend E Rugh and Henrik Zinkernagel. "Weyl's principle, cosmic time and quantum fundamentalism". In: *Explanation, prediction, and confirmation*. Springer, 2011, pp. 411–424.

[69] Hubert Goenner. "Weyl's contributions to cosmology". In: *Hermann Weyl's Raum—Zeit—Materie and a General Introduction to His Scientific Work*. Springer, 2001, pp. 105–137.

[70] Andrei D Linde. "Chaotic inflation". In: *Physics Letters B* 129.3-4 (1983), pp. 177–181.

[71] WJ Handley et al. "Kinetic initial conditions for inflation". In: *Physical Review D* 89.6 (2014), p. 063505.

[72] Moacir Kripka and Rosana Maria Luvezute Kripka. “Big crunch optimization method”. In: *International conference on engineering optimization, Brazil*. 2008, pp. 1–5.

[73] Mir Faizal. “Deformation of the Wheeler–DeWitt equation”. In: *International Journal of Modern Physics A* 29.20 (2014), p. 1450106.

[74] E Schrödinger. “About Heisenberg uncertainty relation”. In: *arXiv preprint quant-ph/9903100* 10 (1999).

[75] Justin Khoury et al. “From big crunch to big bang”. In: *Physical Review D* 65.8 (2002), p. 086007.

[76] José Rafael Hernández Arias. *Nietzsche: la crítica más radical a los valores y a la moral de la cultura occidental*. RBA, 2015.

[77] Elena Medina and Luis Martínez Alonso. “Asymptotic Solutions of a Generalized Starobinski Model: Kinetic Dominance, Slow Roll and Separatrices”. In: *Universe* 7.12 (2021), p. 500.

[78] David H Lyth and Antonio Riotto. “Particle physics models of inflation and the cosmological density perturbation”. In: *Physics Reports* 314.1-2 (1999), pp. 1–146.

[79] Radoje Belušević. “Relativity, Astrophysics and Cosmology, 1 Volume Set”. In: *Relativity* (2008).

[80] Vihan M Patel and Charles H Lineweaver. “Solutions to the cosmic initial entropy problem without equilibrium initial conditions”. In: *Entropy* 19.8 (2017), p. 411.

[81] Investigación y Ciencia. “La vida interior de los quarks”. In: *Investigación y Ciencia* 436 (2013).

[82] Daniel Baumann. “TASI lectures on inflation”. In: *arXiv preprint arXiv:0907.5424* (2009).

[83] Gabriel Álvarez et al. “Separatrices in the Hamilton–Jacobi formalism of inflaton models”. In: *Journal of Mathematical Physics* 61.4 (2020).

[84] Moshe Shapiro. “Derivation of the coordinate-momentum commutation relations from canonical invariance”. In: *Physical Review A—Atomic, Molecular, and Optical Physics* 74.4 (2006), p. 042104.

[85] AO Barvinsky and A Yu Kamenshchik. “Selection rules for the Wheeler-DeWitt equation in quantum cosmology”. In: *Physical Review D* 89.4 (2014), p. 043526.

[86] Alexander Yu Kamenshchik et al. “Superpotential method and the amplification of inflationary perturbations”. In: *Physical Review D* 110.10 (2024), p. 104011.

[87] C Adam and D Varela. "The superpotential method in cosmological inflation". In: *arXiv preprint arXiv:1901.02892* (2019).

[88] David J Griffiths and Darrell F Schroeter. *Introduction to quantum mechanics*. Cambridge university press, 2018.

[89] Carlos Sánchez del Río. *Física cuántica*. Comercial Grupo ANAYA, SA, 2017.

[90] Jun John Sakurai and Jim Napolitano. *Modern quantum mechanics*. Cambridge University Press, 2020.

[91] Stanley C Miller Jr and RH Good Jr. "A WKB-type approximation to the Schrödinger equation". In: *Physical Review* 91.1 (1953), p. 174.

[92] Davide Batic, Marek Nowakowski, and Neelima Govind Kelkar. "Wheeler–Dewitt equation and the late gravitational collapse: effects of factor ordering and the tunneling scenario". In: *Annals of Physics* 469 (2024), p. 169773.

[93] Boris Mikhailovich Karnakov and Vladimir Pavlovich Krainov. *WKB approximation in atomic physics*. Springer Science & Business Media, 2012.

[94] HM Van Horn and EE Salpeter. "WKB approximation in three dimensions". In: *Physical Review* 157.4 (1967), p. 751.

[95] Marcus AM de Aguiar. *The WKB Approximation*. 2013.

[96] Richard Steiner. "History and progress on accurate measurements of the Planck constant". In: *Reports on Progress in Physics* 76.1 (2012), p. 016101.

[97] P Alberto, Carlos Fiolhais, and VMS Gil. "Relativistic particle in a box". In: *European Journal of Physics* 17.1 (1996), p. 19.

[98] Jonathan J Halliwell. "Introductory lectures on quantum cosmology." In: *Introductory lectures on quantum cosmology* (1990).

[99] Stephen W Hawking. "The quantum state of the universe". In: *Nuclear Physics B* 239.1 (1984), pp. 257–276.

[100] Lev Davidovich Landau and Evgenii Mikhailovich Lifshitz. *Quantum mechanics: non-relativistic theory*. Vol. 3. Elsevier, 2013.

[101] Martin Bojowald. *Canonical gravity and applications: cosmology, black holes, and quantum gravity*. Cambridge University Press, 2010.

[102] Alexander Vilenkin. "Boundary conditions in quantum cosmology". In: *Physical Review D* 33.12 (1986), p. 3560.

[103] Alejandro José Florido Tomé. *Ondas gravitacionales: obtención de la ecuación y simulaciones*. University of Cordoba, 2023.

[104] Benjamin P Abbott et al. “Observation of gravitational waves from a binary black hole merger”. In: *Physical review letters* 116.6 (2016), p. 061102.

[105] Michele Maggiore. *Gravitational waves*. Vol. 2. Oxford university press, 2008.

[106] Jürgen Jost and Jeurgen Jost. *Riemannian geometry and geometric analysis*. Vol. 42005. Springer, 2008.

[107] Jürgen Jost. *Geometry and physics*. Springer Science & Business Media, 2009.

[108] Manfredo Perdigao Do Carmo and J Flaherty Francis. *Riemannian geometry*. Vol. 2. Springer, 1992.

[109] Rainer Kurt Sachs and H-H Wu. *General relativity for mathematicians*. Vol. 48. Springer Science & Business Media, 2012.

[110] María Martín Vega. “Completeness and Stability of spacetimes with Lorentz-Minkowski ends”. Trabajo Fin de Máster del Máster en Matemáticas. Master’s thesis. Universidad de Granada, 2020. URL: https://masteres.ugr.es/matematicas/sites/master/matematicas/public/trabajo-fin-master/TFM-MariaMartinVega-CompletenessAndStability.pdf.

[111] Juan Andrés Trillo Gómez Trillo. “Diferenciales holomorfas en superficies de Riemann”. Trabajo Fin de Máster del Máster en Matemáticas. Master’s thesis. Universidad de Granada, 2020. URL: https://masteres.ugr.es/matematicas/sites/master/matematicas/public/trabajo-fin-master/TFM-J.Trillo.pdf.

[112] Dragutin Mihailović et al. *Physics of complex systems: Discovery in the age of Gödel*. CRC Press, 2023.

[113] Yury Aleksandrovich Kubyshin and Igor Pavlovich Volobuev. *Geometria diferencial y algebras de Lie y sus aplicaciones en la teoria de campos*. URSS, 2007.

[114] Matthew P Gaffney. “A special Stokes’s theorem for complete Riemannian manifolds”. In: *Annals of Mathematics* 60.1 (1954), pp. 140–145.

[115] Dexter Kozen and Marc Timme. “Indefinite summation and the Kronecker delta”. In: (2007).

[116] José Ignacio Illana. *Quantum mechanics*. Lecture notes developed in close collaboration with Manuel Masip and Manuel Pérez-Victoria. 2022.

[117] MD Feit, JA Fleck Jr, and A Steiger. “Solution of the Schrödinger equation by a spectral method”. In: *Journal of Computational Physics* 47.3 (1982), pp. 412–433.